# THE ROLE OF COLLOIDAL PARTICLES ON THE MIGRATION OF AIR BUBBLES IN POROUS MEDIA

A Dissertation

by

JI-SEOK HAN

Submitted to the Office of Graduate Studies of
Texas A&M University
in partial fulfillment of the requirements for the degree of

DOCTOR OF PHILOSOPHY

December 2007

Major Subject: Civil Engineering

# THE ROLE OF COLLOIDAL PARTICLES ON THE MIGRATION OF AIR BUBBLES IN POROUS MEDIA

A Dissertation

by

JI-SEOK HAN

Submitted to the Office of Graduate Studies of
Texas A&M University
in partial fulfillment of the requirements for the degree of

DOCTOR OF PHILOSOPHY

Approved by:

| | |
|---|---|
| Chair of Committee, | M. Yavuz Corapcioglu |
| Committee Members, | Hamn-Ching Chen |
| | Roy Hann |
| | Hongbin Zhan |
| Head of Department, | David V. Rosowsky |

December 2007

Major Subject: Civil Engineering

# ABSTRACT

The Role of Colloidal Particles on the Migration of Air Bubbles

in Porous Media. (December 2007)

Ji-Seok Han, B.S, Korea University;

M.S, Texas A&M University

Chair of Advisory Committee: Dr. M. Yavuz Corapcioglu

The contamination of groundwater and soils has been a big issue of great interest and importance to human health. When organic compounds from leaking underground storage tanks or accidental spills on the surface infiltrate into the subsurface environment, they migrate downward through the unsaturated zone. These contaminants are dissolved into groundwater and move with groundwater flow. Thus, there is a need for remediation technologies.

Air sparging is relatively cost-effective, as well as an efficient and safe technique for recovering organic contaminants in the subsurface. This technique introduces air into the subsurface system to enhance the volatilization and bioremediation of the contaminant in the groundwater system. In this operating system, the movement of air phase can take place either as a continuous air phase or as discrete air bubbles. However, the present research focused on continuous air phase assumption and mass balance equations of individual phases rather than taking into account the movement of air bubbles and colloidal particle capture on discrete air-water interface.

Generally colloidal particles are treated as suspended particles in the water, so the hypothesis is that the rising air bubble can collect the particles and transport them up to the water table where the pump extracts the dirty bubbles from the groundwater system to the processing unit on the ground surface.

This dissertation developed a pore-scale study to model the migration of discrete air phase in the presence of colloidal particles captured on the air-water interface. The model was based on the pore-scale balance equation for forces acting on a bubble rising in a porous medium in the presence of colloids. A dimensional analysis of the phenomenon was also conducted to provide a more generalized methodology to evaluate the effect of individual forces acting on an air bubble.

The results indicate that the proposed model can predict the terminal velocity of a rising bubble without or with colloidal particles and provide the effect of numbers of colloidal particles, properties of colloidal particles, and solid grain size. The results showed that the terminal velocity of a discrete bubble was affected by the attachment of particles on a bubble, and then the volatile organic compound (VOC) removal rate was changed by the various radii of a bubble and the number of colloidal particles on a bubble.

# DEDICATION

To God, my Lord Jesus Christ

# ACKNOWLEDGEMENTS

I would like to express my sincere gratitude to my primary co-advisor, Dr. M. Yavuz Corapcioglu, for providing guidance and constant encouragement during the course of this work. I would especially like to thank my committee member, Dr. Roy Hann, for advising my research and counseling me on the all problems that I have had. I am also grateful to Dr. Hamn-Ching Chen and Dr. Hongbin Zhan for serving as members of my advisory committee and for their encouragement, assistance and critical review of this research. And I will always remember Dr. Timothy Kramer, who has passed away, for advising me as a previous member of my committee.

I would like to extend my thanks to my good friends, Seungha Hwang, who has passed away, and Hojoon Lim, for helping and providing an idea for my research.

I thank my wife, Kyunghwan Yoo, and my daughter, Jaein Han, for their love and encouragement. I am also thankful to my sister, Jiyeon Han, my brother-in-law, Hyunseok Choi, their children, Hwansun Choi and Taeun Choi, and my other brother-in-law, Jinsung Yoo, for their constant care and prayers for me in Seoul and New York. Lastly, I have no words to express my gratitude to my father, Kwanghui Han, my mother, Eunju Jung, my farther-in-law, Jungwoong Yoo, and my mother-in-law, Sunmi Yoo, who have shown their limitless support and love throughout the course of my life.

# TABLE OF CONTENTS

Page

ABSTRACT .......... iii

DEDICATION .......... v

ACKNOWLEDGEMENTS .......... vi

TABLE OF CONTENTS .......... vii

LIST OF FIGURES .......... x

LIST OF TABLES .......... xiv

1 INTRODUCTION .......... 1

1-1 Problem Statement .......... 1
1-2 Objectives .......... 6

2 THEORETICAL APPROACH .......... 8

2-1 General Description of Air Sparging .......... 8
2-2 Capture Mechanism of a Particle on a Bubble .......... 10
2-3 Idealization of Packing System in the Porous Media .......... 14
2-4 Air Flow Patterns in Air Sparging System .......... 18

3 FORCE BALANCE EQUATION FOR THE MIGRATION OF AIR BUBBLES IN POROUS MEDIA .......... 21

3-1 Force Balance Equation of Bubble Movement in Porous Media .......... 21
3-1-1 Overview .......... 21
3-1-2 Force Balance Equation of a Bubble without a Particle in Porous Media .......... 22
3-2 Force Balance Equation of the Particle-Bubble Unit in Porous Media .......... 29
3-2-1 Overview .......... 29
3-2-2 Force Balance Equation of the Particle-Bubble Unit in Porous Media .......... 33

Page

4 TERMINAL VELOCITY OF A BUBBLE ATTACHMENT OF PARTICLES.............38

4-1 Terminal Velocity of Bubble in Liquid and in Porous Media ..............................38
4-1-1 Terminal Velocity Equation for a Bubble without a Particle ................38
4-1-2 The Effect of Grain Size ($d_p$) for the Movement of a Bubble without a Particle ....................................................................44
4-2 Terminal Velocity of the Particle-Bubble Unit in Porous Media ..........................50
4-2-1 Terminal Velocity Equation for the Particle-Bubble Unit ......................50
4-2-2 The Effect of Attached Particles for the Particle-Bubble Unit ...............54
4-2-3 The Effect of Grain Size ($d_p$) for the Particle-Bubble Unit's Movement .................................................57

5 DIMENSIONAL ANALYSIS OF BUBBLE IN POROUS MEDIA ..............................68

5-1 Dimensional Analysis of Movement of a Bubble without Particle in Porous Media ...........................................................................................68
5-1-1 General Description of Dimensional Analysis .......................................68
5-1-2 Relationship between the Dimensionless Numbers and Reynolds Number .............................................................................73
5-1-3 Relationship between Bo, Ca, We and Nt .............................................76
5-2 Dimensional Analysis of the Particle-Bubble Unit Movement in Porous Media ...........................................................................................78
5-2-1 General Description of the Modified Dimensionless Number Equations ...................................................................78
5-2-2 Relationship of the Modified Dimensionless Numbers with the Effect of Attached Particles ...................................................90
5-2-3 Relationship between the Modified Dimensionless Numbers and Reynolds Number...........................................................................95
5-2-4 Relationship between Bo′, Ca′, We and Nt' ...........................................101

6 APPLICATION OF TERMINAL VELOCITY OF A SINGLE BUBBLE WITH OR WITHOUT THE PARTICLES IN POROUS MEDIA .................................................109

6-1 Effect of the Property of the Particle during the Movement of the Particle-Bubble Unit in Porous Media ........................................................109
6-1-1 Definition of Hydrophilic and Hydrophobic Particle ...........................109
6-1-2 Effect of Hydrophilic and Hydrophobic Particle for the Movement of the Particle-Bubble Unit in Porous Media .............112
6-2 Application of the Terminal Velocity of the Particle-Bubble Unit in Porous Media ........................................................................................121
6-2-1 Overview ........................................................................................121

Page

6-2-2 Governing Equation of VOC Removal Concentration in a Single Bubble ....122

6-2-3 Effect of a Bubble's Radius and Particle's Numbers for VOC Removal by using the Equation of the Terminal Rise Velocity of a Bubble in Porous Media ....125

7 SUMMARY AND CONCLUSION ....130

REFERENCES ....136

APPENDIX A....141

APPENDIX B....142

VITA ....144

# LIST OF FIGURES

Page

Figure 2. 1 Conceptual model for removal of VOCs dissolved in porous media .......................9

Figure 2. 2 The three important mechanisms during the attachment of particles to bubbles....11

Figure 2. 3 Types of layers (From *Graton and Fraser*, 1935) .................................................15

Figure 2. 4 Type sphere groups of the six cases (From *Graton and Fraser*, 1935)..................16

Figure 2. 5 Sketches of the flow patterns in porous media ......................................................19

Figure 3. 1 External forces acting on a bubble without a particle in porous media................. 23

Figure 3. 2 Schematic diagram of a bubble in a porous medium with orthorhombic packing arrangement ...........................................................................................25

Figure 3. 3 Sketch of the external forces acting on the particle-bubble unit............................30

Figure 3. 4 Three-phase contact between bubble, particle, and liquid (modified by Bloom and Heindel [1997]) ..........................................................32

Figure 3. 5 Schematic diagram of external forces acting on a particle-bubble unit..................34

Figure 4. 1 Terminal velocity of bubble in liquid and in porous media...................................43

Figure 4. 2 Relationship between terminal velocity ($U_b$) and solid grain size ($d_p$)..................46

Figure 4. 3 Relationship between trapped bubble radius and the limiting pore throat radius...48

Figure 4. 4 Comparison of theoretical rise velocity of the particle-bubble unit in porous media with various experimental data which come from Haberman and Morton [1953] and Corapcioglu et al. [2004] ...............................53

Figure 4. 5 The terminal velocity of the particle-bubble unit in porous media as increasing the number of attached particles on the bubble with various radii of bubble ...........................................................................................56

Figure 4. 6 Effect of dp=0.6 cm with various attached particles on the particle-bubble unit in porous media ............................................................................................ 58

Page

Figure 4. 7 Effect of dp=0.5 cm with various attached particles on the particle-bubble unit in porous media ....................................59

Figure 4. 8 Effect of dp=0.4 cm with various attached particles on the particle-bubble unit in porous media ....................................60

Figure 4. 9 Effect of dp=0.3 cm with various attached particles on the particle-bubble unit in porous media ....................................61

Figure 4. 10 Effect of dp=0. 2 cm with various attached particles on the particle-bubble unit in porous media ....................................62

Figure 5. 1 Dimensionless numbers as a function of the equivalent bubble radius ................ .72

Figure 5. 2 Variations of dimensionless numbers (which are Bo, Ca, We, and Nt) as increasing Reynolds number (Re) ....................................75

Figure 5. 3 The ratio of dimensionless numbers (which are Bo, Ca, We) to Trapping number (Nt) with Reynolds number (Re) ....................................77

Figure 5. 4 Modified dimensionless numbers as a function of the bubble radius when 100 particles are attached....................................85

Figure 5. 5 Modified dimensionless numbers as a function of the bubble radius when 500 particles are attached....................................86

Figure 5. 6 Modified dimensionless numbers as a function of the bubble radius when $10^3$ particles are attached....................................87

Figure 5. 7 Modified dimensionless numbers as a function of the bubble radius when $5x10^3$ particles are attached....................................88

Figure 5. 8 Modified dimensionless numbers as a function of the bubble radius when $10^4$ particles are attached....................................89

Figure 5. 9 Relationship between modified Bond number ($Bo'$) and the particle-bubble unit with various number of particles (100, 500, 1000, 5000, and 10000)....................................91

Figure 5. 10 Relationship between modified Capillary number ($Ca'$) and the particle-bubble unit with various number of particles (100, 500, 1000, 5000, and 10000)....................................92

Page

Figure 5. 11 Relationship between Weber number (We) and the particle-bubble unit with various number of particles (100, 500, 1000, 5000, and 10000)........ 93

Figure 5. 12 Relationship between modified Trapping number (Nt′) and the particle-bubble unit with various number of particles (100, 500, 1000, 5000, and 10000)........ 94

Figure 5. 13 Variations of modified dimensionless numbers (Bo′, Ca′, We, and Nt′) as a function of Reynolds number (Re) when 100 particles are attached on a bubble........ 96

Figure 5. 14 Variations of modified dimensionless numbers (Bo′, Ca′, We, and Nt′) as a function of Reynolds number (Re) when 500 particles are attached on a bubble........ 97

Figure 5. 15 Variations of modified dimensionless numbers (Bo′, Ca′, We, and Nt′) as a function of Reynolds number (Re) when $10^3$ particles are attached on a bubble........ 98

Figure 5. 16 Variations of modified dimensionless numbers (Bo′, Ca′, We, and Nt′) as a function of Reynolds number (Re) when $5x10^3$ particles are attached on a bubble........ 99

Figure 5. 17 Variations of modified dimensionless numbers (Bo′, Ca′, We, and Nt′) as a function of Reynolds number (Re) when $10^4$ particles are attached on a bubble........ 100

Figure 5. 18 The ratio of modified dimensionless numbers (Bo′, Ca′, We) to Trapping number (Nt′) with Reynolds number (Re) when 100 particles are attached on a bubble........ 102

Figure 5. 19 The ratio of modified dimensionless numbers (Bo′, Ca′, We) to Trapping number (Nt′) with Reynolds number (Re) when 500 particles are attached on a bubble........ 103

Figure 5. 20 The ratio of modified dimensionless numbers (Bo′, Ca′, We) to Trapping number (Nt′) with Reynolds number (Re) when $10^3$ particles are attached on a bubble........ 104

Figure 5. 21 The ratio of modified dimensionless numbers (Bo′, Ca′, We) to Trapping number (Nt′) with Reynolds number (Re) when $5x10^3$ particles are attached on a bubble........ 105

Page

Figure 5. 22 The ratio of modified dimensionless numbers ($Bo'$, $Ca'$, We) to Trapping number ($Nt'$) with Reynolds number (Re) when $10^4$ of particles are attached on a bubble ................................................ 106

Figure 6. 1 A schematic diagram of hydrophilic and hydrophobic particle attachment on the bubble ........................................................................................ 110

Figure 6. 2 The terminal velocity of the particle-bubble unit in porous media for the hydrophilic particle with various particles attachment ............................ 113

Figure 6. 3 The terminal velocity of the particle-bubble unit in porous media for the hydrophobic particle with various particles attachment .......................... 114

Figure 6. 4 Comparison between the terminal velocity with hydrophilic particles and with hydrophobic particles when 100 particles are attached on a bubble in porous media ........................................................................................ 116

Figure 6. 5 Comparison between the terminal velocity with hydrophilic particles and with hydrophobic particles when 500 particles are attached on a bubble in porous media. ...................................................................................... 117

Figure 6. 6 Comparison between the terminal velocity with hydrophilic particles and with hydrophobic particles when $10^3$ particles are attached on a bubble in porous media. ...................................................................................... 118

Figure 6. 7 Comparison between the terminal velocity with hydrophilic particles and with hydrophobic particles when $5x10^3$ particles are attached on a bubble in porous media ........................................................................................ 119

Figure 6. 8 Comparison between the terminal velocity with hydrophilic particles and with hydrophobic particles when $10^4$ particles are attached on a bubble in porous media ........................................................................................ 120

Figure 6. 9 VOC removal concentrations with various radii of a single bubble without particle. ....................................................................................... 126

Figure 6. 10 VOC removal concentrations with various numbers of attached particle on a single bubble with $R_b$=0.4 cm as increasing the depth Z (cm) .................. 129

## LIST OF TABLES

Page

Table 2. 1 Geometrical relationships of the various packing systems..................................... 17

Table 2. 2 Relationship between the type of air flow and the size of porous medium............. 20

Table 3. 1The summary of the external forces acting on a rising bubble without a particle in porous media ........................................................................ 28

Table 3. 2 The summary of the external forces acting on the particle-bubble unit in porous media .................................................................................................... 36

Table 4. 1 Model parameters ................................................................................................ 42

Table 4. 2 The value of solid grain size ($d_p$), pore throat size (R'), and coefficient of $k_1$, and $k_2$ ................................................................................. 45

Table 4. 3 Summary of the maximum terminal rise velocity of bubble and the starting point of bubble radius (cm)........................................................... 49

Table 4. 4 Reduction rate of the maximum terminal velocity of the particle-bubble unit in dp=0.6 cm.......................................................................................................... 63

Table 4. 5 Reduction rate of the maximum terminal velocity of the particle-bubble unit in dp=0.5 cm.......................................................................................................... 64

Table 4. 6 Reduction rate of the maximum terminal velocity of the particle-bubble unit in dp=0.4 cm.......................................................................................................... 65

Table 4. 7 Reduction rate of the maximum terminal velocity of the particle-bubble unit in dp=0.3 cm.......................................................................................................... 66

Table 4. 8 Reduction rate of the maximum terminal velocity of the particle-bubble unit in dp=0.2 cm.......................................................................................................... 67

Table 5. 1 Summary of dimensionless numbers...................................................................... 71

Table 5. 2 Summary of modified dimensionless numbers ...................................................... 83

Table 5. 3 Summary of a slope of the ratio of the modified dimensionless number to Reynolds number for a bubble without or with a particle .................................... 108

Table 6. 1 Summary of Θ' between a particle and bubble, an angle γ, and an angle ω.......... 111

# 1 INTRODUCTION

## 1-1 PROBLEM STATEMENT

The contamination of groundwater and soils has been a big issue of great interest and importance for human health. When organic compounds from leaking underground storage tank or accidental spills on the surface infiltrate into the subsurface environment, they migrate downward through unsaturated zone. The contaminants may be accumulated on the water table or on the bottom of saturated zone because of the difference of the density of contaminants. These accumulated contaminants are dissolved into groundwater and move with groundwater flow. Thus, there is a need for remediation technologies.

Although various remediation techniques have been proposed, developed and applied to remove contaminants from groundwater and soils, some techniques are expensive and have very low effectiveness. In the last few decades, a lot of researches have been focused on *in-situ* treatment that is relatively cost-effective, as well as efficient and safe technique for recovering organic contaminants in the subsurface. The term *in-situ* comes from Latin and means "in its original place." That is, treatment occurs in the subsurface. A widely used remediation technique is air sparging for removing volatile organic compounds (VOCs) and for treating target compounds in the saturated zone. Many researchers have focused on optimal condition for air sparging. This technique has two main mechanisms: one is volatilization as air moves through porous media and the other is aerobic biodegradation through increased oxygen supply. The main removal mechanism of air sparging is volatilization rather than biodegradation.

This dissertation follows the style of *Water Resources Research*.

When air is injected into the porous media, two types of air flow patterns might be occurred. One is "bubble flow" that means the injected air moves to the water table in the form of discrete air bubbles, and the other is "channel flow" that means the injected air migrates in the vertical direction in the form of discrete air channels. These flow patterns depend on the size of the porous media. As the porous media size increases, air flow patterns move from air channels to bubble flow [*Brooks et al.*, 1999].

A mathematical model has been developed for air sparging by *Wilson et al.* [1998]. They have assumed that the mode of transport of air could be in the form of air channels. Their work is not included in bubble flow system. The quantitative technique about movement of an air bubble has been developed by *Corapcioglu et al.* [2004]. They have developed the model of air movement based on a force balance equation related to inertial force, buoyancy force, surface tension and drag force. These researchers have not considered colloidal particles in porous media.

However, colloids are presented and usually suspended in groundwater. Colloids are generated from chemical and/or physical perturbations in the natural porous matrix or changes in hydraulic system such as pumping or injection of water at high rates. Problems associated with colloid in groundwater have been investigated by many researchers for decades. Colloids naturally present in subsurface environment as mineral particles released from soil matrix in response to various conditions that the soil matrix experiences [*DeNovio et al*., 2004]. The colloids, very tiny particles can be contaminant itself or act as carriers of the contaminant on them in subsurface environment. Due to the very small size, colloids have unique chemical and physical properties. Sometimes colloids facilitate the transport of the contaminant or cause retardation of contaminant transport [*Corapcioglu and Choi*, 1996].

Colloids can also be introduced into the porous medium from the land surface through rapid infiltration of rainfall or injected into subsurface as tracer for an experiment [*Keller and Sirivithayapakorn*, 2004, *Ryan and Elimelech*, 1996]. Colloid mobilization in macro pores in soil matrix due to the changes in solution chemistry is also a colloid generation mechanism in groundwater because mobilized colloids in the pores near the land surface can travel to the water table [*Ryan and Elimelech*, 1996].

Particles present on soil-water interface and in the fluid as suspended form in water saturated porous media. The presence of bubble in the water saturated system affects on the transport phenomena and behaviors of the particles. The moving air bubbles carry the particles attached on their surface if the buoyancy is still big enough to keep rising, or retard when the total mass of the particles produces gravitational resistance which is equal to or exceeds the buoyancy. Force balance equation, population balance equation, and one dimensional advection-dispersion equation describe effects of moving bubble on the behaviors and effects of the particles in porous media.

Attachment of particles on a bubble is explained by many researchers with various theories[*Schulze et al*., 1989, Ralston and *Dukhin*, 1999, *Nguyen*, 1994, *Nguyen and Evans*, 2003]. *Langmuir and Blodgett* [1945] showed that bubble-particle collision efficiency is related to the size of the particle. *Sutherland* [1948] developed a collision model for a bubble-particle system by the derivation of an expression for the ratio of the number of the particles encountering a bubble per unit time to the number of the particles approaching the bubble at a great distance in a flow tube with a cross sectional area equal to the projected area of the bubble's. Recently comprehensive analysis of bubble-particle collision was performed by *Dai et al.* [2000] dealing with the processes in detail. They mainly focused on the bubble surface mobility, the fluid flow regime at the bubble surface, the influence of particle inertial forces on the collision efficiency, and the interfacial forces and the angle of tangency [*Dai et al*., 2000]. *Bloom and Heindel* [1997] introduced the forces acting on a particle as it approaches a bubble in a study on floatation deinking efficiency. They mentioned “the interception of a particle by a bubble can take place only if the trajectory of the particle is within a streaming tube of radius $R_c$, the so-called capture radius”.

When a particle is attached on a bubble, this reaction is assumed to be irreversible. Many researchers reported and discussed that particle straining in thin water film [*Wan and Tokunaga*, 1997] and particle captures on air-water interface [Corapcioglu and Choi, 1996] are treated as irreversible processes. Colloid detachment from solid-water interfaces may occur sometimes in saturated or unsaturated transport models, but is generally negligible if there are no physical/hydrologic or chemical perturbations [*Pinheiro et al*., 1999; *Schäfer et al*., 1998; *Chu et al*., 2001].

The difference between bubble velocity and fluid velocity makes particles collide to bubble when particles move with the velocity of the fluid. However, our study is assumed that there is no water flow in our model system. Presence of bubble affects on the colloid removal efficiency. Comparison will be made on with and without the bubbles. “The residence time of air bubbles in a saturated coarse medium controls the mass transfer of volatile contaminants from water to air phase, thus affecting the efficiency of an air-sparging operation” [*Roosevelt and Corapcioglu*, 1998].

The forces acting on bubble and particle are buoyancy force, surface tension force, and drag force. Sum of these forces is constant. *Corapcioglu et al.* (2004) introduced the force balance concept to explain the rise velocity of the air bubble, however particles attached on the bubble surface may cause changes in the bubble behaviors. This research will set up force balance equation for particle and bubble in pore scale.

By established the force balance equations for particle-bubble interaction, many questions in porous media in the presence of discrete air phase such like capture mechanisms, bubble entrapment in pore body, critical size of bubble to trap, the effect of numbers of colloidal particles, and the property of colloidal particle, etc. can be solved. Understanding the role of moving bubble is essential for improving the effectiveness of air sparging and other technologies which are related to a bubble and colloidal particles in porous media. And pore-scale analysis of interactions between bubble movement and colloids has not been systematically investigated in groundwater system. Furthermore, in addition to investigating the complex interactions between colloidal particles and moving air bubbles, the relationship among colloids, soil particles, and aqueous phase during migration of air bubbles will be studied and modeled.

Another important subject of consideration in this research is properties of the porous medium. The most important factor in unsaturated porous media such as vadose zone is the presence of the air-water interface. In a conventional analysis of contaminant transport, the saturated subsurface is idealized as a two-phase porous medium with contaminants participating between the stationary solid matrix and a mobile fluid phase. When colloidal particles are present in saturated porous media, the subsurface environment can be modeled as a three-phase porous medium with two solid phases. However, in unsaturated porous media, an analysis of the phenomenon should consider the contribution of the air phase in addition to aqueous phase, soil matrix phase, and the colloidal phase. Here comes the unique concept of this research. This research deals with four-phase porous medium that consists of solid phase, aqueous phase, colloidal phase, and discrete air phase (bubble). To emphasize the interaction between the discrete air phase and the colloidal particle, force balance between bubble and colloid particle will be investigated.

## 1-2 OBJECTIVES

Previous studies have been focused on empirical approaches of air sparging design parameters which are air distribution, depth of air injection, air injection pressure and flow rate, injection mode, contaminant type and distribution, soil type and so on. Also, some modeling work for air sparging has been studied. However, the previous research has been centered on continuous air phase or only air bubble migration in porous media without colloidal particles. Hence analyzing particle-bubble interaction and movement of the particle-bubble unit in porous media by setting up the force balance equation which is applied forces acting on particle and bubble in pore scale is performed.

The objective of this research is to develop a quantitative simulation to estimate the particle-bubble units in otherwise saturated porous media. To achieve the objectives of the research the followings are accomplished.

- Describing the relationship between bubble and particle
- Bubbles catch the particles in the fluid while they pass the pore and the particles attached on the bubble surface may cause changes the behaviors of the bubble. The changes of bubble behaviors include reduced velocity, and increased residence time in the pore.
- Setting up force balance equations on a bubble and particles with the assumption that

the sum of all forces acting on bubble and particle are balanced on a critical condition.

- Velocity change of the bubble caused by particles attached on a bubble will be calculated
- Investigating the effect of the property of porous medium such as a solid grain size
- A dimensional analysis of the phenomenon will be provided a more generalized methodology to evaluate the effect of individual forces acting on the particle-bubble unit in porous media
- Investigating the effect of the property of a colloidal particle which are hydrophilic and hydrophobic particle
- Defining roles of particles for mass transfer rate of VOC

# 2 THEORETICAL APPROACH

## 2-1 GENERAL DESCRIPTION OF AIR SPARGING

Understanding the abilities of bacteria in saturated zones is needed. Most types of organic chemicals can be degraded and utilized by bacteria as energy or carbon sources. However, remediation of large amounts of organic chemicals can be limited or out of control by indigenous bacteria because the population and activity of the bacteria in the subsurface environments depends on the depth at which they live. Generally, the microbial population decreases with increasing the depth. When natural biodegradation or attenuation is not sufficient to remove the contaminants, the capabilities of the bacteria to degrade or utilize organic chemical have to be increased by adding air or nutrients in the saturated zone.

Air sparging can remediate volatile organic compounds (VOCs) dissolved in subsurface through basic two mechanisms: one is physical stripping (volatilization) as air rises upward to the surface and aerobic biodegradation of VOCs through increased oxygen supply. Figure 2.1 shows basic VOCs removal mechanisms in the presence of an air phase in porous media. As shown in Figure 2.1, dissolved or sorbed VOCs may be volatilized or biodegraded. When air is injected into saturated zones, discrete air bubbles are formed in the pore and then moved or trapped in the porous media.  At that time, the processes of volatilization and biodegradation are occurred in porous media. Volatilization is governed by the VOC's vapor pressure and biodegradation is related to delivery of oxygen to soil microorganisms. The main mechanism of air sparging is volatilization in short term periods and that of biosparging is biodegradation in long term periods.

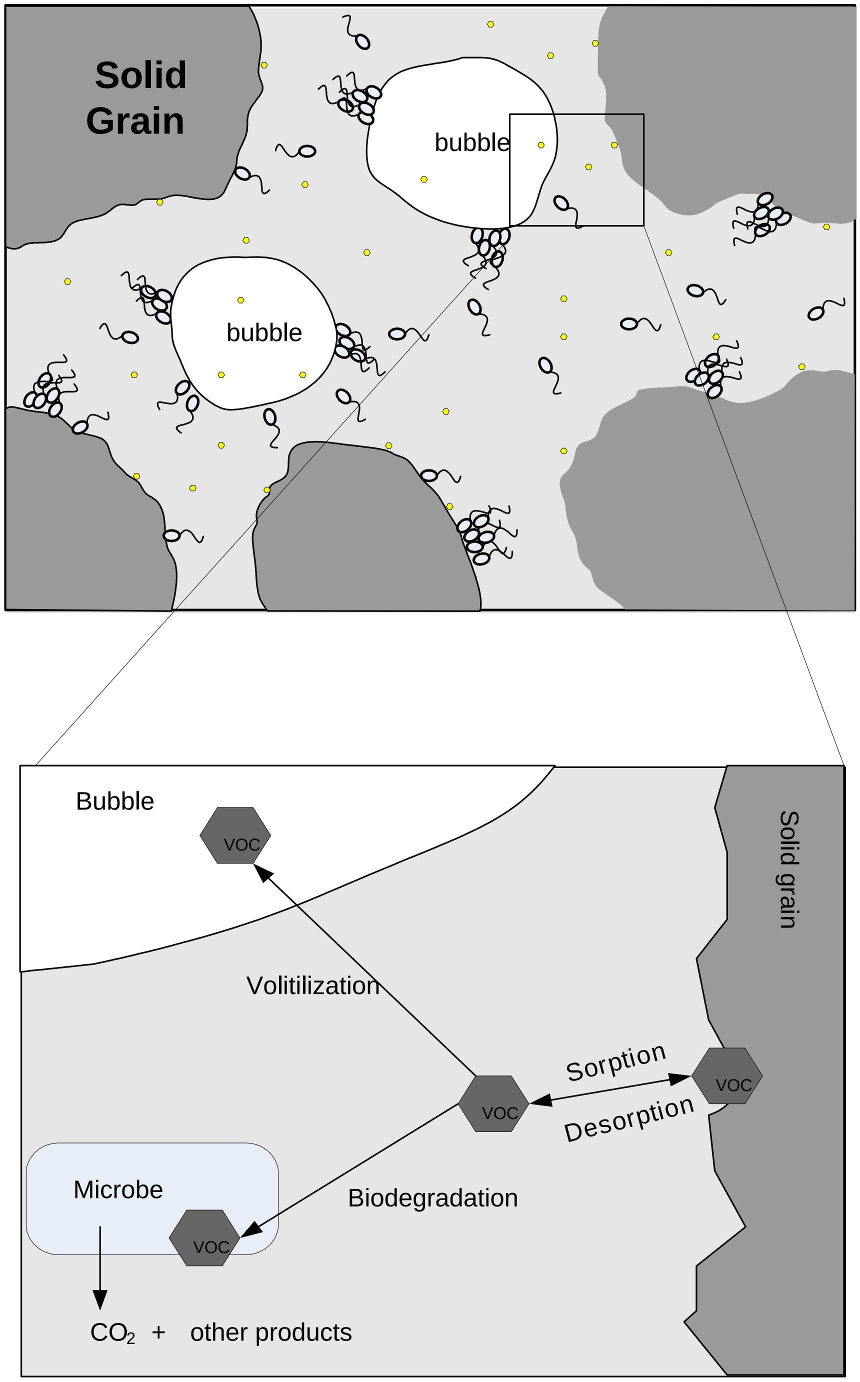


Figure 2. 1 Conceptual model for removal of VOCs dissolved in porous media

## 2-2 CAPTURE MECHANISM OF A PARTICLE ON A BUBBLE

The studies about the attachment of the particle at the air-water interface have been reported and investigated. *Wan et al*. [1994] experimented the transport of a particle in glass bead micro-models with a gas-liquid interface and noted that the retention of a colloidal particle flowing through these systems was proportional to the gas saturation because a colloidal particle preferentially sorbed to the gas-water interface. Also, they found that interfacial attractive force between a gas bubble and a particle was greater than the adhesive force between a glass wall and a particle.

Generally the basic particle's capture mechanisms are sedimentation, interception, and Brownian diffusion in porous media. According to *Weber et al.* [1983], sedimentation is caused by gravity; however, it is not an important attachment mechanism of a colloidal particle because the particles are almost buoyancy neutral. Brownian diffusion can be shown because of the particle's size. Finally, interception is the main mechanism for capturing a particle on the bubble because they have finite size. If one particle moves along a streamline of fluid, it approaches the bubble surface more closely than one particle's radius; thus it will collide with the bubble surface.

According to *Schulze* [1977], he suggested that there were the three important fundamental processes during the attachment of particles to bubbles. Figure 2.2 shows the three mechanism of the attachment of particles on a bubble. That processes are given by:

(1) "Approach of the solid particle to the liquid-gaseous interface upon formation of a thin film between the phase boundaries",

(2) "Formation of the three-phase contact"

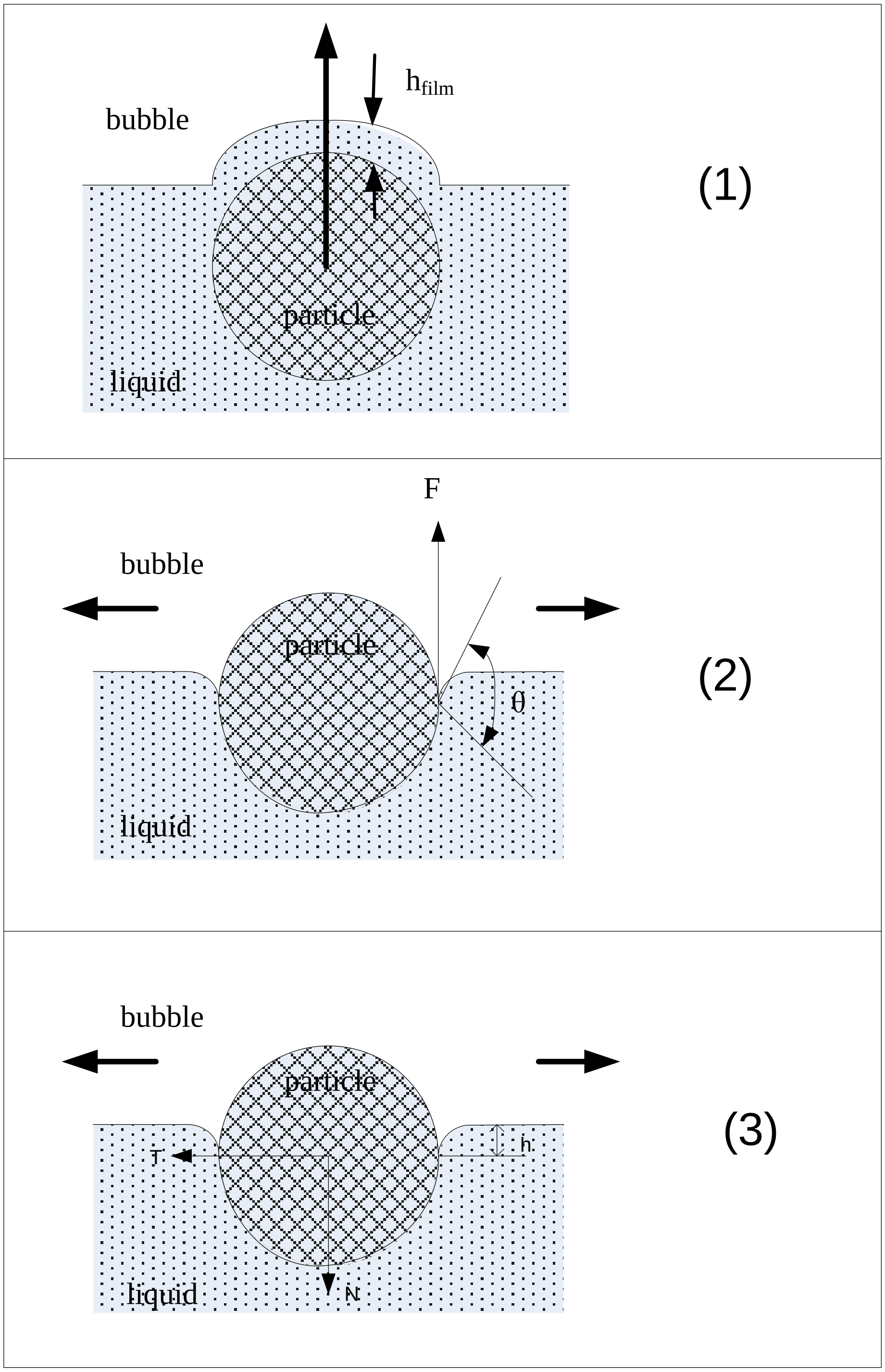


Figure 2. 2 The three important mechanisms during the attachment of particles to bubbles

(3) "Rupture of the particle out of the fluid interface".

After the attachment of the particle to bubbles is completed, we assume that this process is irreversible. One of the widely used theories about sorption of a particle on the gas-water interface is related to particle surface hydrophobicity. *Wan et al*. [1994] have suggested that:

- Hydrophobic particles can be attracted more on gas bubble than hydrophilic particles.
- Hydrophobic forces between a particle and a gas bubble increases with increasing particle surface hydrophobicity.
- Particle surface hydrophobicity is related to water-air contact angles of the cell surfaces.

*Wan et al.* [1994] have concluded that "the sorption appears to be due to the hydrophobic force: sorption at the gas-water interface increases with increasing particle hydrophobicity." *Wan and Wilson* [1994] suggested two energy stages about the sorption of particle onto the gas-water interface. "The DLVO and hydration forces control the first stage, in which the interface is ruptured, the capillary force fixes each particle at an equilibrium position on the interface in the second stage. The capillary force strongly binds particles on the gas-water interface, so they essentially cannot be desorbed from the gas-water interface". *Wan and Wilson* [1994] described that capillary attraction force became stronger "when the system was disturbed, for example, by increasing flow rate, changing flow direction, and especially by moving the bubbles."

*Goldenberg et al*. [1989] also observed that adhesion of hydrophobic colloids (clay minerals) on the surface of bubbles of air and the transport of the composite units formed by bubbles and mineral particles in a glass micro model. The mechanism of the attachment of the particle on a bubble involves a sorption process and an adhesion process. "Sorption process is that clay particles are partitioned between the bulk phase and the gas-liquid interface by movement of the particles from the liquid to the liquid-gas interface. Adhesion process is that interaction between liquid molecules, solid surfaces and gas molecules to form interfaces. The main factors governing these processes are long-range physical interactions through electrostatic or Van der Waals forces." According to *Wan and Wilson* [1994], they classified the six types of particles and their size and surface characteristics:

i. "Hydrophilic, negatively charged latex: These high surface charge density, hydrophilic latexes are manufactured from hydrophobic sulfate charge-stabilized latexes. The process consists of grafting carboxylic acid polymers to the particle surface to produce a porous, highly charged surface layer. The final functional surface groups are predominantly carboxylate with an insignificant amount of sulfate."
ii. "Hydrophobic, negatively charged latex: These microspheres are also stabilized by sulfate charges, but the surface functional groups are sulfate and hydroxylate. Their hydrophobicity is attributed to low charge density."
iii. "Positively charged, hydrophobic latex: The only surface functional group present on these particles is amidine. The surface charge density is relatively low and the particles have a hydrophobic surface."
iv. Na-montmorillonite
v. Hydrophilic bacteria
vi. Hydrophobic bacteria

Although they have performed the experiments for the colloid's transport on the gas-water interface by using these six classified colloidal particles, the results had had two categories.

## 2-3 IDEALIZATION OF PACKING SYSTEM IN THE POROUS MEDIA

In pore-scale analysis, the packing system of solid grain is very important factor for water and bubble movement in porous media. According to *Graton and Fraser* [1935], there are three types of layers which are square layer, simple rhombic layer, and special rhombic layer. These layers depend on the angle of intersection of the sets of rows in the layer. They defined that "the unit solid is an ideal sphere of radius R of solid grain", "the row is an aggregate of uniform spheres arranged with their centers along a straight line and successively spaced at the distance of 2R, so that each sphere along this line is tangent to its neighbors on either side" and "a set of rows is an assemblage of rows in parallel direction". As seen in Figure 2-3, two sets of rows intersect at $90^\circ$ is called "the square layer", three sets of rows intersect at $60^\circ$ is called "simple rhombic layer", and four sets of rows intersect at $75^\circ 31`$ is called "special rhombic layer". And then they have considered only two kinds of systematic packing which were called "loosest" and "tightest" as related with porosity and permeability. Finally, they concluded that solid grain's packing system had six cases as shown in Figure 2.4 and described below [*Graton and Fraser*, 1935]:

- Cases 1 and 4: spheres in second layer vertically over those in first layer.
- Cases 2 and 5: spheres in second layer horizontally offset with respect to those of the first layer, by a distance R along the direction of one of the sets of rows.
- Cases 3 and 6: spheres in second layer horizontally offset with respect to those of the first layer, in a direction bisecting the angle between two sets of rows and by a distance of $R\sqrt{2}$ in case 3 and $2R\sqrt{1/3}$ in case 6.

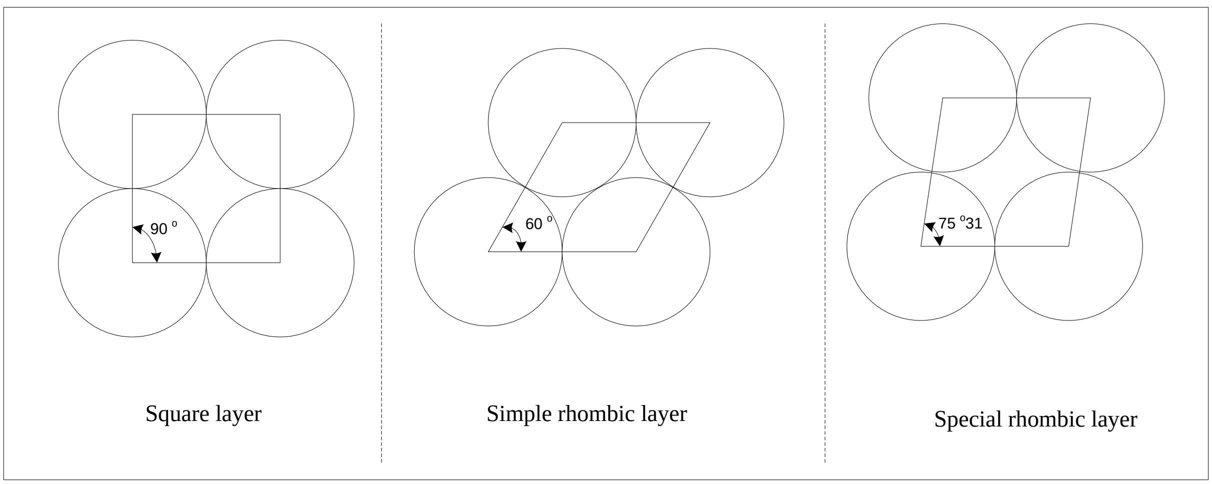


Figure 2. 3 Types of layers (From *Graton and Fraser*, 1935)

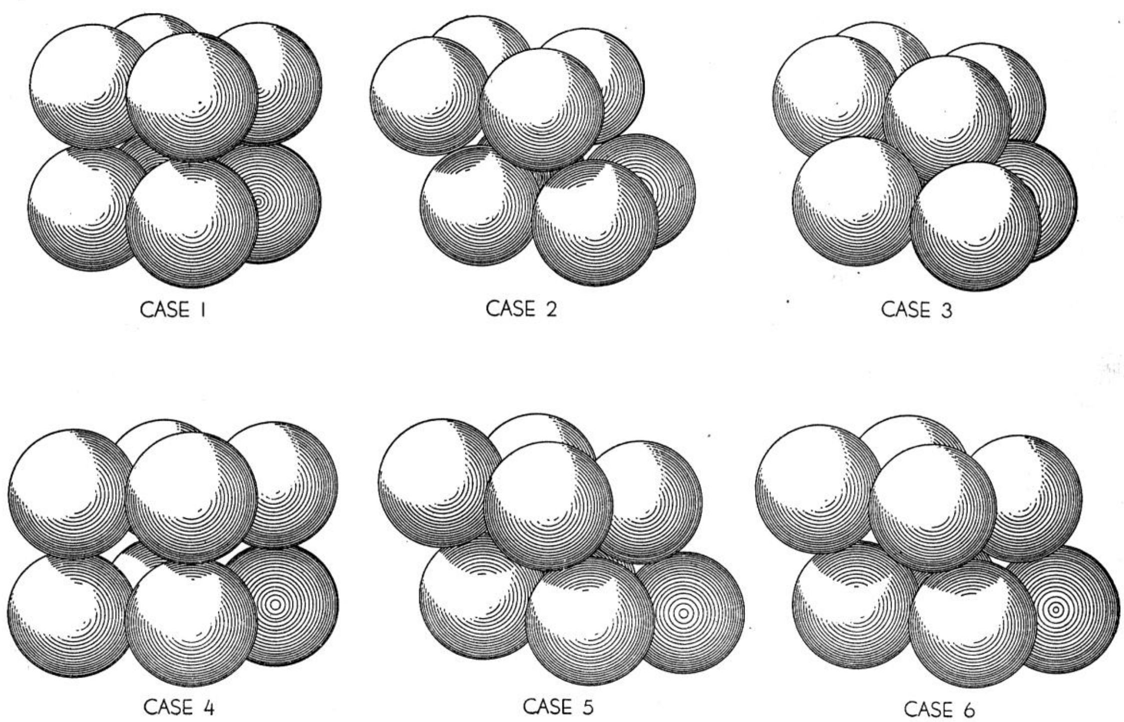


FIG. 3.—Type sphere groups of the six cases

Figure 2. 4 Type sphere groups of the six cases (From *Graton and Fraser*, 1935)

Table 2. 1 Geometrical relationships of the various packing systems

| | *Name* | *Spacing of layers* | *Tangent neighbors* | *Porosity* |
|---|---|---|---|---|
| Case 1 | Cubic | $R\sqrt{4}$ | 6 | 0.4764 |
| Case 2 | Orthorhombic | $R\sqrt{3}$ | 8 | 0.3954 |
| Case 3 | Rhombohedral | $R\sqrt{2}$ | 12 | 0.2595 |
| Case 4 | Orthorhombic | $R\sqrt{4}$ | 8 | 0.3954 |
| Case 5 | Tetragonal-Sphenoidal | $R\sqrt{3}$ | 10 | 0.3019 |
| Case 6 | Rhombohedral | $2R\sqrt{2/3}$ | 12 | 0.2595 |

Figure 2.4 is the picture of the six cases, adapted from Graton and Fraser (1935), and "represented in each instance by an assemblage of eight spheres, four in each of two layers that are stacked one on top of the other". Table 2.1 shows the geometrical relationships of the various packing system and porosity of each case. This study is assumed that packing system is followed by Case 2 which is similar to porosity of sand or gravel.

## 2-4 AIR FLOW PATTERNS IN AIR SPARGING SYSTEM

Before setting up the modeling of air bubble movement in porous media, it is necessary that flow patterns and their geometrical packing systems of soil grain are defined and identified. *Tung and Dhir* [1988] reported that flow regimes in porous media are bubbly flow, slug flow, and annular flow. Figure 2.5 shows sketches of the flow patterns in porous media. However, assumption of our modeling works is that air flow is not continuous, thus both of the bubbly flow and the slug flow are defined as bubble flow which means discrete, non-continuous air bubbles moving through the porous media.

Annular flow is same as channel flow, in which the air phase is continuous. According to *Tung and Dhir* [1988], the theoretical criteria between bubble flow and channel flow are determined by void fraction ($\alpha_0$) which is given by:

$$\alpha_0 = \frac{\pi}{3}\frac{(1-n)}{n}\gamma(1+\gamma)[6\eta-5(1+\gamma)] \qquad (2.1)$$

$$\gamma = \frac{D_b}{d_p} \qquad (2.2)$$

$$\eta = \left[ \frac{\pi\sqrt{2}}{6(1-n)} \right]^{1/3} \quad (2.3)$$

Where n is porosity, $D_b$ is the bubble diameter, and $d_p$ is the diameter of solid grain.

At a higher void fraction ($\alpha_0$) bubble flow can be changed to channel flow. In other words, $d_p$ is a key factor whether gas phase flow is going to be bubble flow or not. Many researchers have studied and reported that the type of air flow pattern was related to the size of solid grain in the air sparging system. [*Brook et al*., 1999, *Elder and Benson*, 1999, *Peterson et al*., 2001]

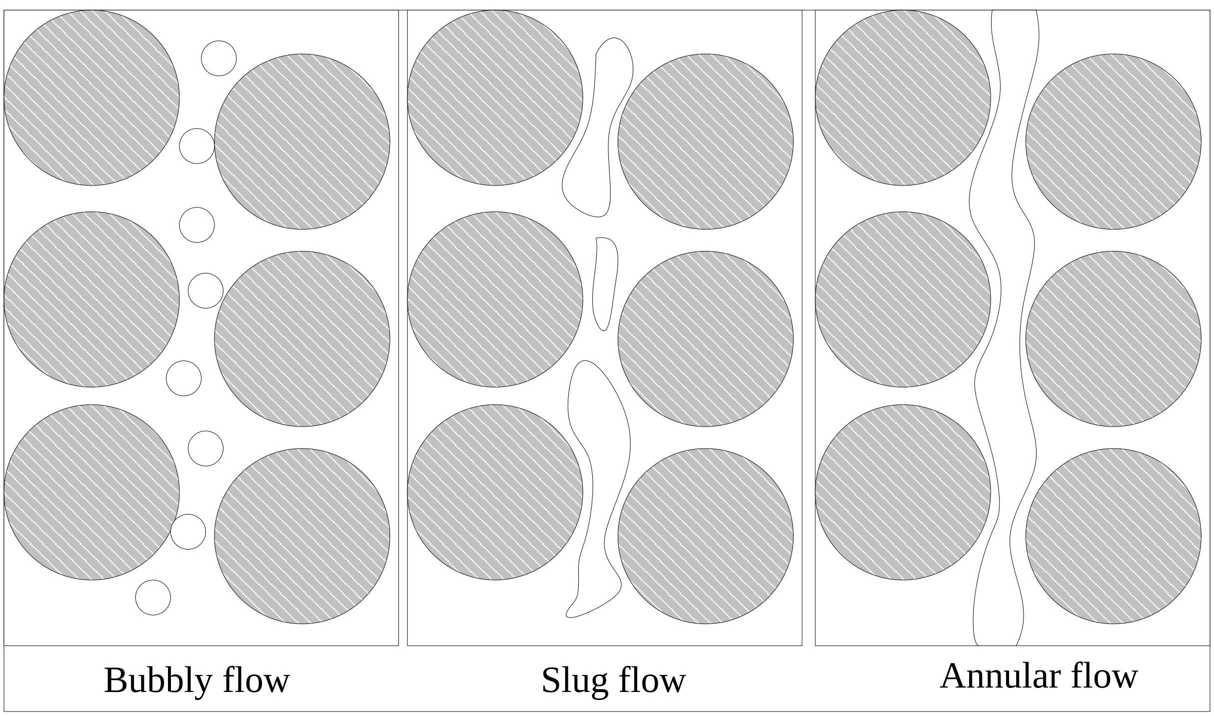


Figure 2. 5 Sketches of the flow patterns in porous media

Table 2.2 shows the relationship between air flow pattern and solid grain size in various laboratory air-sparging experiments. From these results, channel flow in porous media will generally occur equal to or less than 2 mm of grain size, and bubble flow in porous media will generally occur greater than 2 mm of grain size. Thus, $d_p$ in this modeling work is assumed to be 4 mm that means the type of air flow pattern of this study is bubble flow.

Table 2. 2 Relationship between the type of air flow and the size of porous medium

| *Reference* | *Medium* | *Grain size (mm)* | *Air flow pattern* |
|---|---|---|---|
| *Ji et al.* (1993) | Glass beads | 4 | Bubble flow |
| | Glass beads | 2 | Bubble flow and channel flow |
| | Glass beads | 0.75 | Channel flow |
| *Adams and Reddy* (1997) | Sand | 2.5 | Bubble flow |
| | Clay | 0.43 | Channel flow |
| *Brook et al.* (1999) | Glass beads | 3 | Bubble flow |
| | Glass beads | 2 | Slugs of air (bubble flow) |
| | Glass beads | 1.5 | Bubble flow and channel flow |
| | Glass beads | 1 | Channel flow |
| | Glass beads | 0.71~0.8 | Channel flow |

# 3 FORCE BALANCE EQUATION FOR THE MIGRATION OF AIR BUBBLES IN POROUS MEDIA

## 3-1 FORCE BALANCE EQUATION OF BUBBLE MOVEMENT IN POROUS MEDIA

### 3-1-1 Overview

The motion of rising air bubble through porous media is studied in order to determine the rise velocity of an air bubble in porous media. Rising air bubble interacts with the solid grains and groundwater in porous media. When bubble interacts with solid grains and groundwater in porous media, the velocity of an air bubble could be changed because of the momentum exchange between air and solid phase and between air and water phase. The momentum is defined as the product of the mass of the fluid and its velocity. Thus, the momentum balance equation is applied to determine the bubble rise velocity. This equation of momentum indicates that the sum of the external forces acting on a bubble is equal to the rate of change of momentum. This is expressed as following

$$\sum F = \frac{d}{dt}\left(mu_b\right) \tag{3.1}$$

Where ΣF is the sum of the external forces acting on a bubble, t is the time, m is the mass of a bubble, and $u_b$ is a rise velocity of bubble.

The mass of a bubble can be expressed by

$$m = \rho_g \forall_b \tag{3.2}$$

Where $\rho_g$ is a density of a gas bubble, and $\forall_b$ is a volume of the bubble. Assuming that the fluids (gas and water) are incompressible and the bubble radius is the equivalent radius of a sphere with a volume equal to that of a bubble, equation 3.1 can be expressed in the vertical x-direction by

$$\sum F = \frac{4}{3}\pi R_b^3 \rho_g \left( \frac{\partial u_b}{\partial t} + u_b \frac{\partial u_b}{\partial x} \right) \tag{3.3}$$

Where $R_b$ is bubble radius, $\frac{\partial u_b}{\partial t}$ is the local acceleration term, in which the bubble velocity changes with time at the fixed point in space, and $u_b \frac{\partial u_b}{\partial x}$ is the convective acceleration term, in which the bubble velocity changes with space during the bubble's motion through porous media.

### 3-1-2 Force balance equation of a bubble without a particle in porous media

The terminal bubble rise velocity can be obtained from equation 3.3. This study has been accomplished by *Corapcioglu et al.* [2004]. The external forces acting on a bubble in porous media result from gravitational effect which is defined by buoyancy, surface tension effect which is due to interaction between the bubble and solid grain, and drag forces. Other forces (for example, Basset history force, lift force and additional inertial force) can be existed in this system without question. However, *Corapcioglu et al.* [2004] have explained that why these forces could be neglected from this force balance equation. And the buoyant force is balanced by surface tension force and drag force. Thus, the sum of the external forces acting on a bubble are given by

$$\sum F = F_b - F_{st} - F_d \tag{3.4}$$

Where $F_b$ is buoyant force, $F_{st}$ surface tension force, and $F_d$ is drag force.

Figure 3.1 shows external forces acting on a bubble without a particle in porous media.

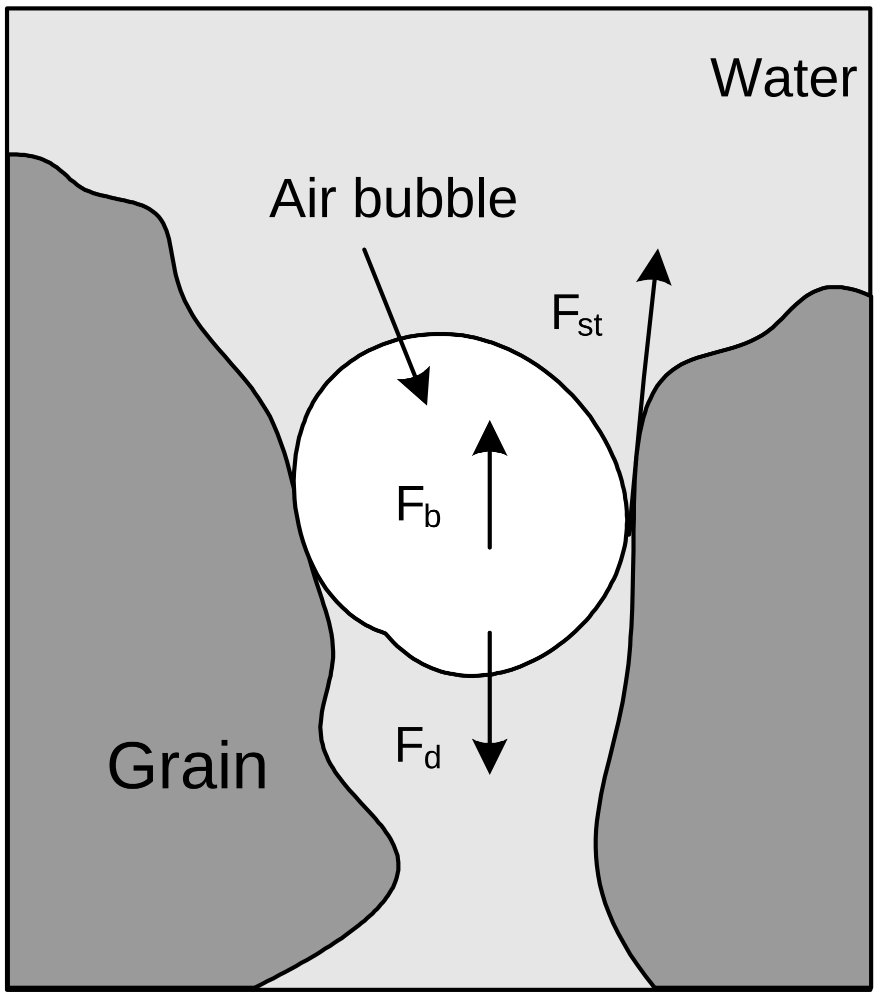


Figure 3. 1 External forces acting on a bubble without a particle in porous media

Buoyant force acts on the bubble in an upward direction because of density difference between the bubble and water. Actually, the bubble in porous media goes up because the density of bubble is smaller than that of water. Its expression is following as:

$$F_b = (\rho_f - \rho_g) g \frac{4}{3} \pi R_b^3 \tag{3.5}$$

Where $\rho_f$ is the density of water

The surface tension force is caused by "the difference between the inward attraction of the molecules inside the bubble and those at the contact surface of the bubble". $F_{st}$ in the vertical direction is given by

$$F_{st} = 2\pi R' \sigma \sin\theta \tag{3.6}$$

Where $\sigma$ is the surface tension, $\Theta$ is the contact angle assumed to be constant during the bubble movement and $R'$ is the equivalent radius of a pore throat through which a bubble can pass in a particular arrangement of grains. Assuming the equilibrium between the phases in porous media, $\Theta$ is $30°$ [*Ortiz-Arroyo et al.*, 2003]

The pore throat size ($R'$) is determined from the property of packing arrangement system in porous media. Assuming that porous medium is orthorhombic packing arrangement, "square layer arrangement is present in three planes that lie at angles of $60°$ to one another. [*Graton and Fraser*, 1935] Figure 3.2 shows the schematic diagram of a bubble in a porous medium with orthorhombic packing arrangement. Maximum radius of a bubble in pore space is presented by a circle with radius $R'$. The center of this circle lies in the center of an equilateral triangle with sides equal to the diameter of the solid grains $d_p$. From the Cosine theorem, the relationship between $R'$ and a solid grain diameter $d_p$ is given by

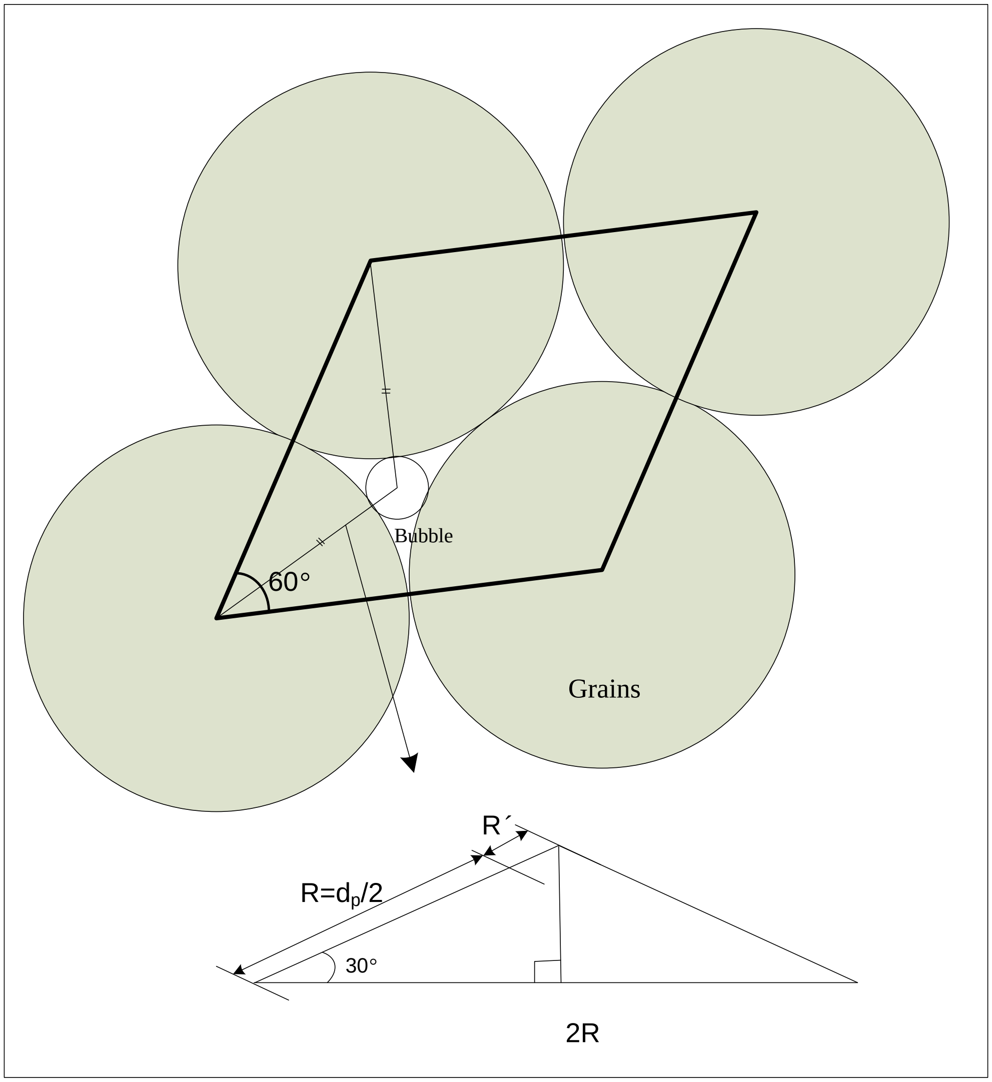


Figure 3. 2 Schematic diagram of a bubble in a porous medium with orthorhombic packing arrangement

$$\cos 30^\circ = \frac{d_p/2}{d_p/2 + R'} \quad (3.7)$$

From rearrangement of equation 3.7, $R'$ is expressed by

$$R' = \left(2\sqrt{3} - 3\right)\frac{d_p}{6} \quad (3.8)$$

In ideal packing arrangement system, the equivalent radius of a pore throat $R'$ can be obtained from a solid grain diameter $d_p$.

Drag forces for rising bubble in porous media is expressed by the momentum transfer terms. *Corpacioglu et al.* [2004] expressed drag forces using modified *Ergun* [1953] equation. According to their research, there are two terms for drag forces acting on bubble in porous media which are for laminar flow and for turbulent flow. Its equation is given by

$$F_d = \left[\frac{\mu_b u_b}{k_1} + \frac{\rho_g u_b^2}{k_2}\right]\frac{4}{3}\pi R_b^3 \quad (3.9)$$

Where $u_b$ is the velocity of bubble in porous medium, $\mu_b$ is the effective dynamic viscosity of the bubble, $k_1$ and $k_2$ are coefficients related to intrinsic permeability, the medium-specific properties, and the partial contact of the bubble with solid grain such as the shape factor, surface area, and tortuosity and so on.

Coefficients $k_1$ and $k_2$ are expressed by

$$k_1 = \frac{d_p^2}{150A}\frac{n^3}{(1-n)^2} \quad (3.10)$$

$$k_2 = \frac{d_p}{1.75A}\frac{n^3}{(1-n)} \quad (3.11)$$

Where n is the porosity, A is the correction factor. *Corapcioglu et al.* [2004] obtained A=26.8 by fitting the experimental data for a range of bubble radii (0.2~0.3 cm) , $\mu_b \approx \mu_g$ by using the expression of *Kovscek and Radke* [1994], and the porosity (n) is 0.3954 by assuming that the porous medium is an orthorhombic arrangement. The external forces acting on a rising bubble in porous media is summarized and presented in Table 3.1.

In order to determine the terminal bubble rise velocity, the force balance equation is established by substituting an each of external force equation presented in Table 3.1 into the equation (3.4), and then the expression for the force balance equation of a rising bubble in porous media is given by

$$\sum F = (\rho_f - \rho_g) g \frac{4}{3}\pi R_b^3 - 2\pi R' \sigma \sin\theta - \left[ \frac{\mu_b u_b}{k_1} + \frac{\rho_g u_b^2}{k_2} \right] \frac{4}{3}\pi R_b^3 \qquad (3.12)$$

The terminal bubble rise velocity will be calculated later in Section 4 by using this equation (3.12).

Table 3. 1 The summary of the external forces acting on a rising bubble without a particle in porous media

| External forces acting on a bubble | Equation for the external forces |
|---|---|
| Buoyant force | $F_b = (\rho_f - \rho_g) g \frac{4}{3} \pi R_b^3$ |
| Surface tension force | $F_{st} = 2\pi R' \sigma \sin\theta$ |
| Drag force | $F_d = \left[ \frac{\mu_b u_b}{k_1} + \frac{\rho_g u_b^2}{k_2} \right] \frac{4}{3} \pi R_b^3$ <br> Where $k_1 = \frac{d_p^2}{150A} \frac{n^3}{(1-n)^2}$ and <br> $k_2 = \frac{d_p}{1.75A} \frac{n^3}{(1-n)}$ |

## 3-2 FORCE BALANCE EQUATION OF THE PARTICLE-BUBBLE UNIT IN POROUS MEDIA

### 3-2-1 Overview

External forces acting on a bubble without a particle are buoyant force, surface tension force, and drag force. When a particle is attached on a bubble, three-phase contact between the bubble, particle, and liquid is formed and there are the additional forces for holding up the particle on bubble/particle aggregate which is called the particle-bubble unit. Figure 3.3 shows a sketch of the external forces acting on the particle-bubble unit. The additional forces which are buoyancy, drag force, and surface tension are related to a bubble and particle. It can be categorized for the buoyant force, drag force, surface tension of a bubble and an attached particle not a particle itself. As mentioned before, drag force equation of a bubble is used by modified Ergun equation and that of a particle is dominated by stoke's law. Buoyant force of a bubble is related to the density difference between air phase and water phase, and that of a particle is related to one between the particle and water phase. Surface tension of a bubble is applied by the capillary force between a bubble and solid grain, and that of a particle is interaction between a bubble and a particle. Any other existing possible forces can be neglected. According to *Corapcioglu et al.*[2004], basset history force and lift force is assumed to be neglected because of various reasons which are high bubble velocities and irrotational flow condition. These assumptions are applied in our study. Each of forces which are buoyant force, drag force, and surface tension can be determined by functional relations obtained through theoretical consideration.

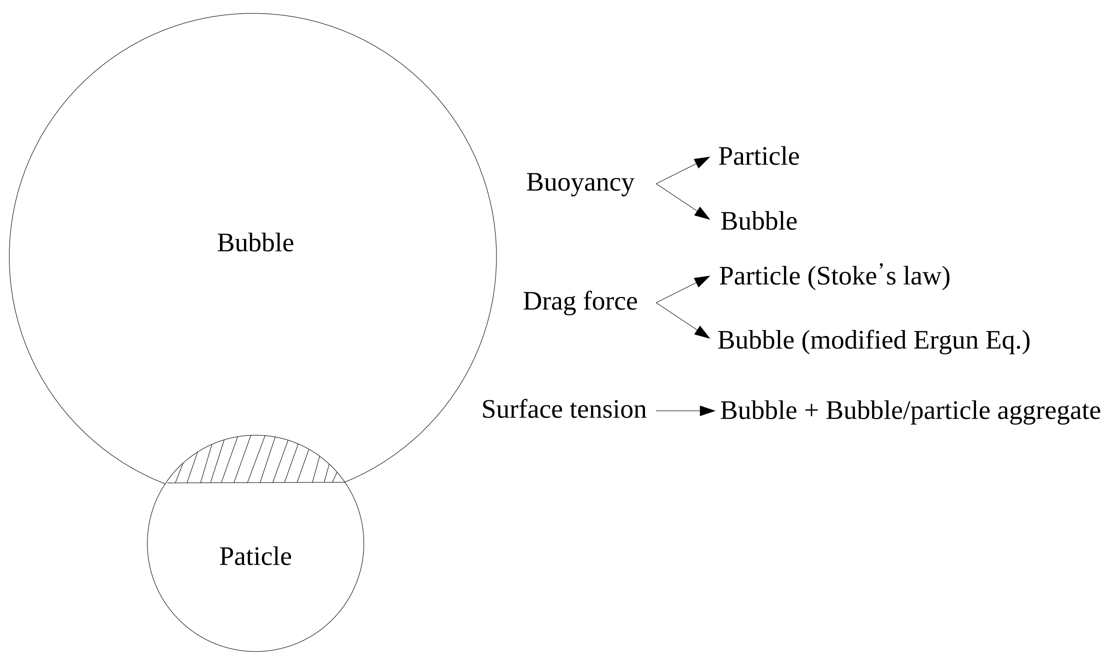


Figure 3. 3 Sketch of the external forces acting on the particle-bubble unit

Figure 3.4 shows three-phase contact between bubble, particle, and liquid. Interaction forces between a bubble and a particle include many forces acting between a bubble and an attached particle. They are usually classified into six categories which are gravitational force, buoyant force, hydrostatic pressure force, capillary force, capillary pressure force, and drag force [*Bloom and Heindel*, 1997]. These forces are expressed by the following equations.

The gravitational force which acts on a particle

$$F_g^p = \frac{4}{3}\pi R_p^3 \rho_p g \tag{3.13}$$

Where $R_p$ is a particle radius assumed that particle is spherical shape, $\rho_p$ is the density of particle

The buoyant force acting on the immersed portion of a particle

$$F_b^p = \frac{\pi}{3} R_p^3 \rho_f g \left[ \left(1-\cos\omega\right)^2 (2+\cos\omega) \right] \tag{3.14}$$

Area of the immersed portion of a particle is solved at Appendix A.

The hydrostatic pressure exerted by a liquid of height $Z_0$ above a contact area of radius $r_p = R_p \sin\omega \left(\sin\omega = \sin\psi\right)$

$$F_{hyd}^p = \pi r_p^2 \rho_f g Z_0 = \pi R_p^2 (\sin^2\omega) \rho_f g Z_0 \tag{3.15}$$

The capillary force exerted on the three-phase contact in the z-direction, Θ′ being contact angle, and $\gamma = \theta' - \psi, \sin(\theta' - \psi) = -\sin(\omega + \theta')$

$$F_{ca}^p = 2\pi r_p \sigma \sin\gamma = -2\pi R_p \sigma \sin\omega \sin(\omega + \theta') \tag{3.16}$$

The force generated by the capillary pressure in the gas bubble which acts on the contact area of the attached particle

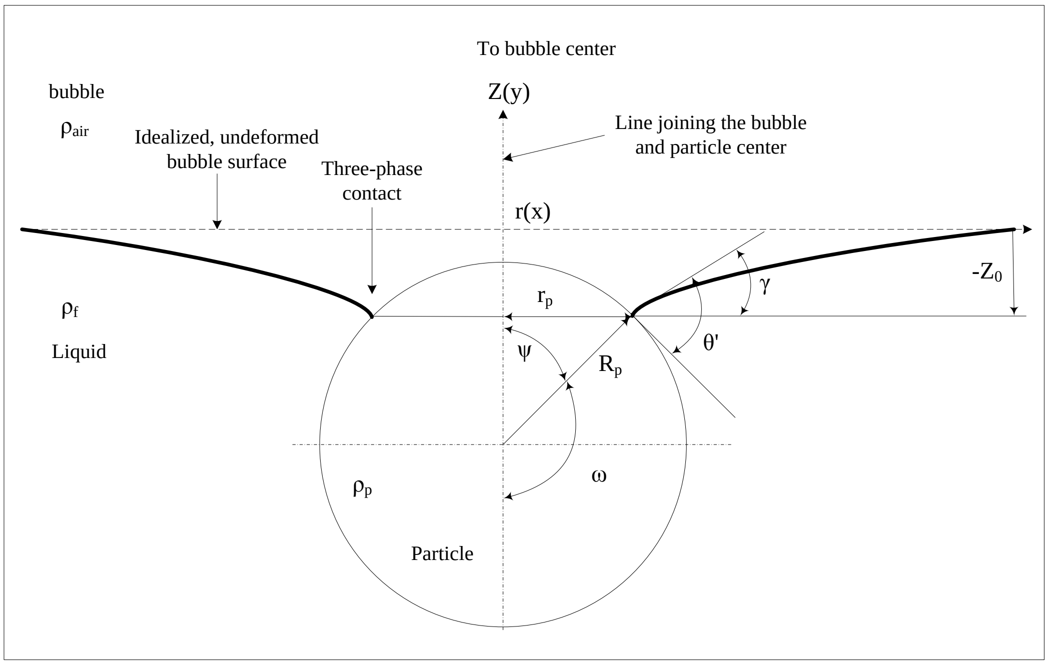


Figure 3. 4 Three-phase contact between bubble, particle, and liquid (modified by *Bloom and Heindel* [1997])

$$F_{\sigma}^{p} = \pi r_p^3 P_{\sigma} \approx \pi R_p^2 \sin^2 \omega \left( \frac{2\sigma}{R_b} - 2R_b \rho_f g \right) \quad (3.17)$$

The darg force acting on a attached particle

$$F_d^p = 6\pi \mu_w R_p u_{bp} \quad (3.18)$$

Where $u_{bp}$ is the velocity of the particle-bubble unit in porous media and $\mu_w$ is the dynamic viscosity of water.

These six forces are explained by the interaction between a bubble and an attached particle. However, the assumption of our study is that the particle attachment is irreversible. When a particle attached on a bubble, the detachment process can not be occurred. Thus, we can neglect any forces which are related to the detachment mechanism. These forces will be discussed later in next paragraph.

**3-2-2 Force balance equation of the particle-bubble unit in porous media**

Figure 3.5 shows schematic diagram of external forces acting on a particle-bubble unit. From this diagram, there are three major forces acting on a particle-bubble unit which are buoyancy, surface tension, and drag force. Hydrostatic pressure force and capillary pressure force is generated by the difference between the excess pressure in the bubble and the hydrostatic force. In this study, we assume that sorption process between a bubble and a particle is irreversible and there is no detachment on a particle-bubble unit. Thus, it can be assumed that hydrostatic pressure force and capillary pressure force can be neglected on the particle-bubble unit.

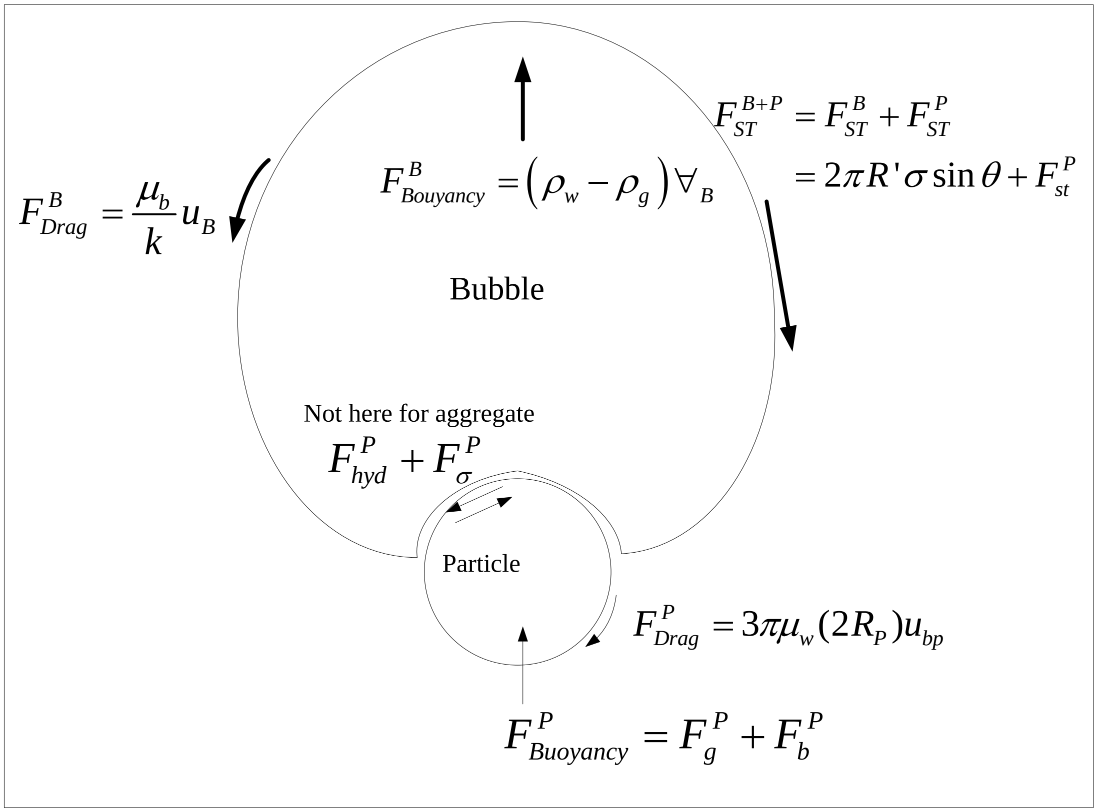


Figure 3. 5 Schematic diagram of external forces acting on a particle-bubble unit

Buoyant force acting on the particle-bubble unit is more complex than that of a bubble in porous media. When a particle is attached on the bubble, bubble shape is not circle. It is meniscus shape of bubble. Thus, buoyant force of the particle-bubble unit is that the buoyant force of bubble adds up the buoyant force of particle. It is expressed by

$$F_b^{B+P} = \rho_f g \frac{4}{3}\pi R_b^3 + \rho_f g \frac{\pi}{3} R_p^3 \left[ \left(1-\cos\omega\right)^2 (2+\cos\omega) \right] \tag{3.19}$$

Gravitational force acting on the particle-bubble unit takes into account the shape of a bubble and a particle. The expression for the gravitational force acting on the particle-bubble unit, $F_g^{B+P}$ is given by

$$\begin{aligned} F_g^{B+P} &= \rho_g g \frac{4}{3}\pi R_b^3 \\ &\quad +(\rho_p - \rho_g) g \frac{4}{3}\pi R_p^3 + \rho_g g \frac{\pi}{3} R_p^3 \left[ \left(1-\cos\omega\right)^2 (2+\cos\omega) \right] \end{aligned} \tag{3.20}$$

Since surface tension acting on the bubble is reduced by surface tension acting on the particle, Surface tension force acting on the particle-bubble unit is carefully considered. It is given by

$$F_{st}^{B+P} = 2\pi R'\sigma \sin\theta - 2\pi R_p \sigma \sin\omega \sin(\omega + \theta') \tag{3.21}$$

The drag force acting on a attached particle is just added into the drag force acting on the bubble. It means that the drag force acting on the particle-bubble unit is equation 3.9 plus equation 3.18. Its expression is given by

$$F_d^{B+P} = \left( \frac{\mu_b u_{bp}}{k_1} + \frac{\rho_g u_{bp}^2}{k_2} \right) \frac{4}{3}\pi R_b^3 + 6\pi\mu_w R_p u_{bp} \tag{3.22}$$

The summary of the external forces acting on the particle-bubble unit in porous media is presented in Table 3.2.

Table 3. 2 The summary of the external forces acting on the particle-bubble unit in porous media

| External forces acting on the particle-bubble unit in porous media | Equation for the external forces acting on the particle-bubble unit in porous media |
|---|---|
| Buoyant force | $F_b^{B+P} = \rho_f g \frac{4}{3}\pi R_b^3 + \rho_f g \frac{\pi}{3} R_p^3 \left[ (1-\cos\omega)^2 (2+\cos\omega) \right]$ |
| Gravitational force | $F_g^{B+P} = \rho_g g \frac{4}{3}\pi R_b^3 + (\rho_p - \rho_g) g \frac{4}{3}\pi R_p^3 + \rho_g g \frac{\pi}{3} R_p^3 \left[ (1-\cos\omega)^2 (2+\cos\omega) \right]$ |
| Surface tension force | $F_{st}^{B+P} = 2\pi R'\sigma \sin\theta - 2\pi R_p \sigma \sin\omega \sin(\omega + \theta')$ |
| Drag force | $F_d^{B+P} = \left( \frac{\mu_b u_{bp}}{k_1} + \frac{\rho_g u_{bp}^2}{k_2} \right) \frac{4}{3}\pi R_b^3 + 6\pi\mu_w R_p u_{bp}$<br>Where $k_1 = \frac{d_p^2}{150A} \frac{n^3}{(1-n)^2}$ and $k_2 = \frac{d_p}{1.75A} \frac{n^3}{(1-n)}$ |

The buoyant force is balanced by gravitational force, surface tension, and drag force. Thus, the sum of the external forces acting on the particle-bubble unit are given by

$$\sum F^{B+P} = F_b^{B+P} - F_g^{B+P} - F_{st}^{B+P} - F_d^{B+P} \tag{3.23}$$

Where $F_b^{B+P}$ is buoyant force, $F_g^{B+P}$ is gravitational force, $F_{st}^{B+P}$ is surface tension force, and $F_d^{B+P}$ is drag force.

As described before, in order to determine the steady-state velocity of the particle-bubble unit in porous media, the force balance equation is applied by substituting a each equation of external force acting on the particle-bubble unit presented in Table 3.2 into the equation 3.23, then the expression for the force balance equation of a rising particle-bubble unit in porous media is given by

$$\begin{aligned} \sum F^{B+P} = & \left(\rho_f - \rho_g\right) g \frac{4}{3}\pi R_b^3 + \left(\rho_f - \rho_g\right) g \frac{\pi}{3} R_p^3 \left[\left(1-\cos\omega\right)^2 (2+\cos\omega)\right] \\ & -(\rho_p - \rho_g) g \frac{4}{3}\pi R_p^3 \\ & -\left(2\pi R'\sigma \sin\theta - 2\pi R_p \sigma \sin\omega \sin(\omega+\theta')\right) \\ & -\left(\left(\frac{\mu_b u_{bp}}{k_1} + \frac{\rho_g u_{bp}^2}{k_2}\right)\frac{4}{3}\pi R_b^3 + 6\pi\mu_w R_p u_{bp}\right) \end{aligned} \tag{3.24}$$

The terminal velocity of the particle-bubble unit in porous media will be calculated later in Section 4 by using this equation (3.24).

# 4 TERMINAL VELOCITY OF A BUBBLE ATTACHMENT OF PARTICLES

## 4-1 TERMINAL VELOCITY OF BUBBLE IN LIQUID AND IN POROUS MEDIA

### 4-1-1 Terminal velocity equation for a bubble without a particle

The bubble rising velocity in liquid has been studied by many researcher. [*Peebles and Garber* [1953], *Mendelson* [1967], and *Haberman and Morton* [1953]] They are determined from the force balance equation for the bubble rising velocity in liquid. There are two external forces acting on a bubble in liquid which are the buoyant force and drag force due to interaction between the bubble and water.

In liquid, the buoyant force acting on a bubble is same as equation 3.5 and given by

$$F_b^W = (\rho_f - \rho_g) g \frac{4}{3} \pi R_b^3 \qquad (3.5)$$

Drag force acting on a bubble in liquid is expressed by

$$F_d^W = \frac{1}{2} C_D \rho_f \pi R_b^2 u_{bw}^2 \qquad (4.1)$$

Where $u_{bw}$ is the velocity of bubble in liquid and $C_D$ is a drag coefficient in liquid.

The sum of two external force acting on a bubble in liquid is given by

$$\sum F^W = (\rho_f - \rho_g) g \frac{4}{3} \pi R_b^3 - \frac{1}{2} C_D \rho_f \pi R_b^2 u_{bw}^2 \qquad (4.2)$$

In steady state, the bubble rise velocity does not explicitly change with time. This is expressed by

$$\sum F^W = 0 \qquad (4.3)$$

Substituting equation 4.3 into equation 4.2, we obtain

$$(\rho_f - \rho_g) g \frac{4}{3}\pi R_b^3 - \frac{1}{2} C_D \rho_f \pi R_b^2 u_{bw}^2 = 0 \tag{4.4}$$

Rearranging equation 4.4 for obtaining terminal velocity of bubble, its expression is given by

$$u_{bw} = \sqrt{\frac{8(\rho_f - \rho_g) g}{3\rho_f C_D} R_b} \tag{4.5}$$

In porous media, the sum of external force acting on a bubble is expressed in Section 3 by

$$\sum F = (\rho_f - \rho_g) g \frac{4}{3}\pi R_b^3 - 2\pi R'\sigma \sin\theta - \left[\frac{\mu_b u_b}{k_1} + \frac{\rho_g u_b^2}{k_2}\right]\frac{4}{3}\pi R_b^3 \tag{3.12}$$

In steady state, the sum of external force acting on a bubble in porous media is zero as same as equation 4.4 and is given by

$$(\rho_f - \rho_g) g \frac{4}{3}\pi R_b^3 - 2\pi R'\sigma \sin\theta - \left[\frac{\mu_b u_b}{k_1} + \frac{\rho_g u_b^2}{k_2}\right]\frac{4}{3}\pi R_b^3 = 0 \tag{4.6}$$

Equation 4.6 has two unknown variables which are the bubble velocity and radius. The other variables such as liquid properties which are density, viscosity, and surface tension of water, gas properties which are density and viscosity of gas in a bubble, and porous medium properties which are porosity and radius of pore throat, are known constants. Thus, equation 4.6 can be rearranged to lump the terms with the same exponent of $u_b$. This is expressed by

$$u_b^2\left(\frac{4\rho_g \pi R_b^3}{3k_2}\right) + u_b\left(\frac{4\mu_b \pi R_b^3}{3k_1}\right) + 2\pi R'\sigma \sin\theta - \frac{4}{3}\left(\rho_f - \rho_g\right) g \pi R_b^3 = 0 \tag{4.7}$$

From this equation, we know that terminal bubble rise velocity is a function of bubble radius and it can be expressed by

$$C_1 u_b^2 + C_2 u_b + C_3 = 0 \quad (4.8)$$

Where constant coefficients of $C_1$, $C_2$, and $C_3$ are given by

$$C_1 = \frac{4\rho_g \pi R_b^3}{3k_2} \quad (4.9)$$

$$C_2 = \frac{4\mu_b \pi R_b^3}{3k_1} \quad (4.10)$$

$$C_3 = 2\pi R'\sigma \sin\theta - \frac{4}{3}\left(\rho_f - \rho_g\right) g\pi R_b^3 \quad (4.11)$$

As mentioned before, coefficient $k_1$, and $k_2$ is dependent on the porous medium properties such as permeability, shape factor, and tortuosity. Its expression is given by

$$k_1 = \frac{d_p^2}{150A}\frac{n^3}{(1-n)^2} \quad (3.10)$$

$$k_2 = \frac{d_p}{1.75A}\frac{n^3}{(1-n)} \quad (3.11)$$

Typically, equation 4.8 has two solutions which are given by

$$u_b = \frac{-C_2 + \sqrt{C_2^2 - 4C_1C_3}}{2C_1} \quad (4.12)$$

$$u_b = \frac{-C_2 - \sqrt{C_2^2 - 4C_1C_3}}{2C_1} \quad (4.13)$$

The second solution expressed by equation 4.13 will be neglected since bubble rise velocity cannot be negative. Thus, equation 4.12 is used by model parameters given in Table 4.1 and represents the bubble rise velocity in a steady state as a function of bubble radius. The solution of a steady state bubble rise velocity is given by

$$u_b = \sqrt{\left(\frac{\mu_b k_2}{2k_1\rho_g}\right)^2 - \frac{3\sigma\sin\theta k_2}{2\rho_g}\frac{R'}{R_b^3} + \left(\rho_f - \rho_g\right)\frac{k_2}{\rho_g}g} - \frac{\mu_b}{2\rho_g k_1}k_2 \qquad (4.14)$$

Figure 4.1 shows the terminal bubble rise velocity in liquid and in porous media. This figure includes data obtained by *Haberman and Morton* [1953] and *Corapcioglu et al.* [2004] and simulation calculated by equation 4.14.

As seen in Figure 4.1, the terminal velocity of bubble in porous medium is about 5 cm/s slower than in liquid. The reason is that "A bubble rising through the porous medium is confined to traveling through the available pore space and hence is subjected to a boundary effect from the solid particles." [*Corapcioglu et al.* [2004]]

From figure 4.1, it can be concluded that

- The bubble with a larger radius has a higher velocity
- The terminal velocity of bubble in liquid is much higher than that of bubble in porous medium because there is no surface tension effect in liquid.
- There is a good agreement between experimental data and simulation value calculated by equation 4.14.

Less than 0.2 mm radius of bubble in porous media cannot be observed by experiment of *Corapcioglu et al*. [2004] in which they suggested that "bubbles with diameters approximately 1.5 to 2 times the grain diameter are more frequently observed than other-sized bubbles." However, we can predict and simulate the terminal velocity of bubble with radii $< 0.2$ mm in porous medium by using equation 4.14. The solution of bubble's terminal velocity in porous media shows that the bubble rise velocity depends on the bubble size. It is higher when the bubble radius is larger.

Table 4. 1 Model parameters

| Parameters | Units | Values |
|---|---|---|
| $\rho_g$ | g/cm$^3$ | 0.00123 |
| $\rho_f$ | g/cm$^3$ | 0.9973 |
| $\mu_b$ | g/cm·s | 0.00018 |
| $\mu_f$ | g/cm·s | 0.01 |
| $\sigma$ | g/s$^2$ | 72 |
| g | cm/s$^2$ | 981 |
| n | | 0.3954 |
| $d_p$ | cm | 0.4 |

Data from *Corapcioglu et al*. [2004]

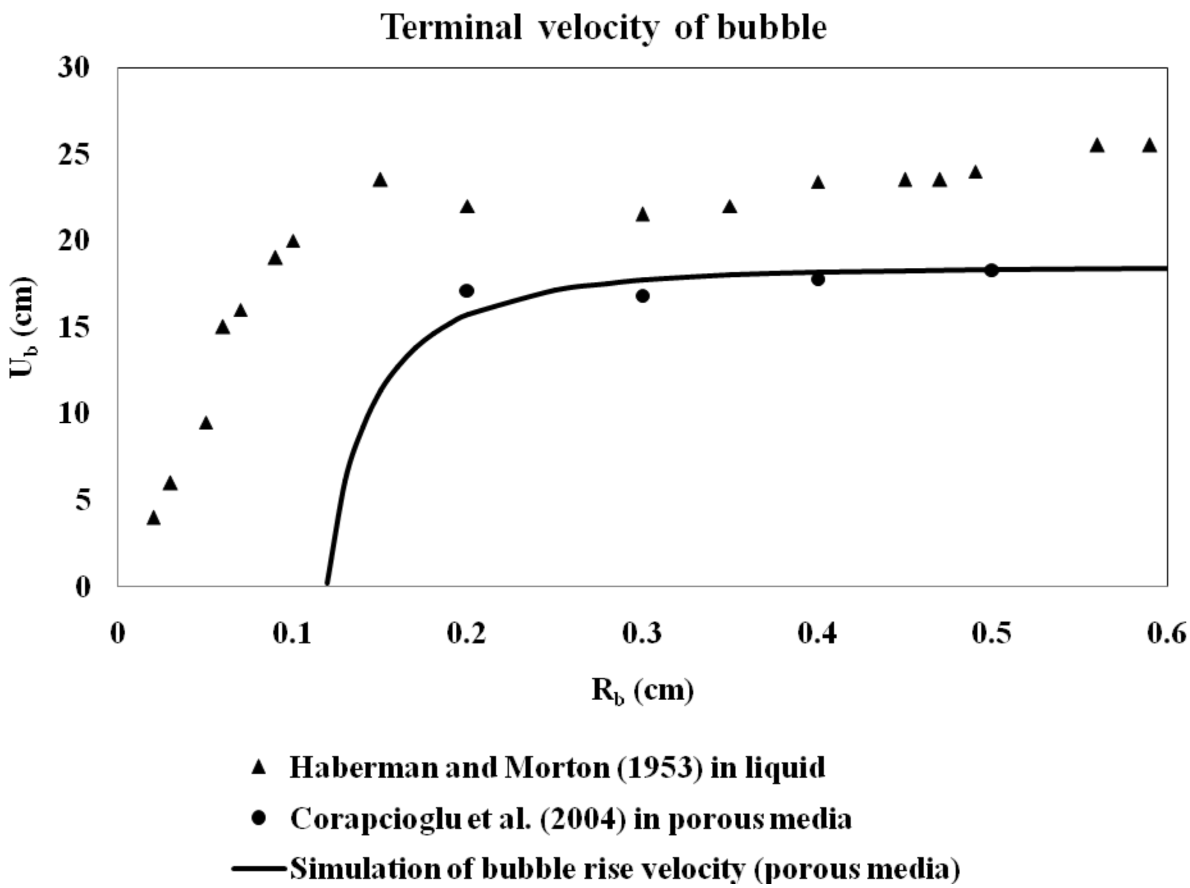


Figure 4. 1 Terminal velocity of bubble in liquid and in porous media

**4-1-2 The effect of grain size ($d_p$) for the movement of a bubble without a particle**

We can calculate from equation 4.14 that the steady state bubble rise velocity in porous media cannot exceed 18.5 cm/s. In simulation of our study, starting point of bubble size is 0.119 cm because a single bubble might become stuck in an idealized homogeneous medium due to the pore throat size. Thus, solid grain size ($d_p$) and pore throat size (R') is sensitive and critical factor for movement of bubble in porous media. As mentioned before in section 2, simulation of bubble movement without attached particle in porous media is assumed that the diameter of solid grain ($d_p$) is 0.4 cm for bubble flow. If the diameter of solid grain is changed, the value of R', $k_1$, and $k_2$ should be changed and then bubble rise velocity also should be changed. Based on equation 3.8 and 3.10~11, we can calculate the value of $d_p$, R', $k_1$, and $k_2$. Solid grain size ($d_p$) is decreased with decreasing pore throat size, coefficient $k_1$ and $k_2$, and with decreasing the terminal velocity of bubble.

Table 4.2 indicates the value of $d_p$, R', $k_1$, and $k_2$, and figure 4.2 shows relationship between the terminal velocity of bubble ($u_b$) and solid grain size ($d_p$). As seen in figure 4.2, the terminal velocity of bubble in porous media is decreased with decreasing the diameter of solid grain. When solid grain size ($d_p$) is 0.6 cm, the terminal rise velocity of a single bubble in porous media cannot exceed 26.5 cm/s and starting point of bubble radius ($R_b$) is 0.136 cm. And the terminal rise velocity of bubble in porous medium with $d_p$ = 0.4 cm cannot exceed 18.5 cm/s and starting point of bubble radius ($R_b$) is 0.119 cm. *Levich* [1962] has reported that the rise velocity of a single bubble in a stationary water phase cannot exceed 30 cm/s.

Table 4. 2 The value of solid grain size ($d_p$), pore throat size (R'), and coefficient of $k_1$, and $k_2$

| $d_p$ (cm) | R' (cm) | $k_1$ ($cm^2$) | $k_2$ (cm) |
|---|---|---|---|
| 0.6 | 0.0464102 | 1.5144 $x10^{-5}$ | 1.308 $x10^{-3}$ |
| 0.5 | 0.0386751 | 1.0517 $x10^{-5}$ | 1.09 $x10^{-3}$ |
| 0.4 | 0.0309401 | 6.7308 $x10^{-6}$ | 8.72 $x10^{-4}$ |
| 0.3 | 0.0232051 | 3.7861 $x10^{-6}$ | 6.54 $x10^{-4}$ |
| 0.2 | 0.0154701 | 1.6827 $x10^{-6}$ | 4.36 $x10^{-4}$ |

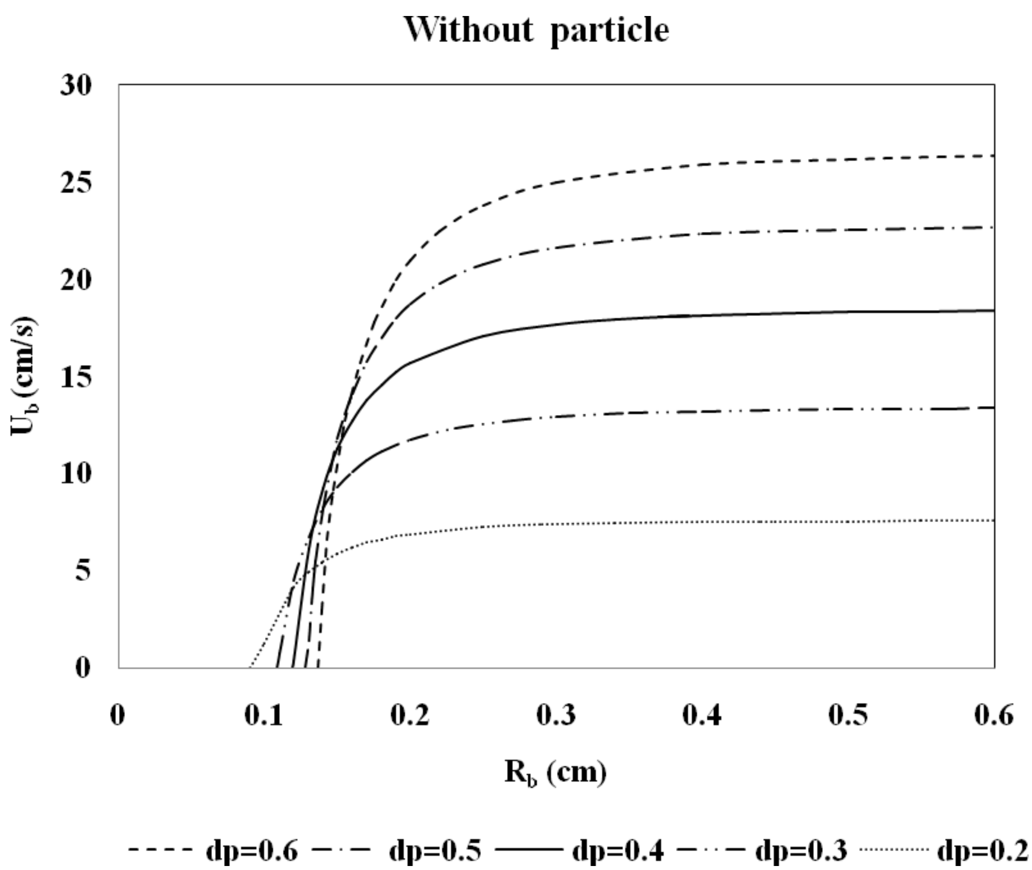


Figure 4. 2 Relationship between terminal velocity ($U_b$) and solid grain size ($d_p$)

The maximum terminal rise velocity of bubble in porous media with $d_p$ = 0.6 cm is lower than that of bubble in a water phase and higher than that of bubble in porous media with $d_p$=0.4 cm. Table 4.3 shows that Summary of the maximum terminal rise velocity of bubble and the starting point of bubble radius ($R_b$).

Difference between the terminal velocity of bubble in water phase and in porous media is caused by the surface tension effect and difference between the terminal velocity of bubble in porous media with $d_p$=0.6 cm and with $d_p$=0.4 cm is caused by effect of the pore throat size. Effect of pore throat size has been studied by *Corapcioglu et al.* [2004]. When the surface tension force is equal to the buoyant force, the bubble can be trapped in pore. Its expression is given by

$$F_b = F_{st} \tag{4.15}$$

$$F_b = (\rho_f - \rho_g) g \frac{4}{3} \pi R_b^3 \tag{3.5}$$

$$F_{st} = 2\pi R' \sigma \sin\theta \tag{3.6}$$

Substituting equation 3.5~6 to equation 4.15, it can be expressed by

$$(\rho_f - \rho_g) g \frac{4}{3} \pi R_{b\_T}^3 = 2\pi R' \sigma \sin\theta \tag{4.16}$$

Rearranging equation 4.16, it is given by

$$R_{b\_T} = \sqrt[3]{\frac{3R' \sigma \sin\theta}{2(\rho_f - \rho_g) g}} \tag{4.17}$$

Where $R_{b\_T}$ is a trapped bubble radius in porous media, R' is the limiting pore throat radius. Trapped bubble radius in porous media can be expressed by the function of the limiting pore throat radius. Figure 4.3 shows that the relationship between trapped bubble radius and the limiting pore throat radius. If bubble move through the porous medium, starting point of bubble radius should exceed this trapped bubble radius. In other words, the maximum trapped bubble radius is almost equal to minimum starting point of bubble radius. Thus, solid grain size ($d_p$) decrease with decreasing the starting point of bubble radius in Table 4.3. And the terminal velocity of bubble in porous media is decreased with decreasing the diameter of solid grain. The reason may be that bubble is hard to pass through smaller pore throat and need more driving force such as buoyant force in porous media.

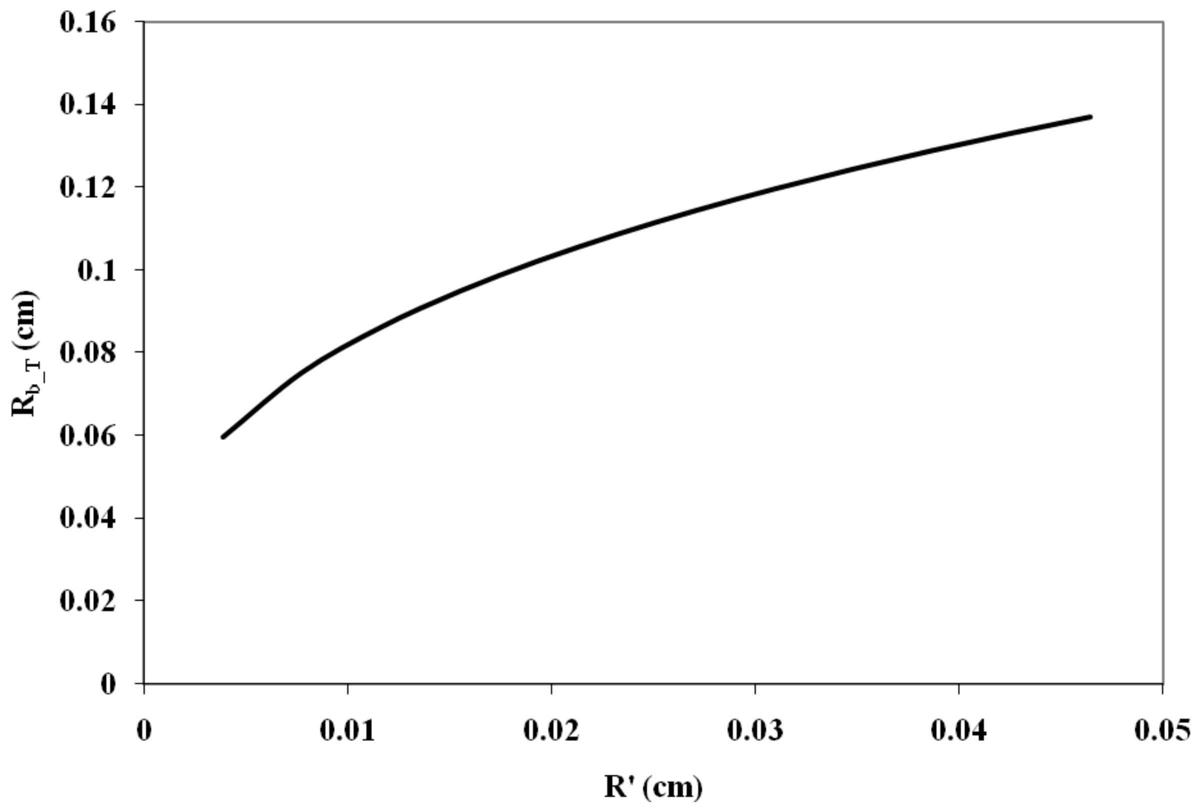


Figure 4. 3 Relationship between trapped bubble radius and the limiting pore throat radius

Table 4. 3 Summary of the maximum terminal rise velocity of bubble and the starting point of bubble radius (cm)

| *Solid grain size (cm)* | *The maximum terminal rise velocity of bubble in porous media (cm/s)* | *The starting point of bubble radius (cm)* |
|---|---|---|
| 0.6 | 26.5 | 0.136 |
| 0.5 | 22.7 | 0.128 |
| 0.4 | 18.5 | 0.119 |
| 0.3 | 13.4 | 0.108 |
| 0.2 | 7.6 | 0.09 |

## 4-2 TERMINAL VELOCITY OF THE PARTICLE-BUBBLE UNIT IN POROUS MEDIA

### 4-2-1 Terminal velocity equation for the particle-bubble unit

When the particle is attached on the bubble in porous medium, force balance equation for movement of the particle-bubble unit has some different formation other than that for movement of a bubble only in porous media.

As describe in Section 3, the sum of external force acting on bubble in porous media is expressed by

$$\sum F = (\rho_f - \rho_g) g \frac{4}{3}\pi R_b^3 - 2\pi R'\sigma \sin\theta - \left[\frac{\mu_b u_b}{k_1} + \frac{\rho_g u_b^2}{k_2}\right]\frac{4}{3}\pi R_b^3 \qquad (3.12)$$

However, when a particle is attached on a bubble in porous media, additional force acting on the particle-bubble in porous medium is considered, and then its expression is given by equation 3.24 such as

$$\begin{aligned}\sum F^{B+P} =& \left(\rho_f - \rho_g\right) g \frac{4}{3}\pi R_b^3 + \left(\rho_f - \rho_g\right) g \frac{\pi}{3} R_p^3 \left[\left(1-\cos\omega\right)^2 (2+\cos\omega)\right] \\ & -(\rho_p - \rho_g) g \frac{4}{3}\pi R_p^3 \\ & -\left(2\pi R'\sigma \sin\theta - 2\pi R_P \sigma \sin\omega \sin(\omega + \theta')\right) \\ & -\left(\left(\frac{\mu_b u_{bp}}{k_1} + \frac{\rho_g u_{bp}^2}{k_2}\right)\frac{4}{3}\pi R_b^3 + 6\pi\mu_w R_p u_{bp}\right)\end{aligned} \qquad (3.24)$$

This equation can be applied by just in case of one single particle. However, attached particle is not one single particle, it can be one hundred or the more particle. Summation of particles can be inserted into the term of force acting on particle. Thus, equation 3.24 can be expressed by

$$\sum F^{B+P} = \left(\rho_f - \rho_g\right) g \frac{4}{3}\pi R_b^3 + \sum_{i=1}^{n}\left(\rho_f - \rho_g\right) g \frac{\pi}{3} R_{pi}^3 \left[\left(1-\cos\omega\right)^2 (2+\cos\omega)\right]$$
$$-(\rho_p - \rho_g) g \sum_{i=1}^{n} \frac{4}{3}\pi R_{pi}^3$$
$$-\left(2\pi R'\sigma \sin\theta - \sum_{i=1}^{n} 2\pi R_{Pi}\sigma \sin\omega \sin(\omega+\theta')\right) \tag{4.18}$$
$$-\left(\left(\frac{\mu_b u_{bp}}{k_1} + \frac{\rho_g u_{bp}^2}{k_2}\right)\frac{4}{3}\pi R_b^3 + \sum_{i=1}^{n} 6\pi\mu_w R_{pi} u_{bp}\right)$$

Solution of the terminal velocity of the particle-bubble unit in porous media is same as that of bubble without particle in porous media. Thus, equation 4.18 can be rearranged and transformed by

$$u_{bp}^2\left(-\frac{4\rho_g \pi R_b^3}{3k_2}\right) + u_{bp}\left(-\frac{4\mu_b \pi R_b^3}{3k_1} - \sum_{i=1}^{n} 6\pi\mu_w R_{pi}\right)$$
$$+\frac{4}{3}\left(\rho_f - \rho_g\right) g\pi R_b^3$$
$$+\left(\rho_f - \rho_g\right) g \sum_{i=1}^{n} \frac{\pi}{3} R_{pi}^3 \left[\left(1-\cos\omega\right)^2 (2+\cos\omega)\right] \tag{4.19}$$
$$-\left(\rho_p - \rho_g\right) g \sum_{i=1}^{n} \frac{4}{3}\pi R_{pi}^3$$
$$-2\pi R'\sigma \sin\theta + \sum_{i=1}^{n} 2\pi R_{Pi}\sigma \sin\omega \sin(\omega+\theta') = 0$$

Same as equation 4.8, this equation is the form of quadratic equation and expressed by

$$C_1' u_{bp}^2 + C_2' u_{bp} + C_3' = 0 \tag{4.20}$$

Where $C'_1$, $C'_2$, and $C'_3$ are constant coefficients given by

$$C_1' = -\frac{4\rho_g \pi R_b^3}{3k_2} \tag{4.21}$$

$$C_2' = -\frac{4\mu_b \pi R_b^3}{3k_1} - \sum_{i=1}^{n} 6\pi\mu_w R_{pi} \tag{4.22}$$

$$\begin{aligned} C_3' = {} & \frac{4}{3}\left(\rho_f - \rho_g\right) g\pi R_b^3 \\ & -2\pi R'\sigma \sin\theta \\ & +\left(\rho_f - \rho_g\right) g \sum_{i=1}^{n} \frac{\pi}{3} R_{pi}^3 \left[ (1-\cos\omega)^2 (2+\cos\omega) \right] \\ & -\left(\rho_p - \rho_g\right) g \sum_{i=1}^{n} \frac{4}{3}\pi R_{pi}^3 \\ & +\sum_{i=1}^{n} 2\pi R_{Pi}\sigma \sin\omega \sin(\omega+\theta') \end{aligned} \tag{4.23}$$

As described before, this quadratic equation 4.20 has two solutions which are given by

$$u_{bp} = \frac{-C_2' + \sqrt{C_2'^2 - 4C_1'C_3'}}{2C_1'} \tag{4.24}$$

$$u_{bp} = \frac{-C_2' - \sqrt{C_2'^2 - 4C_1'C_3'}}{2C_1'} \tag{4.25}$$

In the terminal velocity of the particle-bubble unit in porous media, negative value of the terminal velocity can be neglected, thus equation 4.25 can be neglected in our model system.

Figure 4.4 shows the terminal velocity of the particle-bubble unit in porous media as increasing number of particle which are 100, 500, 1000, 5000, 10000. There is no reason to choose this numbers of particles. Also, this figure includes data obtained by *Haberman and Morton* [1953] and *Corapcioglu et al.* [2004]. As seen in Figure 4.4, the terminal velocity of the particle-bubble unit in porous media decreases with increasing the number of particle. In our modeling work, we can predict that the terminal velocity of 100 particles attached bubble in porous media has no big difference with that of bubble only in porous media.

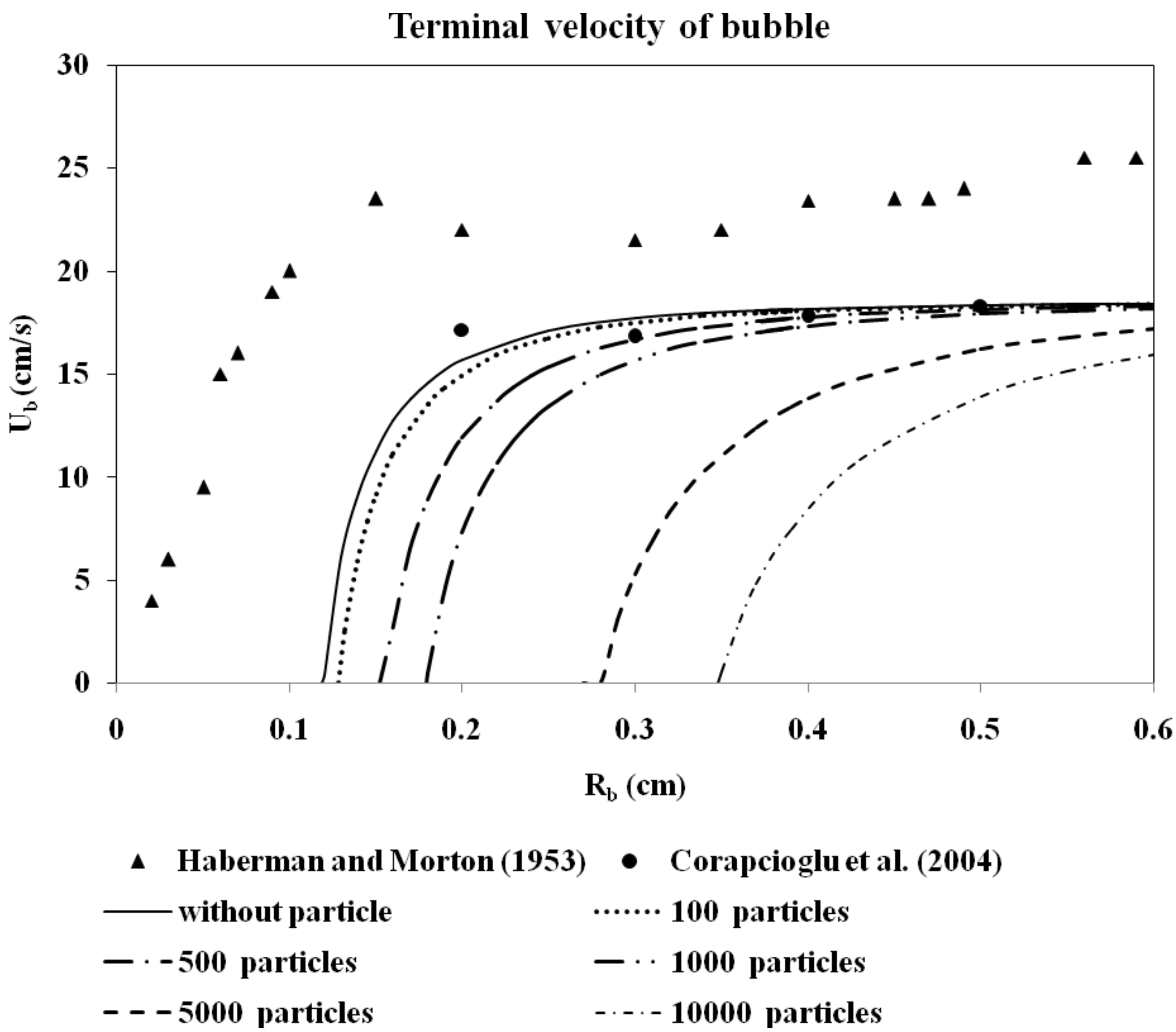


Figure 4. 4 Comparison of theoretical rise velocity of the particle-bubble unit in porous media with various experimental data which come from *Haberman and Morton* [1953] and *Corapcioglu et al*. [2004]

However, the terminal velocity of 10,000 particles attached bubble in porous media is much slower than that of bubble only in porous media. As mentioned before, starting point of bubble only radius is 0.119 cm. When 10,000 particles are attached on the bubble, starting point of bubble radius is 0.348 cm. As a result, we can conclude that

- As increased number of attached particle, the terminal velocity of the particle-bubble unit in porous media is decreased.
- Attached particle on the bubble in porous media might prevent the movement of bubble in porous media due to surface tension of particle.
- Surface tension of particle is more strong than buoyant force of particle

There is no experimental data about movement of the particle-bubble unit in porous media. Thus, we cannot compare our modeling work with experimental data. We can just predict about the effect of attached particle in movement of the particle-bubble unit in porous media by using equation 4.24.

### 4-2-2 The effect of attached particles for the particle-bubble unit

We can predict and simulate the starting point of the particle-bubble unit in porous media. This situation is similar to the effect of solid grain size ($d_p$). As the number of attached particle on the particle-bubble unit in porous media is increased, the starting point of the particle-bubble unit in porous media is increased. For example, when 100, 500, 1000, 5000, and 10,000 of particles are attached on the bubble, the starting point of bubble radius is 0.128, 0.152, 0.179, 0.27, and 0.348 cm. The meaning of the starting point is that when the particle-bubble unit moves to upward, the minimum radius of a bubble is needed for our simulation. In less than this starting point, a bubble can be trapped or stuck among the porous media.

Thus, trapping possibility of the particle-bubble unit with smaller bubble in porous media is much higher than that of the particle-bubble unit with larger bubble. This critical trapping condition is a very important factor for predicting the particle-bubble unit in porous media. The presence of particle in porous media has some advantage and disadvantage for air sparging remediation. For example, if the particles are the target of contaminant as a harmful substance, the smaller bubbles are not good operating factor for the remediation of the particles. However, if the goal of contaminant remediation is volatile organic compound in groundwater, the smaller bubbles might be great operating factor for bioremediation since trapped bubbles provide oxygen into groundwater. Figure 4.5 shows the terminal velocity of the particle-bubble unit in porous media as increasing the number of attached particle with various radius of bubble. From Figure 4.5, in all of bubble radius, the terminal velocity of the particle-bubble unit in porous media decrease with increasing the number of attached particle as mentioned previously. Small size of bubble can be more affected than large size of bubble in movement of the particle-bubble unit in porous media. This simulation indicate that the terminal velocity of the particle-bubble unit with $R_b$=0.2 cm is more rapidly decreased than that of the particle-bubble unit with $R_b$=0.6 cm. Thus, the effect of numbers of particles is sensitive and critical for a rising the particle-bubble unit in porous media with small size of bubble. If over 3000 of particles is attached on the particle-bubble unit with $R_b$=0.2 cm, this bubble might becomes stuck and trapped among the pore body or the pore throat. However, the terminal velocity of the particle-bubble unit in porous media with $R_b$=0.6 cm is almost same as that of bubble only in porous media. Otherwise, over 10,000 of particles are attached on the particle-bubble unit with $R_b$=0.6 cm, and then the terminal velocity of the particle-bubble unit is decreased.

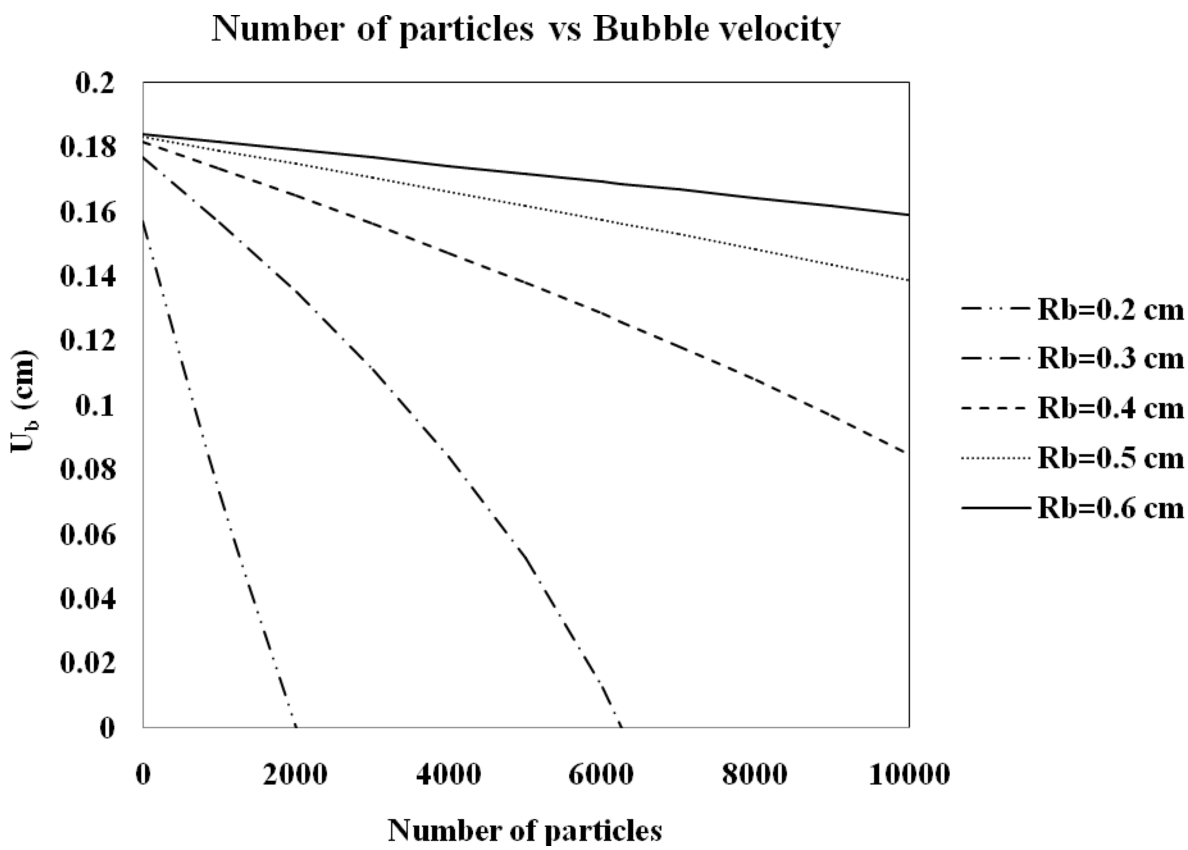


Figure 4. 5 The terminal velocity of the particle-bubble unit in porous media as increasing the number of attached particles on the bubble with various radii of bubble

### 4-2-3 The effect of grain size ($d_p$) for the particle-bubble unit's movement

We can predict from equation 4.24 that the terminal velocity of the particle-bubble unit in porous media cannot exceed 18.5 cm/s as same as that of bubble only in porous media, and starting point of bubble size is various with different value of number of the particle. Thus, in the particle-bubble unit, solid grain size ($d_p$) and pore throat size (R') is a important factor for analysis of movement of the particle-bubble unit in porous media. Figure 4.6 - 4.10 show effect of $d_p$ with various number of attached particles on the particle-bubble unit in porous media. The pattern of rise terminal velocity of the particle-bubble unit in porous media is similar to all of solid grain size ($d_p$). However, the value of terminal velocity of the particle-bubble unit in porous media is different in each of solid grain size ($d_p$). From Figures 4.6 - 4.10, the maximum terminal rise velocity of the particle-bubble unit in porous media is similar to that of a bubble without a particle in porous media. In $d_p$=0.6, the maximum terminal rise velocity of 100 particle attached bubble unit is 26.4 cm/s, and that of 10,000 particle attached bubble unit is 23.2 cm/s. As compared with that of bubble only in porous media, that of 100 particle attached bubble unit is almost same as that of bubble without particle. However, 10,000 particle attached bubble unit's terminal rise velocity is reduced by almost 13 %. From this data analysis, the maximum terminal velocity of 100, 500, 1000 particle attached bubble is reduced less than 1 %. Otherwise, that of 5000, 10000 particle attached bubble is reduced more than 10 %. Thus, it can be concluded that higher particle attachment on a bubble in porous media is caused by reduction of the maximum terminal velocity of the particle-bubble unit. Tables 4.4 - 4.8 show the reduction rate of maximum terminal velocity of the particle-bubble unit in various solid grain size ($d_p$).

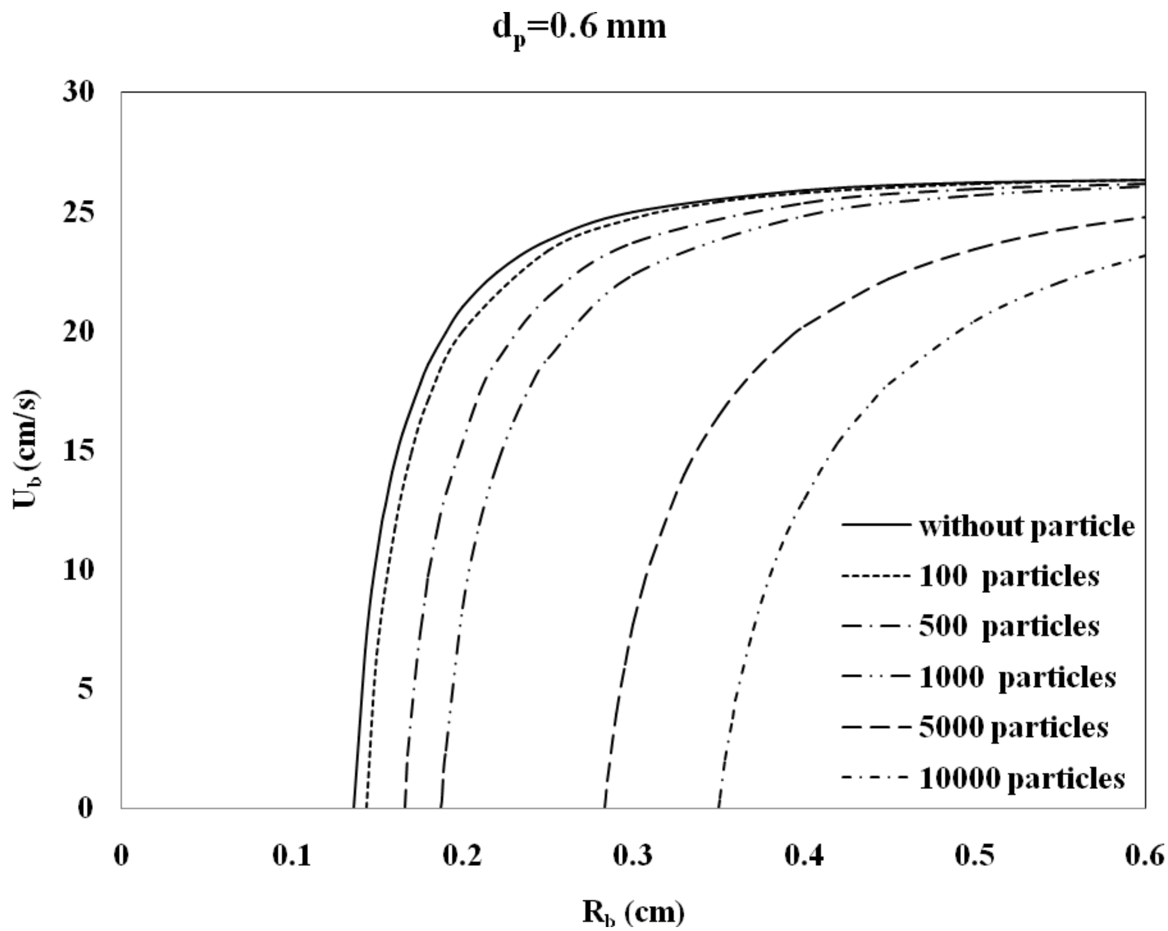


Figure 4. 6 Effect of $d_p$=0.6 cm with various attached particles on the particle-bubble unit in porous media

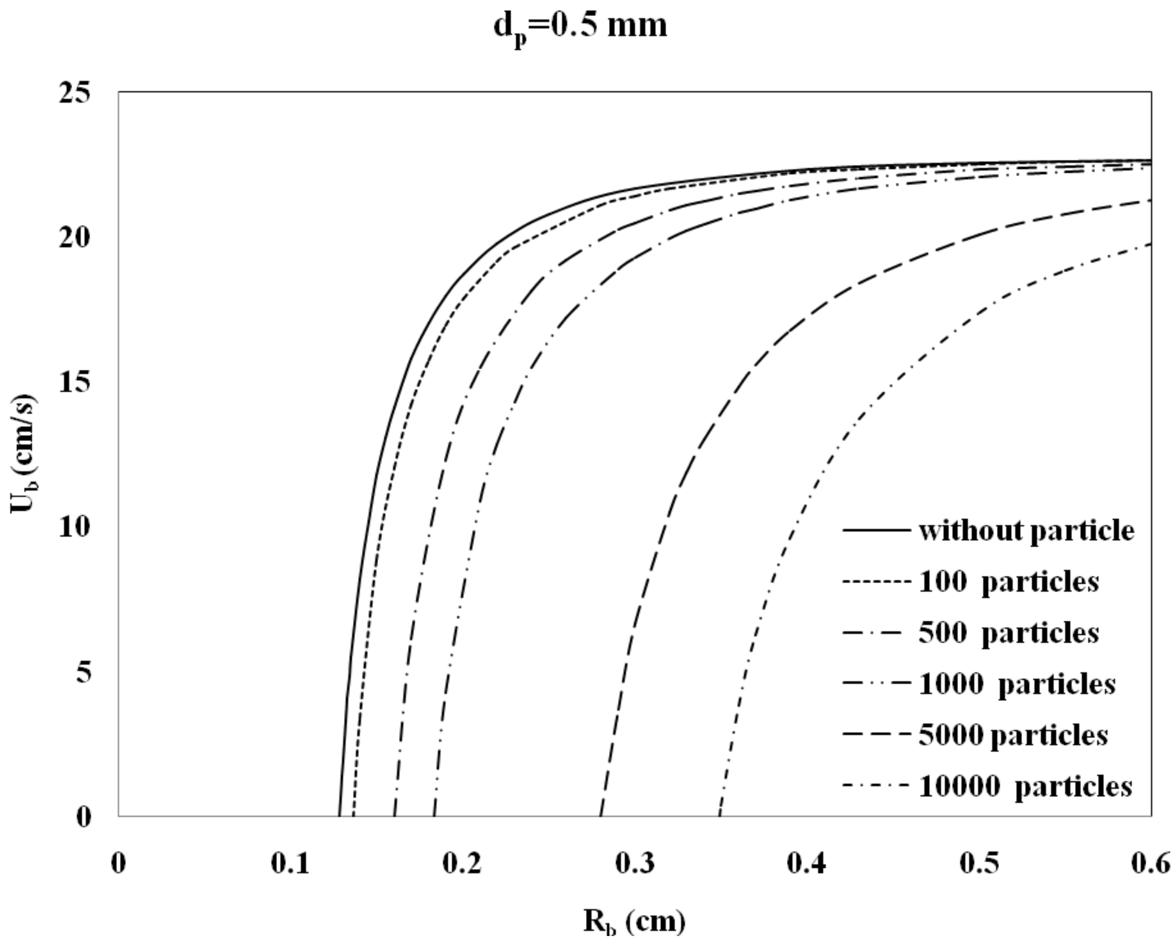


Figure 4. 7 Effect of $d_p$=0.5 cm with various attached particles on the particle-bubble unit in porous media

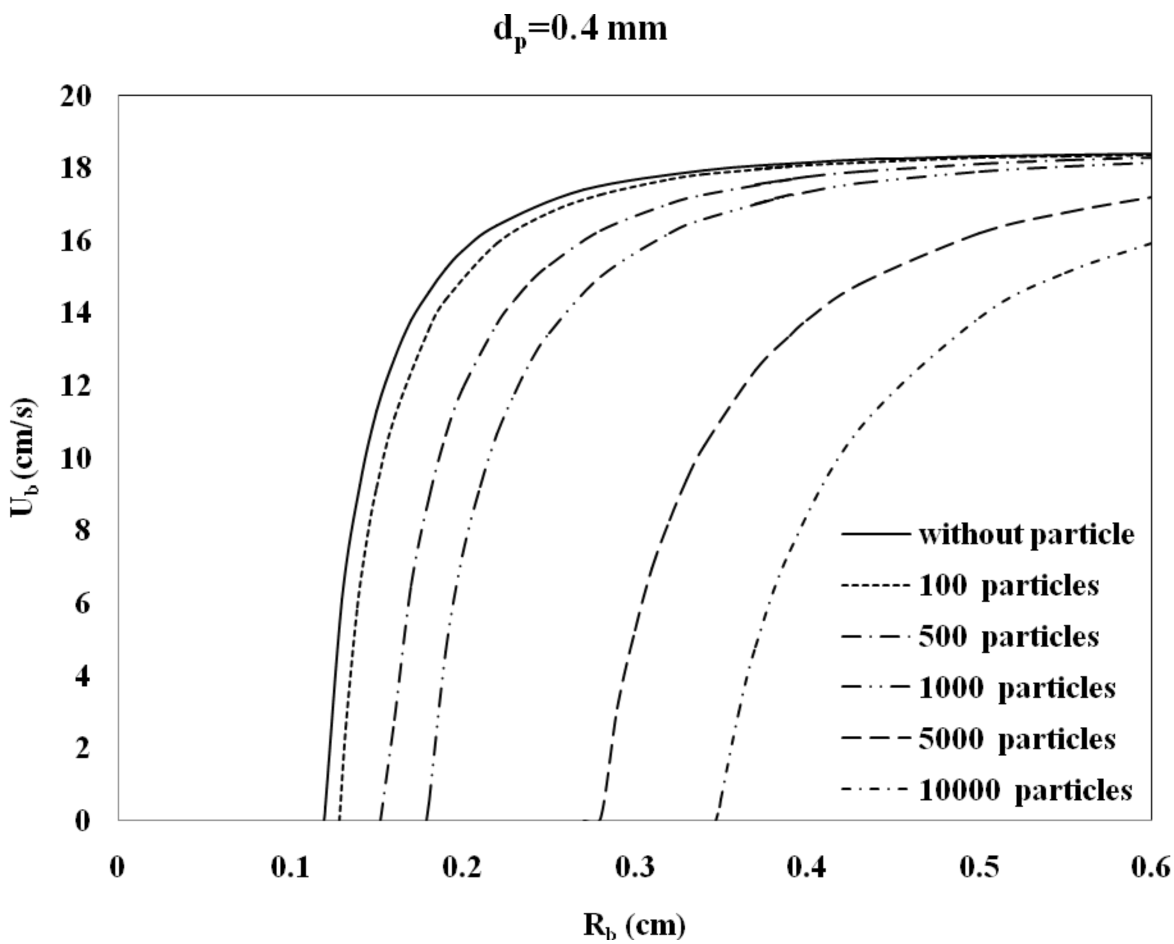


Figure 4. 8 Effect of $d_p$=0.4 cm with various attached particles on the particle-bubble unit in porous media

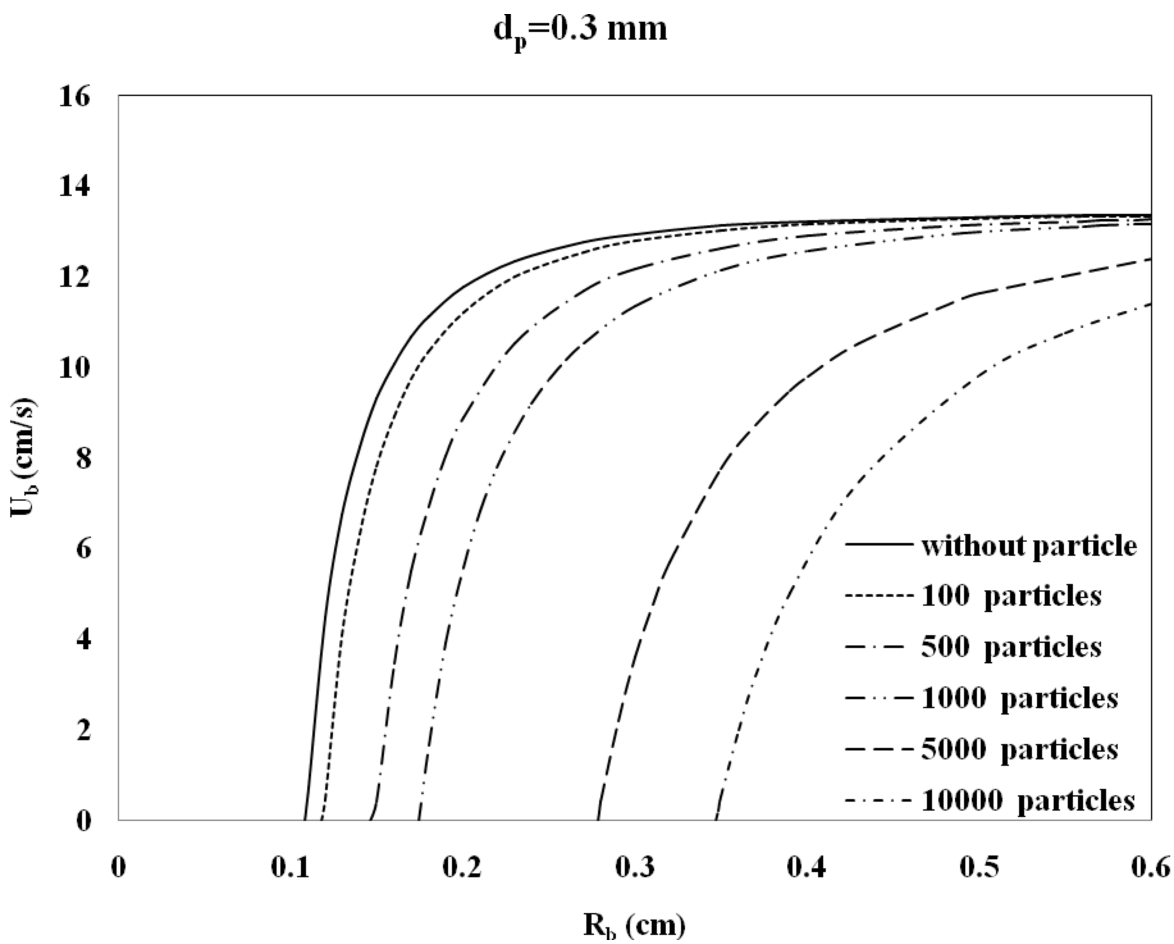


Figure 4. 9 Effect of $d_p$=0.3 cm with various attached particles on the particle-bubble unit in porous media

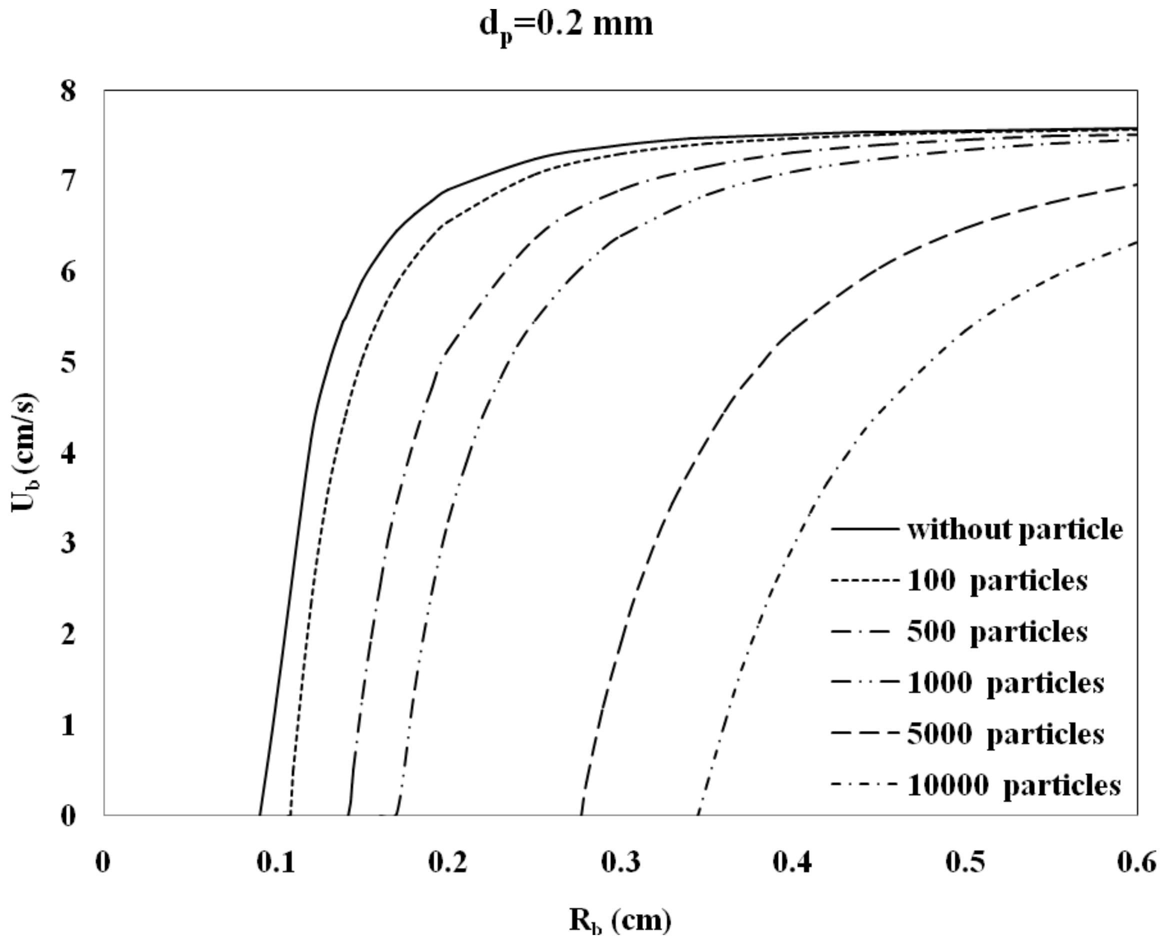


Figure 4. 10 Effect of $d_p$=0.2 cm with various attached particles on the particle-bubble unit in porous media

Table 4. 4 Reduction rate of the maximum terminal velocity of the particle-bubble unit in dp=0.6 cm

| *Number of particles* | *Maximum terminal velocity of the particle-bubble unit (cm/s)* | *Reduction rate of velocity (%)* |
|---|---|---|
| 100 | 26.31 | 0.1 |
| 500 | 26.18 | 0.6 |
| 1000 | 26.03 | 1.2 |
| 5000 | 24.77 | 5.9 |
| 10000 | 23.13 | 12.2 |

Table 4. 5 Reduction rate of the maximum terminal velocity of the particle-bubble unit in dp=0.5 cm

| *Number of particles* | *Maximum terminal velocity of the particle-bubble unit (cm/s)* | *Reduction rate of velocity (%)* |
|---|---|---|
| 100 | 22.64 | 0.1 |
| 500 | 22.53 | 0.6 |
| 1000 | 22.39 | 1.2 |
| 5000 | 21.26 | 6.2 |
| 10000 | 19.80 | 12.7 |

Table 4. 6 Reduction rate of the maximum terminal velocity of the particle-bubble unit in dp=0.4 cm

| *Number of particles* | *Maximum terminal velocity of the particle-bubble unit (cm/s)* | *Reduction rate of velocity (%)* |
|---|---|---|
| 100 | 18.37 | 0.1 |
| 500 | 18.28 | 0.6 |
| 1000 | 18.16 | 1.3 |
| 5000 | 17.19 | 6.6 |
| 10000 | 15.93 | 13.4 |

Table 4. 7 Reduction rate of the maximum terminal velocity of the particle-bubble unit in dp=0.3 cm

| *Number of particles* | *Maximum terminal velocity of the particle-bubble unit (cm/s)* | *Reduction rate of velocity (%)* |
|---|---|---|
| 100 | 13.35 | 0.1 |
| 500 | 13.27 | 0.7 |
| 1000 | 13.17 | 1.4 |
| 5000 | 12.40 | 7.2 |
| 10000 | 11.40 | 14.7 |

Table 4. 8 Reduction rate of the maximum terminal velocity of the particle-bubble unit in dp=0.2 cm

| *Number of particles* | *Maximum terminal velocity of the particle-bubble unit (cm/s)* | *Reduction rate of velocity (%)* |
|---|---|---|
| 100 | 7.57 | 0.1 |
| 500 | 7.52 | 0.8 |
| 1000 | 7.46 | 1.6 |
| 5000 | 6.96 | 8.2 |
| 10000 | 6.32 | 16.6 |

# 5 DIMENSIONAL ANALYSIS OF BUBBLE IN POROUS MEDIA

## 5-1 DIMENSIONAL ANALYSIS OF MOVEMENT OF A BUBBLE WITHOUT PARTICLE IN POROUS MEDIA

### 5-1-1 General description of dimensional analysis

When a bubble goes up through a porous medium, there are some external forces acting on bubble which are buoyant force, surface tension, and drag force. Their equation expressions are presented in Table 3.1. Each of these forces is affected by bubble's motion in porous media. In steady state, dimensional analysis can be performed to provide a more generalized methodology to determine which one of these external forces has the most dominant impact on the bubble's motion in porous media. It is accomplished in the following steps:

Dimensional analysis comes from force balance equation which is given by equation 3.12

$$\sum F = (\rho_f - \rho_g) g \frac{4}{3}\pi R_b^3 - 2\pi R' \sigma \sin\theta - \left[\frac{\mu_b u_b}{k_1} + \frac{\rho_g u_b^2}{k_2}\right]\frac{4}{3}\pi R_b^3 \qquad (3.12)$$

Then, buoyant force is balanced by surface tension and drag force in steady state, its expression is given by

$$(\rho_f - \rho_g) g \frac{4}{3}\pi R_b^3 = \frac{\mu_b u_b}{k_1}\frac{4}{3}\pi R_b^3 + \frac{\rho_g u_b^2}{k_2}\frac{4}{3}\pi R_b^3 + 2\pi R' \sigma \sin\theta \qquad (5.1)$$

Where $k_1$ and $k_2$ is related to the medium's permeability and is expressed by

$$k_1 = \frac{d_p^2}{150A}\frac{n^3}{(1-n)^2} \qquad (3.10)$$

$$k_2 = \frac{d_p}{1.75A}\frac{n^3}{(1-n)} \tag{3.11}$$

Then, both sides of equation 5.1 are divided by $\frac{4}{3}\pi R_b^3 \sigma \sin$ and multiplied by $k_1$,

$$\frac{(\rho_f - \rho_g) g k_1}{\sigma \sin\theta} = \frac{\mu_b u_b}{\sigma \sin\theta} + \frac{\rho_g u_b^2}{\sigma \sin\theta}\frac{k_1}{k_2} + \frac{3R' k_1}{2R_b^3} \tag{5.2}$$

The left hand side of equation 5.2 can be interpreted as a type of Bond number (Bo) which expresses the ratio of gravitational to surface tension force as given by

$$Bo = \frac{(\text{gravitational force})}{(\text{surface tention force})} = \frac{(\rho_f - \rho_g) g k_1}{\sigma \sin\theta} \tag{5.3}$$

The first term on the right hand side of equation 5.2 is Capillary number (Ca) which presents the ratio of viscous to surface tension force as given by

$$Ca = \frac{(\text{viscous force})}{(\text{surface tention force})} = \frac{\mu_b u_b}{\sigma \sin\theta} \tag{5.4}$$

The second term on the right hand side of equation 5.2 is Weber number (We) which defines as the ratio of the inertial to surface tension force as given by

$$We = \frac{(\text{inertial force})}{(\text{surface tention force})} = \frac{\rho_g u_b^2}{\sigma \sin\theta}\frac{k_1}{k_2} \tag{5.5}$$

The third term on the right hand side of equation 5.2 is called as Trapping number (Nt) which represents the relative medium-specific ease of a bubble to move through the porous medium as given by

$$Nt = \frac{(\text{Gravitational force})\text{-}(\text{viscous force})\text{-}(\text{inertial force})}{(\text{surface tention force})} = \frac{3R' k_1}{2R_b^3} \tag{5.6}$$

Substituting and rearranging equation 5.3~6 into equation 5.2 is expressed as

$$Bo - Ca - We = Nt \tag{5.7}$$

Table 5.1 shows the summary of dimensionless numbers. Equation 5.2 can be transformed to equation 5.7 and these four dimensionless numbers can be expressed as the function of bubble rise velocity, its radius, and the specific properties of porous medium. As mentioned in Section 4, a bubble rise velocity can be expressed as the function of a bubble radius in porous media, thus these dimensionless numbers can be presented by a function of the equivalent bubble radius as presented in Figure 5.1. From Figure 5.1, the Bond number does not change with a bubble radius since the increase in the bubble density with decreasing bubble volume is not important enough compared to the density of the water that means the bubble movement is not affected by the bubble density with this range of bubble volume. Capillary number (Ca) and Weber number (We) increases with increasing the bubble radius as shown in Figure 5.1. This is explained that the viscous force and the inertial force dominate the surface tension force heavily. Compared the Capillary number with Weber number, the viscous force is more affected than the inertial force by a bubble movement in porous media. Otherwise, Trapping number (Nt) decrease with increasing the bubble radius as seen in Figure 5.1. This indicates that the small size of a bubble in porous media can be more easily trapped than the large size of a bubble. The higher trapping number means that a bubble can be easily trapped among the pore body. Thus, the small size of a bubble has higher possibility of trapping in the pore body or the pore throat than the large size of a bubble in porous media. From Figure 5.1, the Bond number does not change with a bubble radius since the increase in the bubble density with decreasing bubble volume is not important enough compared to the density of the water that means the bubble movement is not affected by the bubble density with this range of bubble volume.

Capillary number (Ca) and Weber number (We) increases with increasing the bubble radius as shown in Figure 5.1. This is explained that the viscous force and the inertial force dominate the surface tension force heavily. Compared the Capillary number with Weber number, the viscous force is more affected than the inertial force by a bubble movement in porous media. Otherwise, Trapping number (Nt) decrease with increasing the bubble radius as seen in Figure 5.1. This indicates that the small size of a bubble in porous media can be more easily trapped than the large size of a bubble. The higher trapping number means that a bubble can be easily trapped among the pore body. Thus, the small size of a bubble has higher possibility of trapping in the pore body or the pore throat than the large size of a bubble in porous media. This analysis shows general effect of a bubble movement in porous media.

Table 5. 1 Summary of dimensionless numbers

| Dimensionless number | Definition and expression |
|---|---|
| Bond number | The ratio of gravitational to surface tension force<br>$Bo = \frac{(\rho_f - \rho_g) g k_1}{\sigma \sin\theta}$ |
| Capillary number | The ratio of viscous to surface tension force<br>$Ca = \frac{\mu_b u_b}{\sigma \sin\theta}$ |
| Weber number | The ratio of inertial force to surface tension force<br>$We = \frac{\rho_g u_b^2}{\sigma \sin\theta} \frac{k_1}{k_2}$ |
| Trapping number | The relative medium-specific ease of a bubble to move through the porous medium<br>$Nt = \frac{3R' k_1}{2R_b^3}$<br>Where $k_1$ and $k_2$ is expressed by<br>$k_1 = \frac{d_p^2}{150A} \frac{n^3}{(1-n)^2}$ and $k_2 = \frac{d_p}{1.75A} \frac{n^3}{(1-n)}$ |

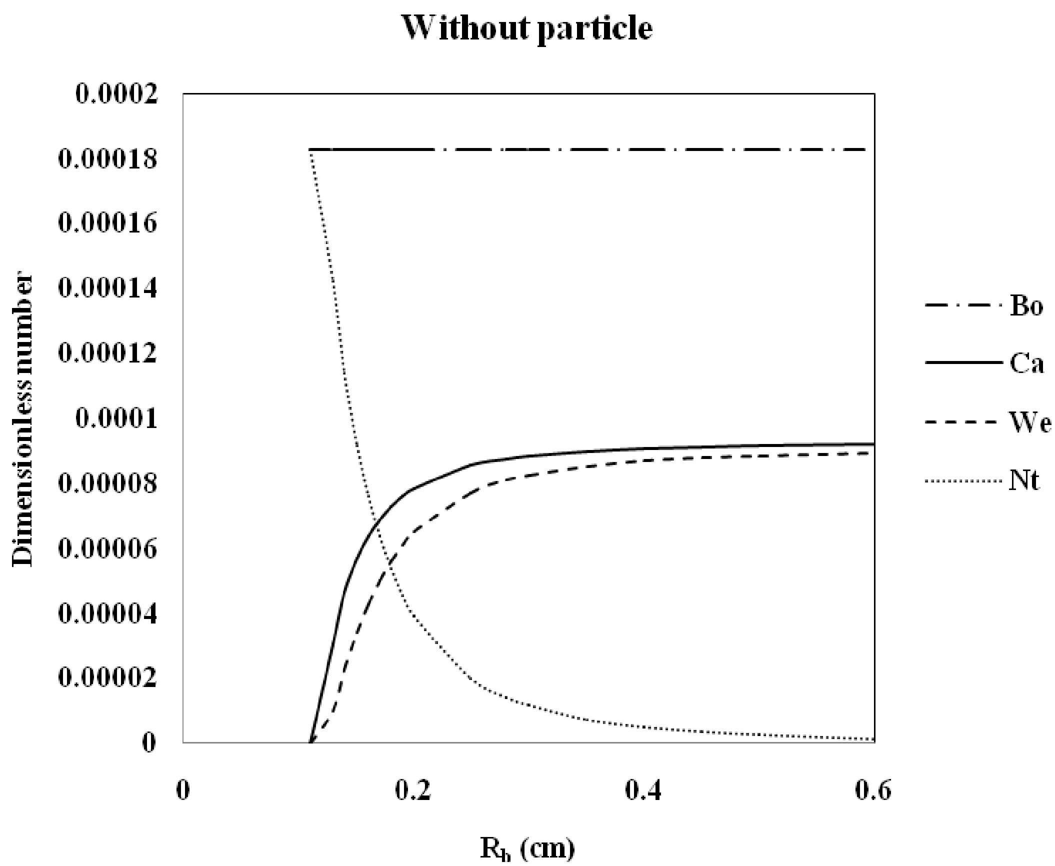


Figure 5. 1 Dimensionless numbers as a function of the equivalent bubble radius

**5-1-2 Relationship between the dimensionless numbers and Reynolds number**

Relationship between various dimensionless numbers and Reynolds number can provide more specific inspection for a bubble movement in porous media. Reynolds number (Re) defines as the ratio of inertial to viscous force and expresses as

$$R_e = \frac{(\text{inertial force})}{(\text{viscous force})} = \frac{2R_b u_b \rho_f}{\mu_f} \qquad (5.8)$$

Variations of the dimensionless numbers (which are Bo, Ca, We, and Nt) with Reynolds number (Re) can explain to the effect of individual forces acting on a bubble in porous media and are presented in Figure 5.2. As describe before, the Bond number (Bo) is also constant with the Reynolds number (Re) because of the density difference between a bubble and water. However, A log-log plot of Capillary number (Ca), Weber number (We) and Trapping number (Nt) as increasing Reynolds number (Re) indicates different lines with sharp changes at the almost same range of Re value. This sharp change in behavior indicates that different types of bubble movement are predicted before and after turning point. The critical Re at the turning point, calculated with using equation 5.3~6 and 5.8 is about 520 for $d_p$ = 4mm. At this point, a bubble radius is about 0.18 cm. Thus, the magnitude of inertial force and viscous force of a bubble is much smaller than that of surface tension force of a bubble without particle with less than 0.18cm which means that small size of a bubble is dominated by surface tension. Trapping number (Nt) which is inversely proportional to $R_b^3$, is initially almost constant with increasing Reynolds number (Re). Thus, in less than 0.18 cm of bubble radius, bubble size is insignificant for the Trapping number (Nt). After turning point, Trapping number is gradually decreased with increasing Reynolds number (Re) since bubble size is important for the Trapping number. Capillary number (Ca) which is proportional to $\mu_b u_b$, initially increases with increasing Reynolds number (Re) until the effect of viscous forces against the drag forces becomes insignificant at the turning point. Then, Capillary number (Ca) is almost constant as increasing Reynolds number (Re) after turning point, thus the effect of viscous forces against the drag forces become a significant factor for rising bubble movement in porous media. The Weber number (We) which is proportional to $\rho_g u_b^2$, initially increases with increasing Reynolds number (Re) until the effect of inertial forces against the drag forces becomes negligible at the turning point. Then, Weber number (We) is also constant as increasing Reynolds number (Re) after turning point, thus the effect of inertial forces against the drag forces become a important factor for rising bubble movement in porous media. As seen in figure 5.2, after the turning point which is larger than 0.18 cm of a bubble radius, the value of Capillary number (Ca) is equal to that of Weber number (We) which means that effect of viscous force is same as that of inertial force.

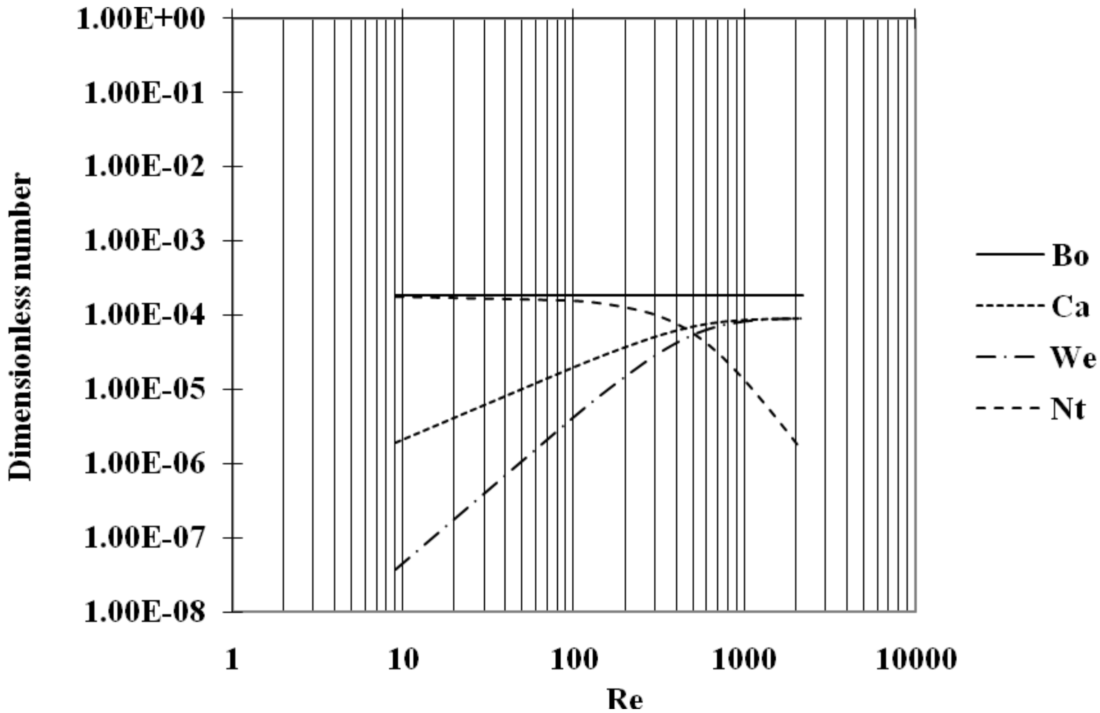


Figure 5. 2 Variations of dimensionless numbers (which are Bo, Ca, We, and Nt) as increasing Reynolds number (Re)

**5-1-3 Relationship between Bo, Ca, We and Nt**

If each of dimensionless numbers is divided by Trapping number (Nt), we can obtain the functional dependence of one dimensionless group in response to orders of magnitude changes in another dimensionless group. Dividing equation 5.7 to Trapping number (Nt) is given by

$$\frac{Bo}{Nt}-\frac{Ca}{Nt}-\frac{We}{Nt}=1 \tag{5.9}$$

The first term on the left hand side of equation 5.9 indicates the ratio of Bond number (Bo) to total driving force acting on a bubble in porous media. The second term and third term on the left hand side of equation 5.9 present the ratio of Capillary number (Ca) and the ratio of Weber number (We) to total driving force acting on a bubble in porous media. Thus, Bo/Nt = 1 means that bubble is trapped among pore body or pore throat. Figure 5.3 shows the ratio of dimensionless numbers (which are Bo, Ca, We) to Trapping number (Nt) with Reynolds number (Re). As mentioned above, three variables which are Bo/Nt, Ca/Nt, and We/Nt have three different lines with sharp changes at the almost same range of Re value which is about 520. When $R_b \leq 0.18$ cm, Re ≤ 520, Bo/Nt is almost constant and a slope of We/Nt to Re is 2 and a slope of Ca/Nt to Re is 1. Thus, the surface tension is balanced to the gravitational forces in bubbles with $R_b \leq 0.18$ cm and inertial force is more dominant force than viscous force for bubbles with $R_b \leq 0.18$. Reversely, When $R_b \geq 0.18$ cm, Re ≥ 520, a slope of Bo/Nt to Re is 2.6, a slope of We/Nt to Re is 2 and a slope of Ca/Nt to Re is 2. Thus, the gravitational force dominates more than the surface tension with $R_b \geq 0.18$ cm and the effect of inertial force is equal to that of viscous force with $R_b \geq 0.18$.

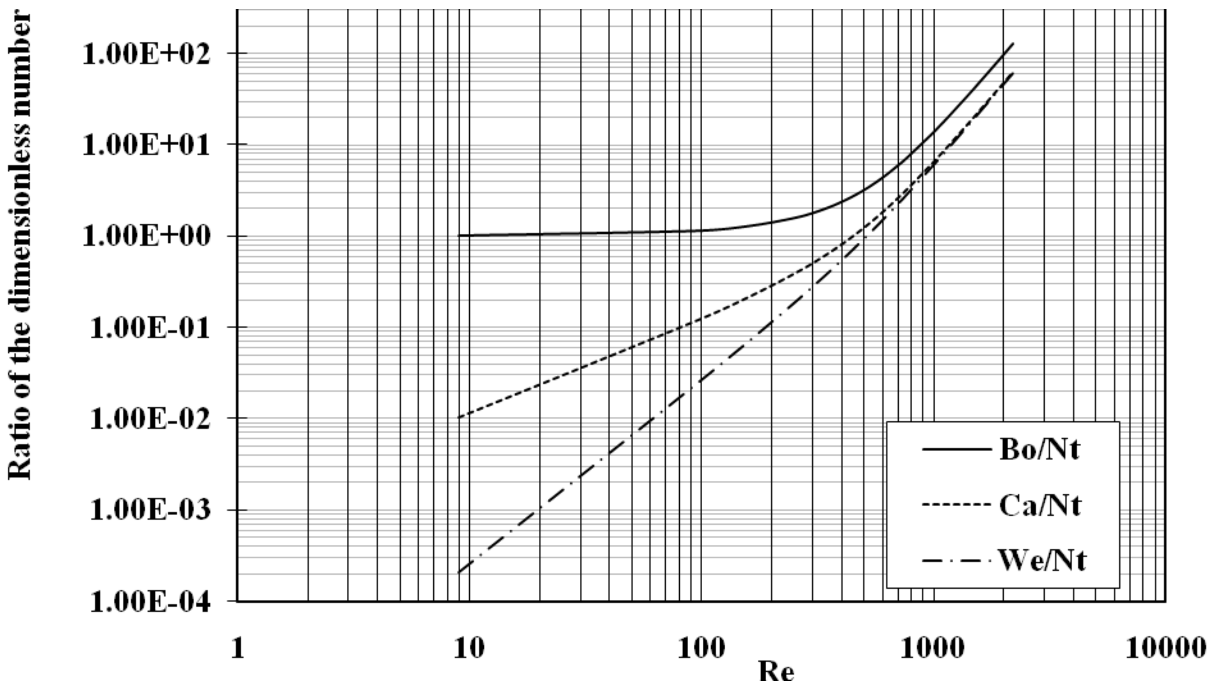


Figure 5. 3 The ratio of dimensionless numbers (which are Bo, Ca, We) to Trapping number (Nt) with Reynolds number (Re)

## 5-2 DIMENSIONAL ANALYSIS OF THE PARTICLE-BUBBLE UNIT MOVEMENT IN POROUS MEDIA

### 5-2-1 General description of the modified dimensionless number equations

As described as Section 4-2, when a particle is attached on a bubble in porous medium, dimensional analysis of movement of a bubble without a particle differs from that of motion of the particle-bubble unit. Of course, there are Bond number, Capillary number, Weber number, and Trapping number in dimensional analysis of the particle-bubble unit movement in porous media. Although they need some correction and modification, external forces acting on the particle-bubble unit in porous media are similar to external forces acting on bubble without a particle such as buoyant force, surface tension force, and drag force. Force balance equation for the particle-bubble unit is given by

$$\begin{aligned}\sum F^{B+P} = & \left(\rho_f - \rho_g\right) g \frac{4}{3}\pi R_b^3 + \left(\rho_f - \rho_g\right) g \frac{\pi}{3} R_p^3 \left[\left(1-\cos\omega\right)^2 (2+\cos\omega)\right] \\ & -(\rho_p - \rho_g) g \frac{4}{3}\pi R_p^3 \\ & -\left(2\pi R'\sigma \sin\theta - 2\pi R_p \sigma \sin\omega \sin(\omega+\theta')\right) \\ & -\left(\left(\frac{\mu_b u_{bp}}{k_1} + \frac{\rho_g u_{bp}^2}{k_2}\right)\frac{4}{3}\pi R_b^3 + 6\pi\mu_w R_p u_{bp}\right)\end{aligned} \tag{3.24}$$

This equation is considered by attachment of one single particle on the bubble in porous media. If a number of particle is more than one, this equation is changed and modified as following below

$$\sum F^{B+P} = \left(\rho_f - \rho_g\right) g \frac{4}{3}\pi R_b^3 + \sum_{i=1}^{n}\left(\rho_f - \rho_g\right) g \frac{\pi}{3} R_{pi}^3 \left[\left(1-\cos\omega\right)^2 (2+\cos\omega)\right]$$
$$-(\rho_p - \rho_g) g \sum_{i=1}^{n} \frac{4}{3}\pi R_{pi}^3$$
$$-\left(2\pi R'\sigma\sin\theta - \sum_{i=1}^{n} 2\pi R_{Pi}\sigma\sin\omega\sin(\omega+\theta')\right) \quad (4.18)$$
$$-\left(\left(\frac{\mu_b u_{bp}}{k_1} + \frac{\rho_g u_{bp}^2}{k_2}\right)\frac{4}{3}\pi R_b^3 + \sum_{i=1}^{n} 6\pi\mu_w R_{pi} u_{bp}\right)$$

Dimensional analysis of the particle-bubble unit movement provides the effect of individual forces acting on a bubble. It is accomplished in the following steps:

Dimensional analysis come from force balance equation which is given by equation 4.14 as shown above Then, buoyant force acting on the particle-bubble unit is balanced by surface tension and drag force acting on the particle-bubble unit  in steady state, its expression is rearranged and given by

$$\left(\rho_f - \rho_g\right) g \frac{4}{3}\pi R_b^3$$
$$+\left(\rho_f - \rho_g\right) g \sum_{i=1}^{n} \frac{\pi}{3} R_{pi}^3 \left[\left(1-\cos\omega\right)^2 (2+\cos\omega)\right]$$
$$-(\rho_p - \rho_g) g \sum_{i=1}^{n} \frac{4}{3}\pi R_{pi}^3 \quad (5.10)$$
$$-\frac{\mu_b u_{bp}}{k_1}\frac{4}{3}\pi R_b^3 - \frac{\rho_g u_{bp}^2}{k_2}\frac{4}{3}\pi R_b^3 - \sum_{i=1}^{n} 6\pi\mu_w R_{pi} u_{bp}$$
$$-2\pi R'\sigma\sin\theta + \sum_{i=1}^{n} 2\pi R_{Pi}\sigma\sin\omega\sin(\omega+\theta')$$
$$= 0$$

Then, both sides of equation 5.10 are divided by $\frac{4}{3}\pi R_b^3\sigma\sin$ and multiplied by $k_1$, it can be expressed by

$$\frac{\left(\rho_f-\rho_g\right)gk_1}{\sigma\sin\theta}+\frac{\left(\rho_f-\rho_g\right)g\sum_{i=1}^{n}\frac{\pi}{3}R_{pi}^3\left[\left(1-\cos\omega\right)^2(2+\cos\omega)\right]k_1}{\frac{4}{3}\pi R_b^{\ 3}\sigma\sin\theta}$$
$$-\frac{(\rho_p-\rho_g)g\sum_{i=1}^{n}\frac{4}{3}\pi R_{pi}^3k_1}{\frac{4}{3}\pi R_b^{\ 3}\sigma\sin\theta}-\frac{\mu_b u_{bp}}{\sigma\sin\theta}-\frac{\rho_g u_{bp}^2 k_1}{k_2\sigma\sin\theta}-\frac{\sum_{i=1}^{n}9\mu_w R_{pi}u_{bp}k_1}{2R_b^{\ 3}\sigma\sin\theta} \tag{5.11}$$
$$-\frac{3R'k_1}{2R_b^{\ 3}}+\frac{\sum_{i=1}^{n}3R_{Pi}\sin\omega\sin(\omega+\theta')k_1}{2R_b^{\ 3}\sigma\sin\theta}=0$$

The first term on the left hand side of equation 5.11 can be interpreted as a type of Bond number (Bo) as presented in Table 5.1.

The second term on the left hand side of equation 5.11 can be expressed by Bond number as given by

$$\frac{\left[\left(1-\cos\omega\right)^2(2+\cos\omega)\right]\sum_{i=1}^{n}R_{pi}^3}{4R_b^{\ 3}}Bo \tag{5.12}$$

The third term on the left hand side of equation 5.11 can be also expressed by Bond number as given by

$$\frac{\left(\rho_p-\rho_g\right)\sum_{i=1}^{n}R_{pi}^3}{\left(\rho_f-\rho_g\right)R_b^{\ 3}}Bo \tag{5.13}$$

The fourth term on the left hand side of equation 5.11 can be expressed by Capillary number as shown in Table 5.1.

The fifth term on the left hand side of equation 5.11 can be interpreted as a type of Weber number as presented in Table 5.1.

The sixth term on the left hand side of equation 5.11 can be expressed by Capillary number as given by

$$\frac{\sum_{i=1}^{n} 9\mu_w R_{pi} k_1}{2\mu_b R_b{}^3} Ca \tag{5.14}$$

The seventh term on the left hand side of equation 5.11 can be interpreted as a type of Trapping number as presented in Table 5.1.

Substituting equation 5.12~14 into equation 5.11, then its expression is given by

$$\begin{aligned} &Bo + \frac{\left[(1-\cos\omega)^2 (2+\cos\omega)\right]\sum_{i=1}^{n} R_{pi}^3}{4R_b{}^3} Bo \\ &-\frac{\left(\rho_p - \rho_g\right)\sum_{i=1}^{n} R_{pi}^3}{\left(\rho_f - \rho_g\right) R_b{}^3} Bo - Ca - We - \frac{\sum_{i=1}^{n} 9\mu_w R_{pi} k_1}{2\mu_b R_b{}^3} Ca \\ &-Nt + \frac{\sum_{i=1}^{n} 3R_{Pi} \sin\omega \sin(\omega+\theta') k_1}{2R_b{}^3 \sigma \sin\theta} = 0 \end{aligned} \tag{5.15}$$

Rearranging equation 5.15 and then dimensional analysis equation for the particle-bubble unit in porous media is expressed by

$$\begin{aligned} &\left(1 + \frac{\left[(1-\cos\omega)^2 (2+\cos\omega)\right]\sum_{i=1}^{n} R_{pi}^3}{4R_b{}^3} - \frac{\left(\rho_p - \rho_g\right)\sum_{i=1}^{n} R_{pi}^3}{\left(\rho_f - \rho_g\right) R_b{}^3}\right) Bo \\ &-\left(1 + \frac{\sum_{i=1}^{n} 9\mu_w R_{pi} k_1}{2\mu_b R_b{}^3}\right) Ca - We - \left(Nt - \frac{\sum_{i=1}^{n} 3R_{Pi} \sin\omega \sin(\omega+\theta') k_1}{2R_b{}^3 \sigma \sin\theta}\right) = 0 \end{aligned} \tag{5.16}$$

From equation 5.16, first term on the left hand side of equation 5.16 can be expressed as "modified Bond number" which is given by

$$Bo' = \left( 1 + \frac{\left[ \left(1 - \cos\omega\right)^2 (2 + \cos\omega) \right] \sum_{i=1}^{n} R_{pi}^3}{4R_b{}^3} - \frac{\left(\rho_p - \rho_g\right) \sum_{i=1}^{n} R_{pi}^3}{\left(\rho_f - \rho_g\right) R_b{}^3} \right) Bo \qquad (5.17)$$

Second term on the left hand side of equation 5.16 is called "modified Capillary number" which is given by

$$Ca' = \left( 1 + \frac{\sum_{i=1}^{n} 9\mu_w R_{pi} k_1}{2\mu_b R_b{}^3} \right) Ca \qquad (5.18)$$

Third term on the left hand side of equation 5.16 is the Weber number which was expressed by equation 5.5.

Fourth term on the left hand side of equation 5.16 can be expressed as "modified Trapping number" which is given by

$$Nt' = Nt - \frac{\sum_{i=1}^{n} 3R_{Pi} \sin\omega \sin(\omega + \theta') k_1}{2R_b{}^3 \sigma \sin\theta} \qquad (5.19)$$

Substituting equation 5.17~19 into equation 5.16 is given by

$$Bo' - Ca' - We - Nt' = 0 \qquad (5.20)$$

Table 5.2 shows the summary of modified dimensionless numbers. Equation 5.20 for dimensionless number analysis of the particle-bubble unit is similar to equation 5.7 for that of a bubble without a particle in porous media. As seen in equation 5.20, these three modified dimensionless numbers are related to dimensionless number for a bubble without particle, the function of bubble radius, the size of particle, a number of particle and contact angle between the particle and bubble.

Table 5. 2 Summary of modified dimensionless numbers

| *Dimensionless number* | *Definition and expression* |
|---|---|
| Modified Bond number | The ratio of gravitational to surface tension force acting on the particle-bubble unit in porous media $$Bo' = \left( 1 + \frac{\left[ (1-\cos\omega)^2 (2+\cos\omega) \right] \sum_{i=1}^{n} R_{pi}^3}{4R_b^{\ 3}} - \frac{\left(\rho_p - \rho_g\right) \sum_{i=1}^{n} R_{pi}^3}{\left(\rho_f - \rho_g\right) R_b^{\ 3}} \right) Bo$$ |
| Modified Capillary number | The ratio of viscous to surface tension force acting on the particle-bubble unit in porous media $$Ca' = \left( 1 + \frac{\sum_{i=1}^{n} 9\mu_w R_{pi} k_1}{2\mu_b R_b^{\ 3}} \right) Ca$$ |
| Modified Trapping number | The relative medium-specific ease of the particle-bubble unit to move through the porous medium $$Nt' = Nt - \frac{\sum_{i=1}^{n} 3R_{Pi} \sin\omega \sin(\omega + \theta')k_1}{2R_b^{\ 3} \sigma \sin\theta}$$ |

As seen in equation 5.20, these three modified dimensionless numbers are related to dimensionless number for a bubble without particle, the function of bubble radius, the size of particle, a number of particle and contact angle between the particle and bubble. Figure 5.4 - 5.8 shows modified dimensionless numbers as a function of the bubble radius when various number (100, 500, 1000, 5000, and 10000) of particles are attached.

Modified dimensionless number profile for the particle-bubble unit is similar to dimensionless number profile for a bubble without particle in porous media. Modified dimensionless number decrease with increasing the number of particles. As seen in Figures 5.4 - 5.8, the modified Bond number ($Bo'$) does not change with a bubble radius as same as Bond number does not change.

The modified Capillary number ($Ca'$) and Weber number (We) increases with increasing the bubble radius as shown in Figures 5.4 - 5.8. This pattern is also same as Capillary number (Ca) for movement of a bubble without particle.

The modified Trapping number ($Nt'$) decrease with increasing the bubble radius as same as Trapping number (Nt) for movement of a bubble without particle. The terminal rise velocity's profile of a bubble without a particle is similar to that of a bubble with various attached particles.

When attached particles on a bubble are increased, all of the modified dimensionless numbers except the modified Bond number ($Bo'$) are decreased. It can be concluded that

- Increasing attached particles on a bubble does not affect gravitational force acting on the particle-bubble unit in porous media.
- Effect of attached particles on a bubble occurs the movement of the particle-bubble

unit in porous media since the modified Capillary number ($Ca'$) and Weber number (We) is decreased with increasing attached particles.

When attached particles on a bubble is increased, the modified Trapping number ($Nt'$) is increased which means that attached particles on a bubble affect trapping of the particle-bubble unit among pore body or pore throat. Difference between the modified Capillary number ($Ca'$) and Weber number (We) is increased with increasing the number of attached particles on a bubble in porous media. Thus, the ratio of inertial force to surface tension force is more affected than that of viscous force to surface tension force with increasing the number of particles. In other words, effect of attached particles on a bubble in porous media occurs that inertial force is more sensitive and critical than viscous force for rising bubble through pore.

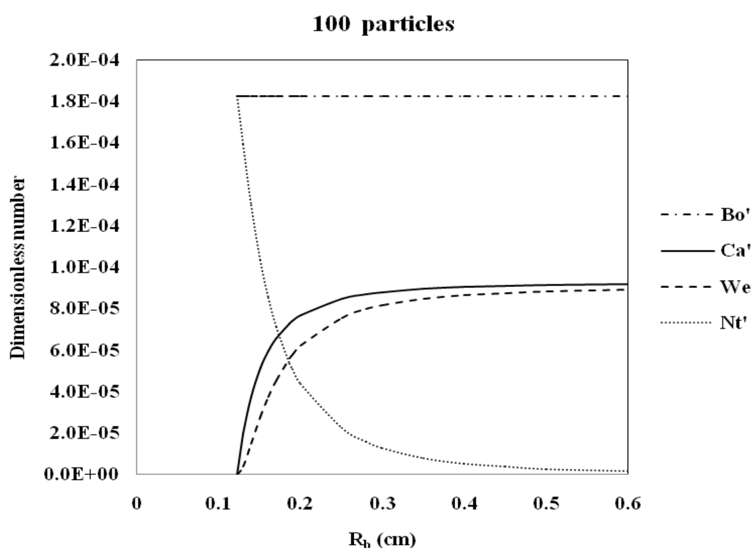


Figure 5.4 Modified dimensionless numbers as a function of the bubble radius when 100 particles are attached

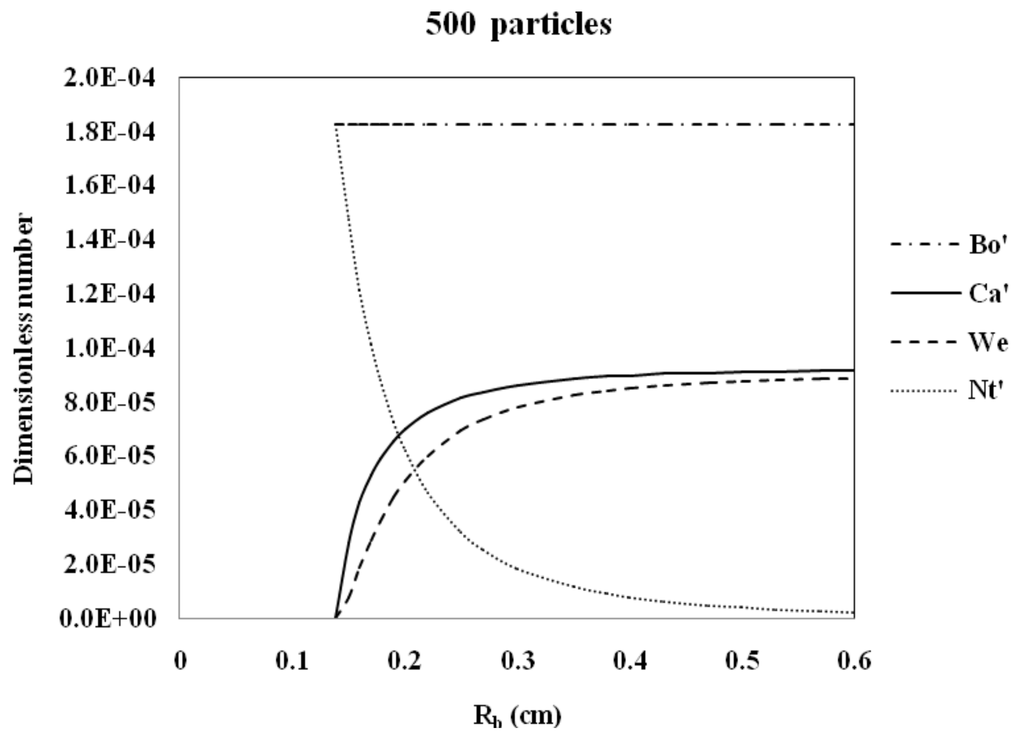


Figure 5.5 Modified dimensionless numbers as a function of the bubble radius when 500 particles are attached

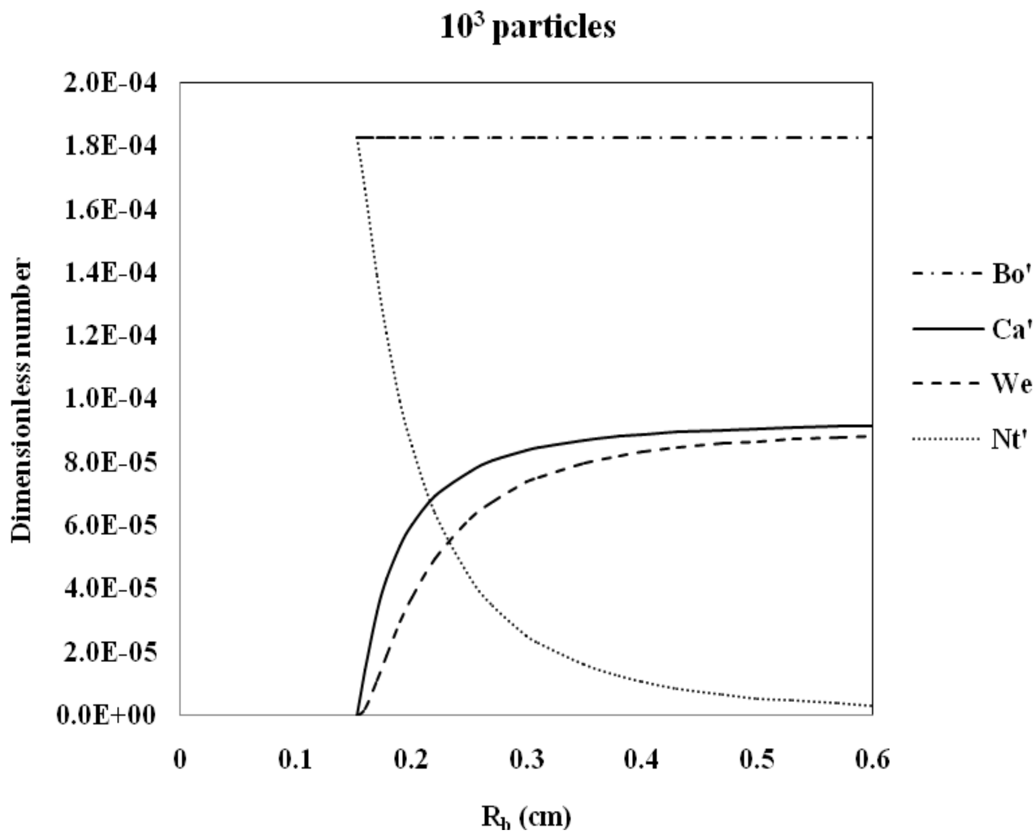


Figure 5.6 Modified dimensionless numbers as a function of the bubble radius when $10^3$ particles are attached

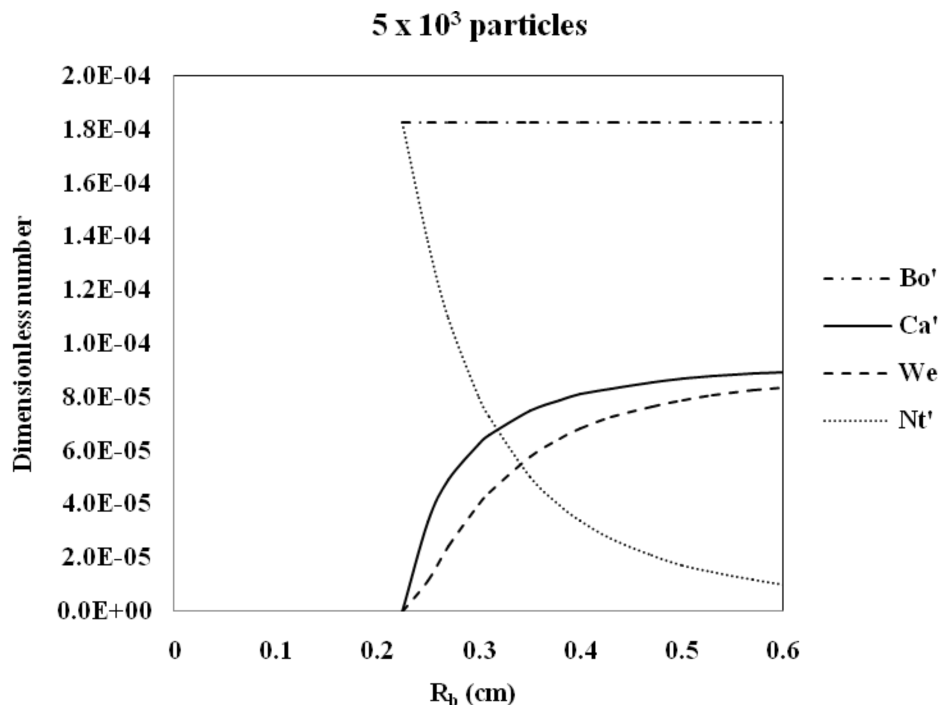


Figure 5.7 Modified dimensionless numbers as a function of the bubble radius when $5x10^3$ particles are attached

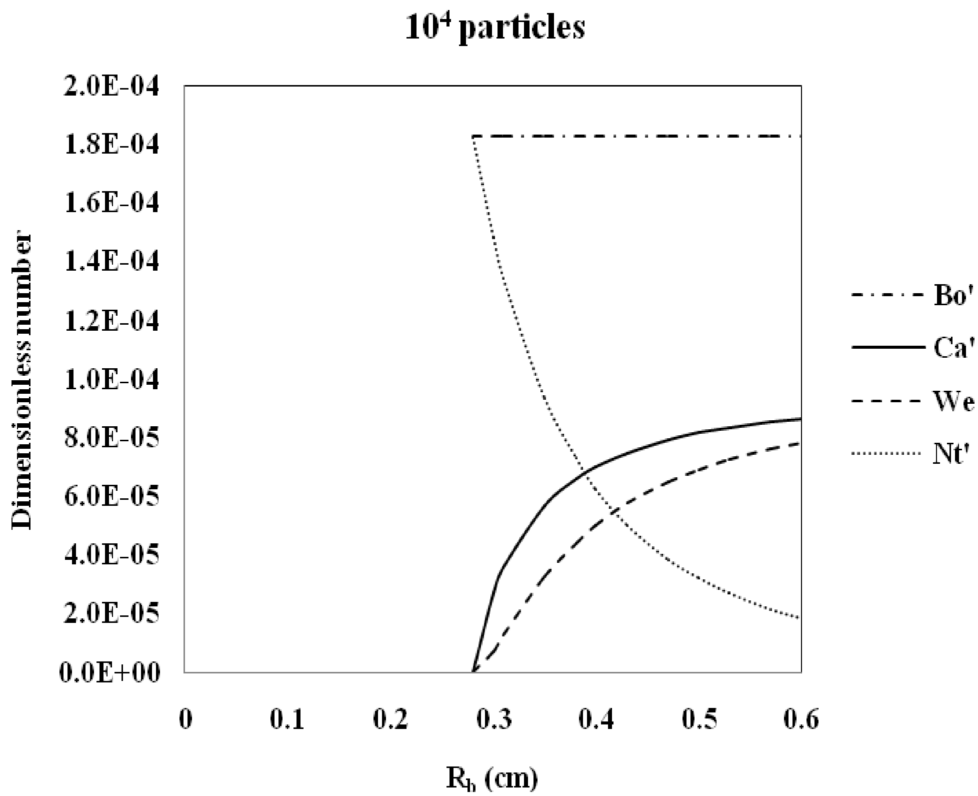


Figure 5.8 Modified dimensionless numbers as a function of the bubble radius when $10^4$ of particles are attached

**5-2-2 Relationship of the modified dimensionless numbers with the effect of attached particles**

Figure 5.9 - 5.12 illustrate relationship between the modified dimensionless numbers ($Bo'$, $Ca'$, We, and $Nt'$) and the particle-bubble unit with various number of particles (100, 500, 1000, 5000, and 10000). In figure 5.9, the modified Bond number ($Bo'$) is increased with increasing the radius of the particle-bubble unit in porous media. When attached particles on a bubble are increased, the profile of the modified Bond number ($Bo'$) moves left hand side to right hand side which means that the number of particles are increased with decreasing the modified Bond number ($Bo'$). However, the range of the modified Bond number ($Bo'$) is $10^{-10}$. Thus, as seen in figure 5.4 - 5.8, the modified Bond number ($Bo'$) does not change with increasing a radius of bubble. In figure 5.10, the modified Capillary number ($Ca'$) and Weber number (We) is increased with increasing the bubble's radius. However, the modified Capillary number ($Ca'$) and Weber number (We) is decreased with increasing attached particles on a bubble and the starting points of bubble's radius are different. On the other hand, the modified Trapping number ($Nt'$) is increased with increasing attached particles on a bubble. The starting points of bubble's radius with 100 particles is 0.122 cm, that of bubble's radius with 500 particles is 0.138 cm, that of bubble's radius with 1000 particles is 0.153 cm, that of bubble's radius with 5000 particles is 0.225 cm, and that of bubble's radius with 10,000 particles is 0.28 cm. As a result, the particle-bubble unit in porous media can be stuck or trapped among pore body or pore throat by attachment of particles on a bubble. As mentioned previously, relationship between various dimensionless numbers and Reynolds number can provide more specific analysis for the particle-bubble unit movement and the effect of individual forces acting on the particle-bubble unit in porous media.

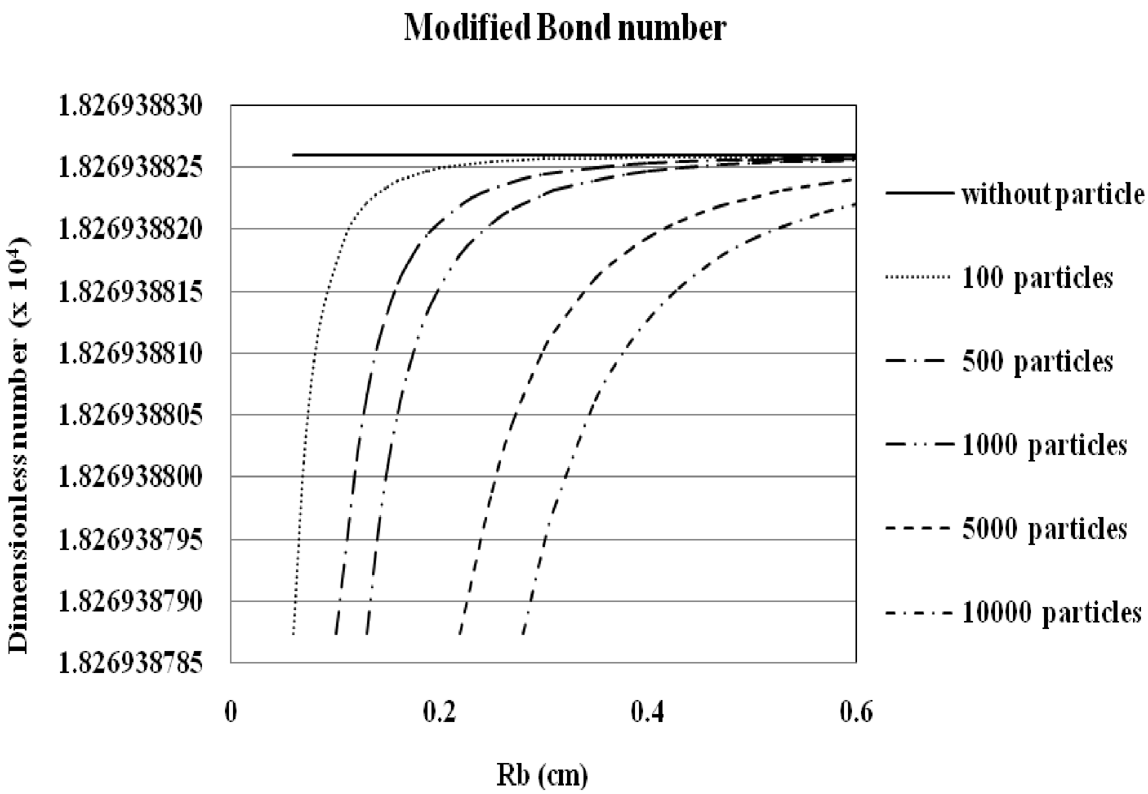


Figure 5.9 Relationship between modified Bond number (Bo′) and the particle-bubble unit with various number of particles (100, 500, 1000, 5000, and 10000)

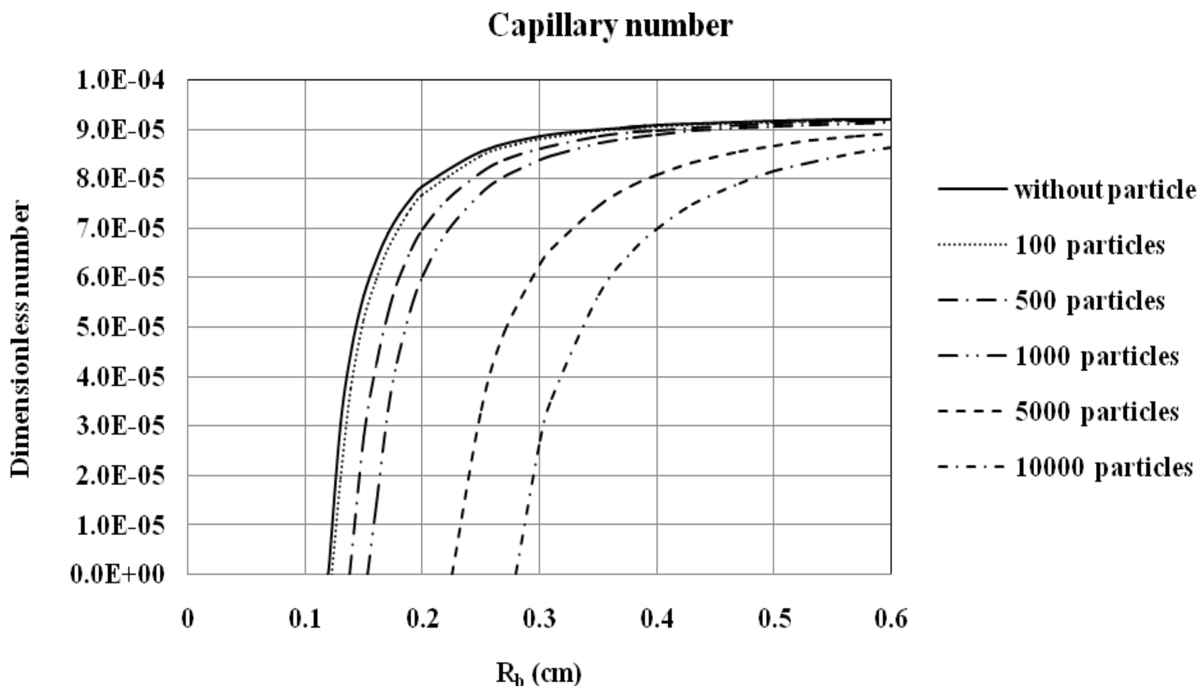


Figure 5.10 Relationship between modified Capillary number (Ca′) and the particle-bubble unit with various number of particles (100, 500, 1000, 5000, and 10000)

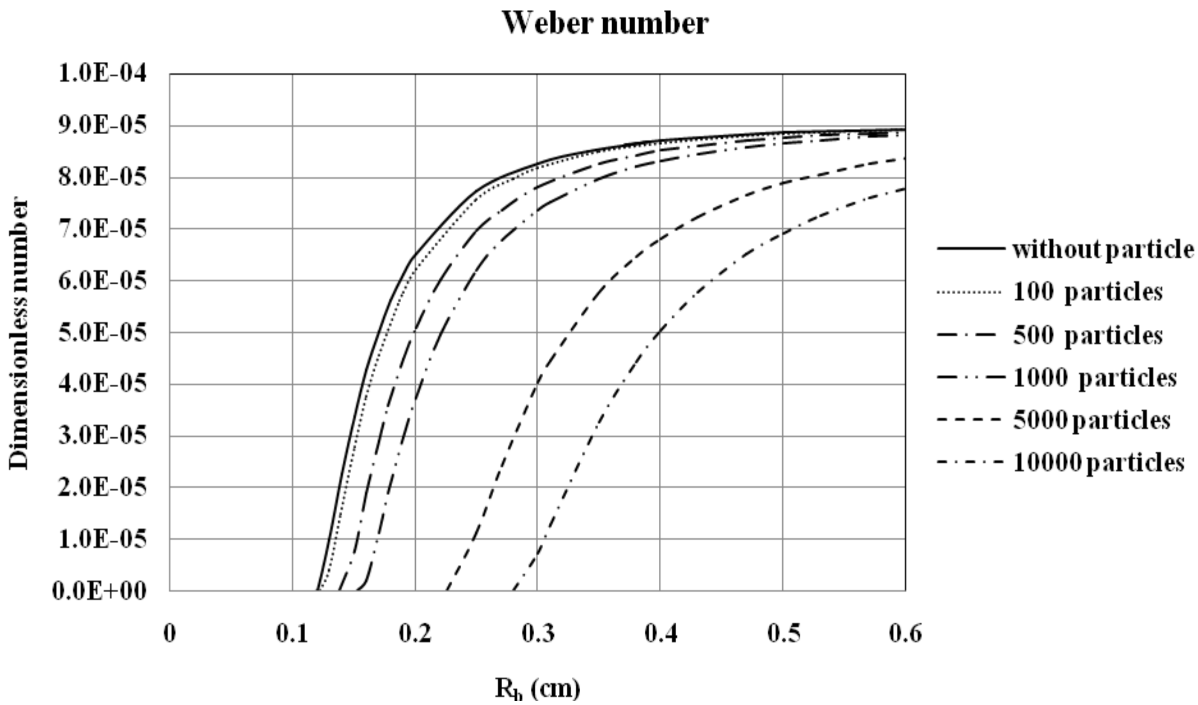


Figure 5.11 Relationship between Weber number (We) and the particle-bubble unit with various number of particles (100, 500, 1000, 5000, and 10000)

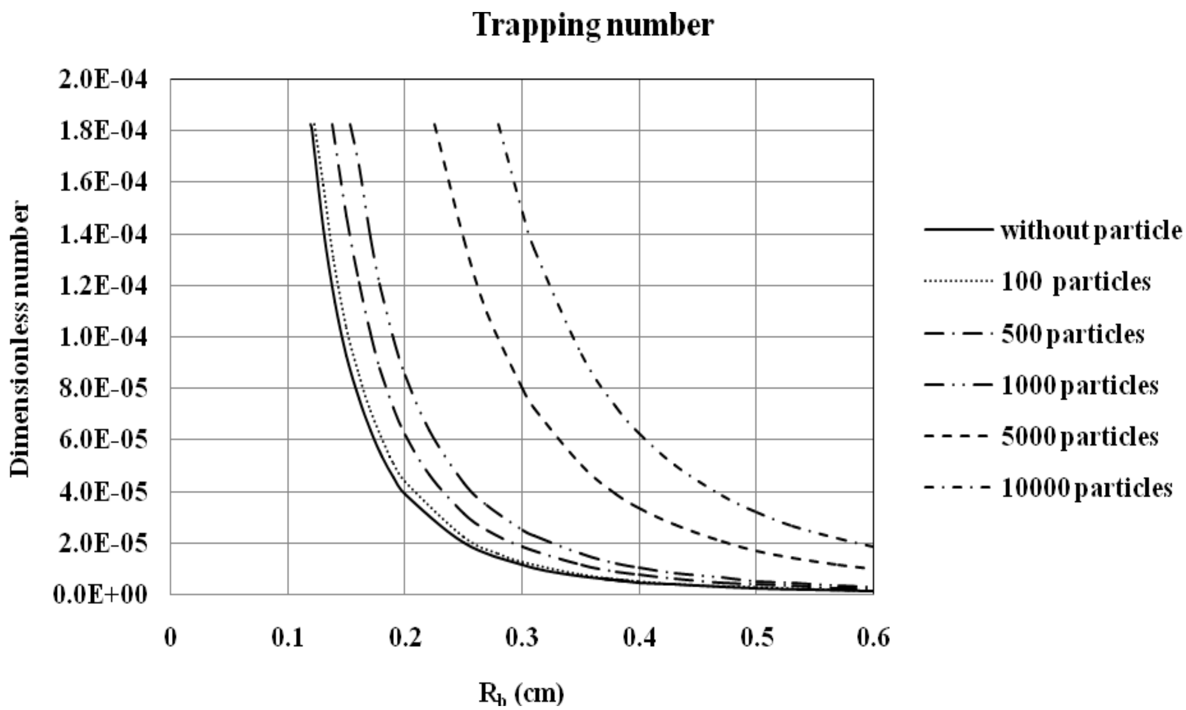


Figure 5.12 Relationship between modified Trapping number (Nt) and the particle-bubble unit with various number of particles (100, 500, 1000, 5000, and 10000)

**5-2-3 Relationship between the modified dimensionless numbers and Reynolds number**

Figure 5.13 - 5.17 shows a log-log plot of the modified Bond number ($Bo'$), the modified Capillary number (Ca), Weber number, and the modified Trapping number with a function of Reynolds number as increasing attached particles on a bubble. Lines of the modified dimensionless number for the particle-bubble unit's movement have a turning point in the same manner of dimensionless number lines for a bubble without particle. In figure 5.13, the critical Re at the turning point is about 540 and the particle-bubble unit's radius at this point is about 0.19 cm for a bubble with 100 particles in porous media. Compared with a bubble without particle, critical Re and radius of the particle-bubble unit with 100 particles is almost similar. In figure 5.14 - 5.17, the critical Re at the turning point is about 601, 670, 1000, and 1440 for a bubble with 500, 1000, 5000, and 10000 particles. The particle-bubble unit's radius at this point is about 0.22, 0.25, 0.38 and 0.51cm for a bubble with 500, 1000, 5000, and 10000 particles. When attached particles on a bubble in porous media are increased, the critical Re at the turning point is increased and the particle-bubble unit's radius at this point is also increased. Thus, the particle-bubble unit's radius dominated by surface tension at the turning point is getting larger since surface tension of a particle adds up that of a bubble in porous media. As same as Trapping number (Nt) for a bubble without particle, the modified Trapping number ($Nt'$ ) is also constant with increasing Reynolds number. Thus, insignificant radius of the particle-bubble unit is increased with increasing the modified Trapping number (($Nt'$ ) at the turning point.

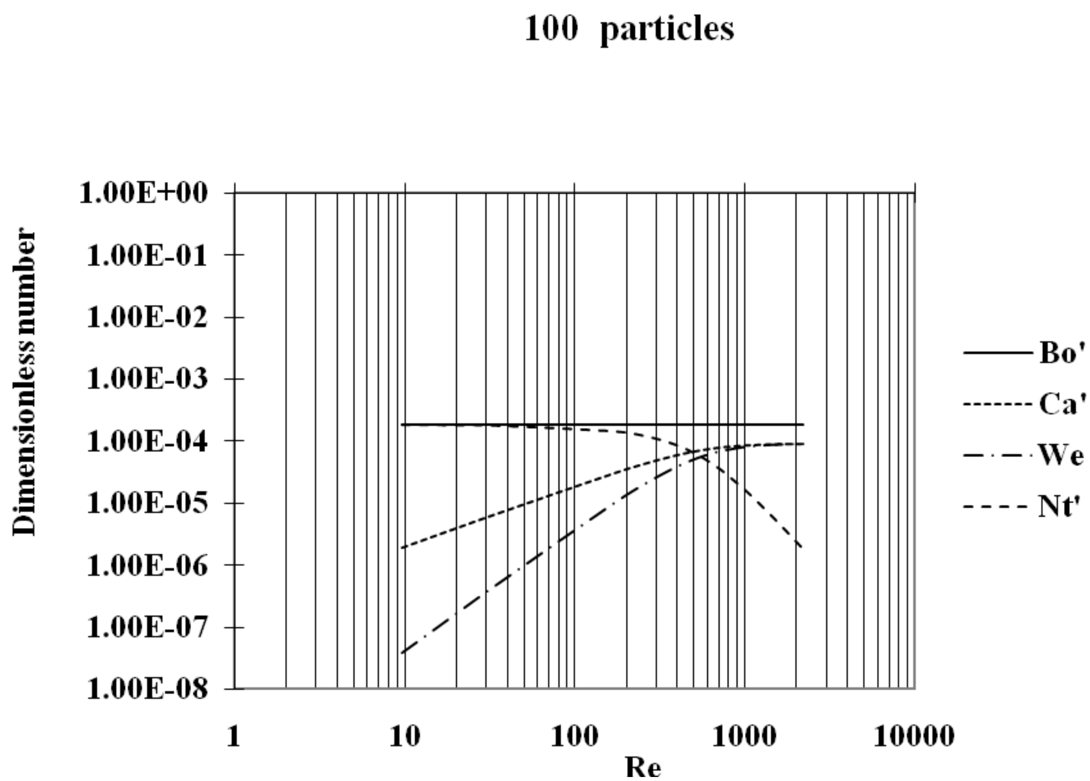


Figure 5.13 Variations of modified dimensionless numbers (Bo′, Ca′, We, and Nt′) as a function of Reynolds number (Re) when 100 particles are attached on a bubble

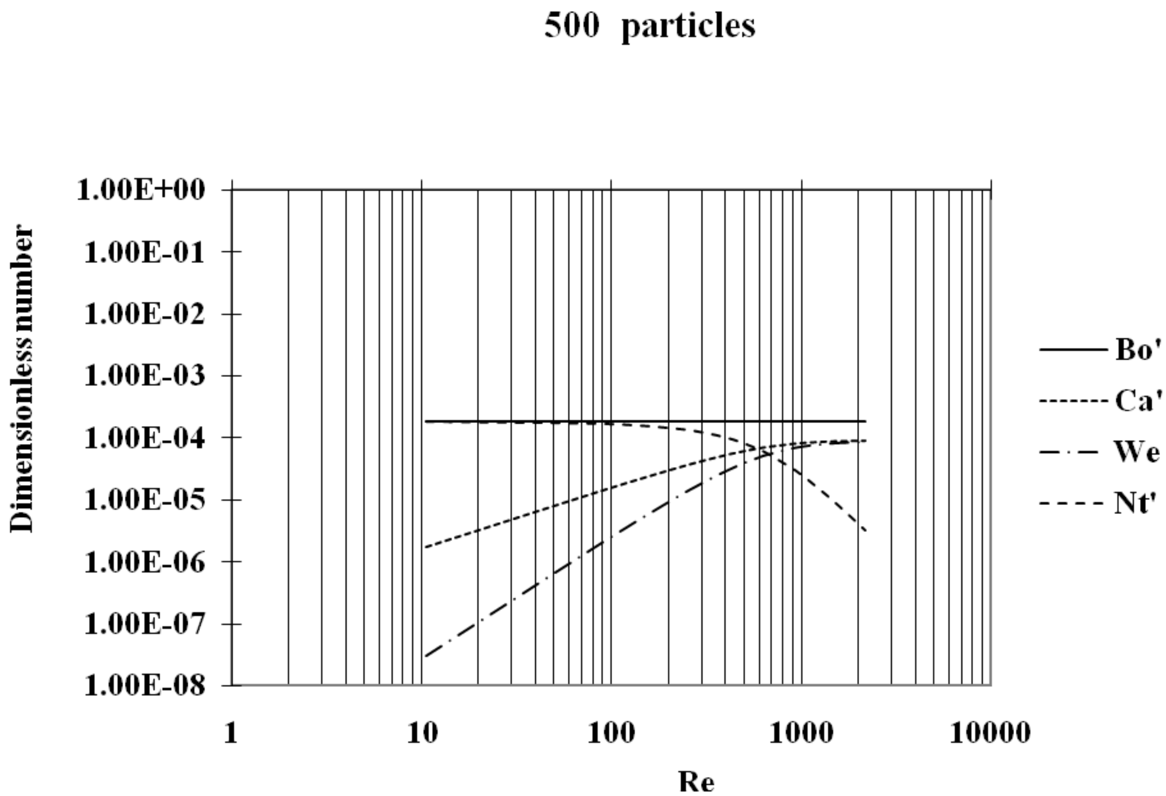


Figure 5.14 Variations of modified dimensionless numbers (Bo′, Ca′, We, and Nt′) as a function of Reynolds number (Re) when 500 particles are attached on a bubble

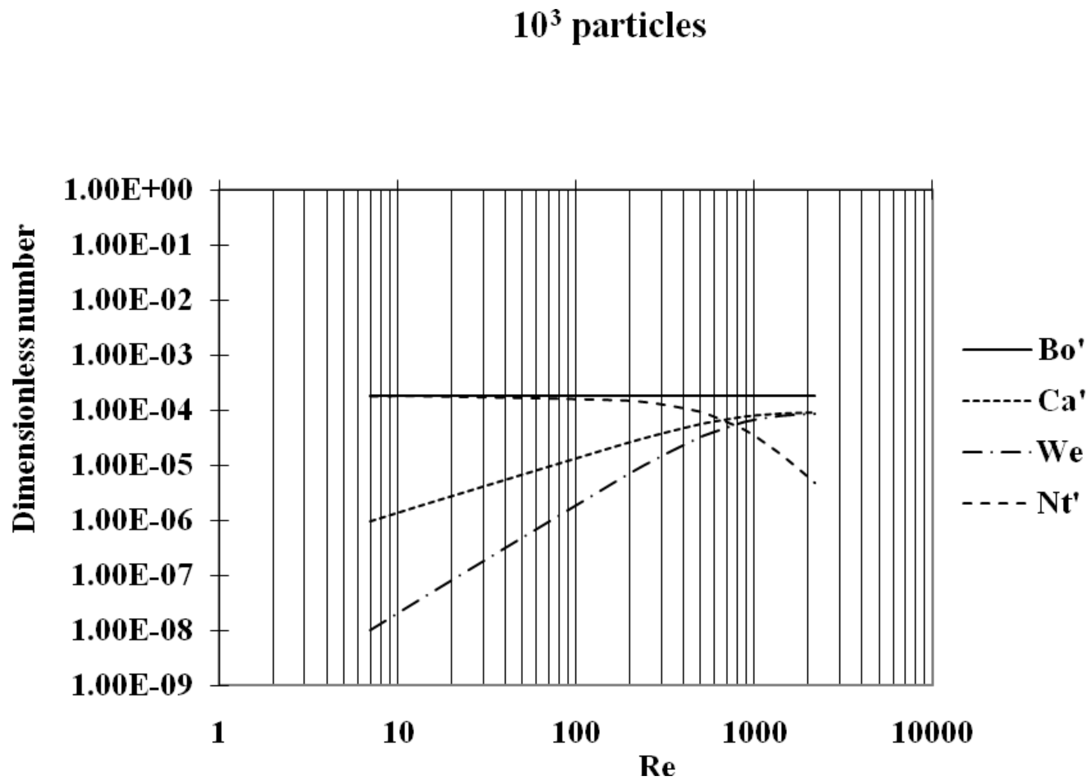


Figure 5.15 Variations of modified dimensionless numbers (Bo′, Ca′, We, and Nt′) as a function of Reynolds number (Re) when $10^3$ particles are attached on a bubble

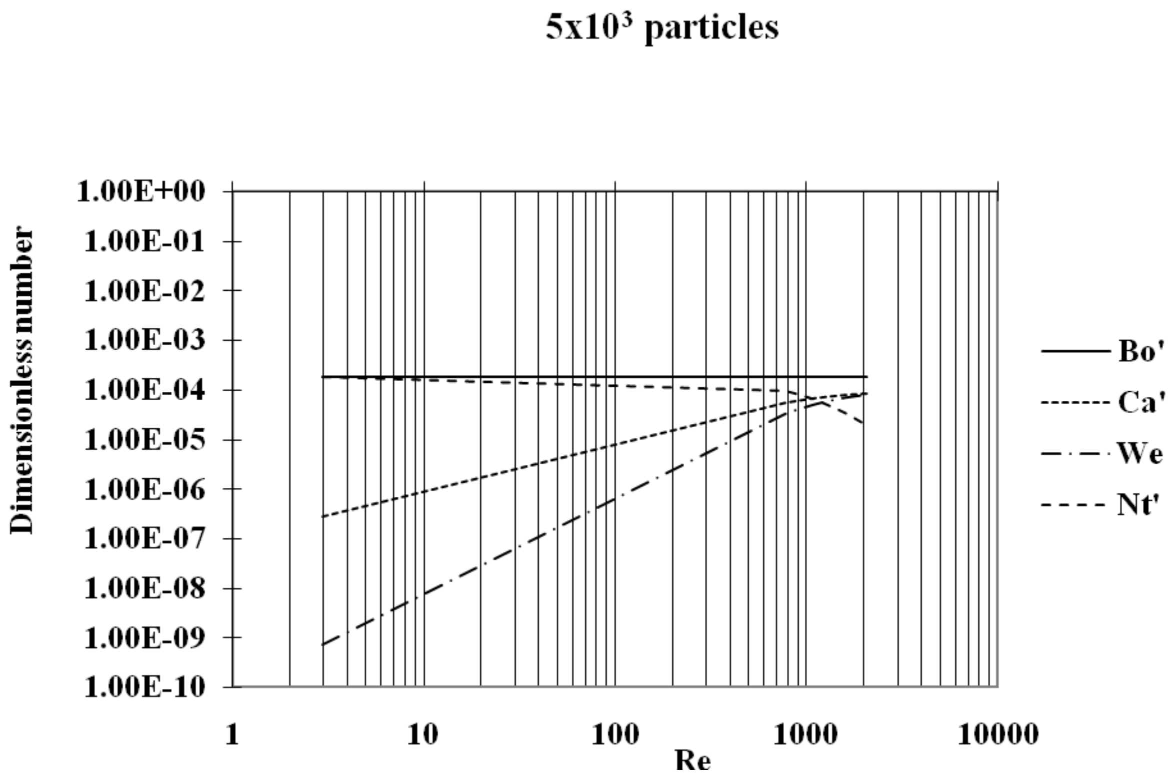


Figure 5.16 Variations of modified dimensionless numbers (Bo′, Ca′, We, and Nt′) as a function of Reynolds number (Re) when $5x10^3$ particles are attached on a bubble

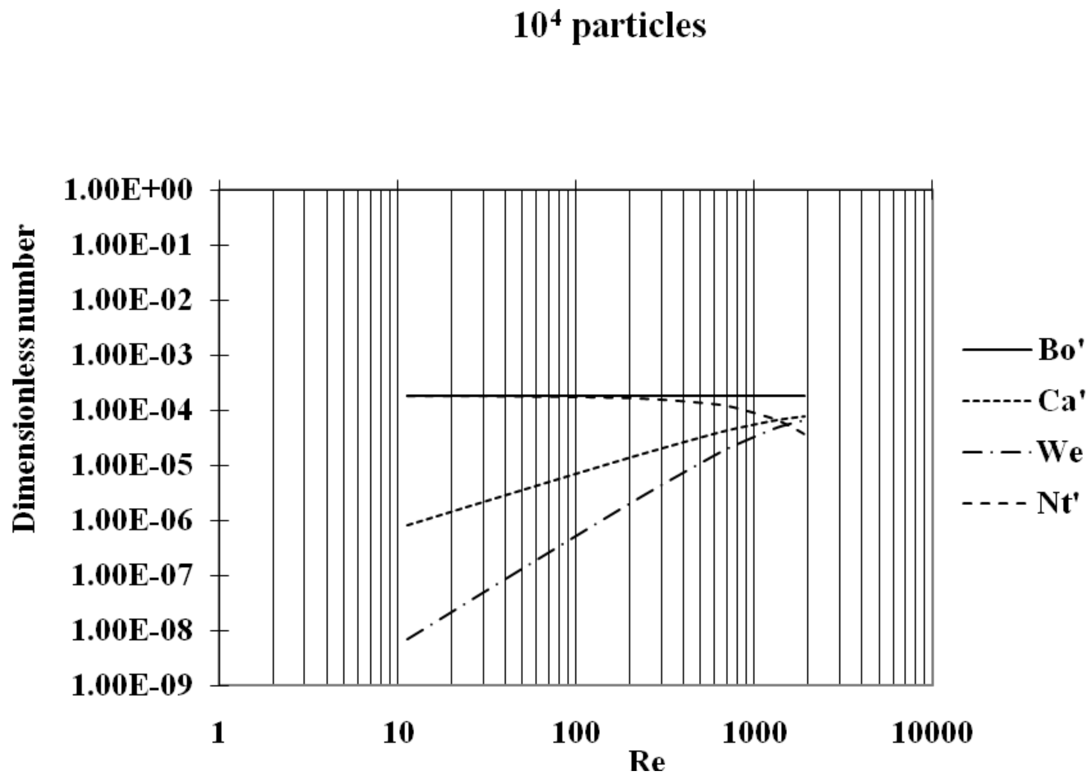


Figure 5.17 Variations of modified dimensionless numbers (Bo′, Ca′, We, and Nt′) as a function of Reynolds number (Re) when $10^4$ particles are attached on a bubble

**5-2-4 Relationship between Bo′, Ca′, We and Nt′**

As same as the dimensionless analysis for a bubble without a particle, each of the modified dimensionless numbers is divided by the modified Trapping number (Nt′), and then another dimensionless analysis for predicting the functional dependence of one modified dimensionless group in response to orders of magnitude changes in another dimensionless group is obtained. Its expression is given by

$$\frac{Bo'}{Nt} - \frac{Ca'}{Nt} - \frac{We'}{Nt} = 1 \qquad (5.21)$$

The definition of the ratio of the modified dimensionless number for the particle-bubble unit is same as that of the ratio of dimensionless number for a bubble without a particle in porous media. Thus, the meaning of Bo′/Nt′ = 1 is that the particle-bubble unit might be stuck or trapped in porous media. Figure 5.18 - 5.22 illustrate the ratio of the modified dimensionless numbers (Bo′, Ca′, We) to Trapping number (Nt′) with a function of Reynolds number (Re) when various numbers of particles are attached on the particle-bubble unit. Each term of equation 5.21 has three different lines with sharp changes at same value of Re. When 100 particles are attached on the particle-bubble unit, the critical Re at the turning point is 540 and the particle-bubble unit's radius at this point is 0.19 cm. When $R_b \leq 0.19$ cm, Re ≤ 540, Bo′/Nt′ is almost constant and a slope of We/ Nt′ to Re is 2 and a slope of Ca′/ Nt′ to Re is 1. Reversely, When $R_b \geq 0.19$ cm, Re ≥ 540, a slope of Bo′/Nt′to Re is 2.6, a slope of We/ Nt′ to Re is 2 and a slope of Ca′/ Nt′ to Re is 2. These values for the particle-bubble unit with 100 particles are almost same as for a bubble without a particle. In case of the particle-bubble unit with 500 particles, the critical Re at the turning point is 601 and the particle-bubble unit's radius at this

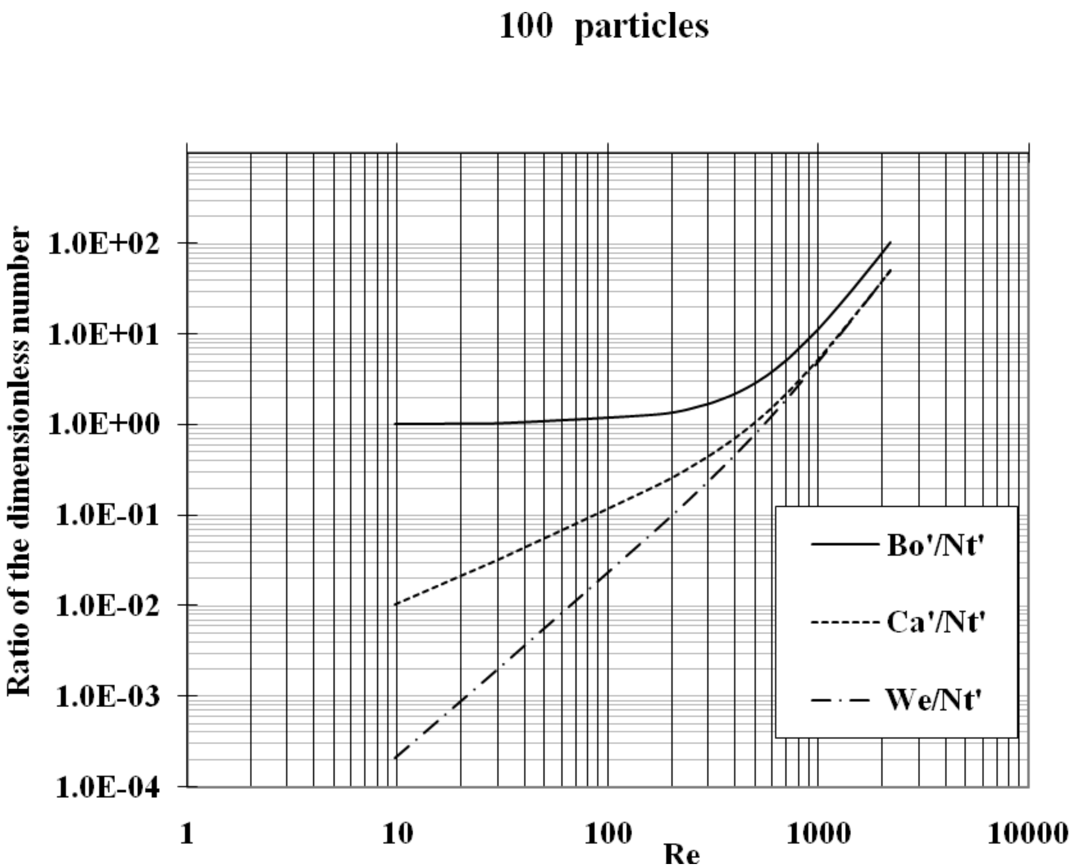


Figure 5.18 The ratio of modified dimensionless numbers (Bo′, Ca′, We) to Trapping number (Nt′) with Reynolds number (Re) when 100 particles are attached on a bubble

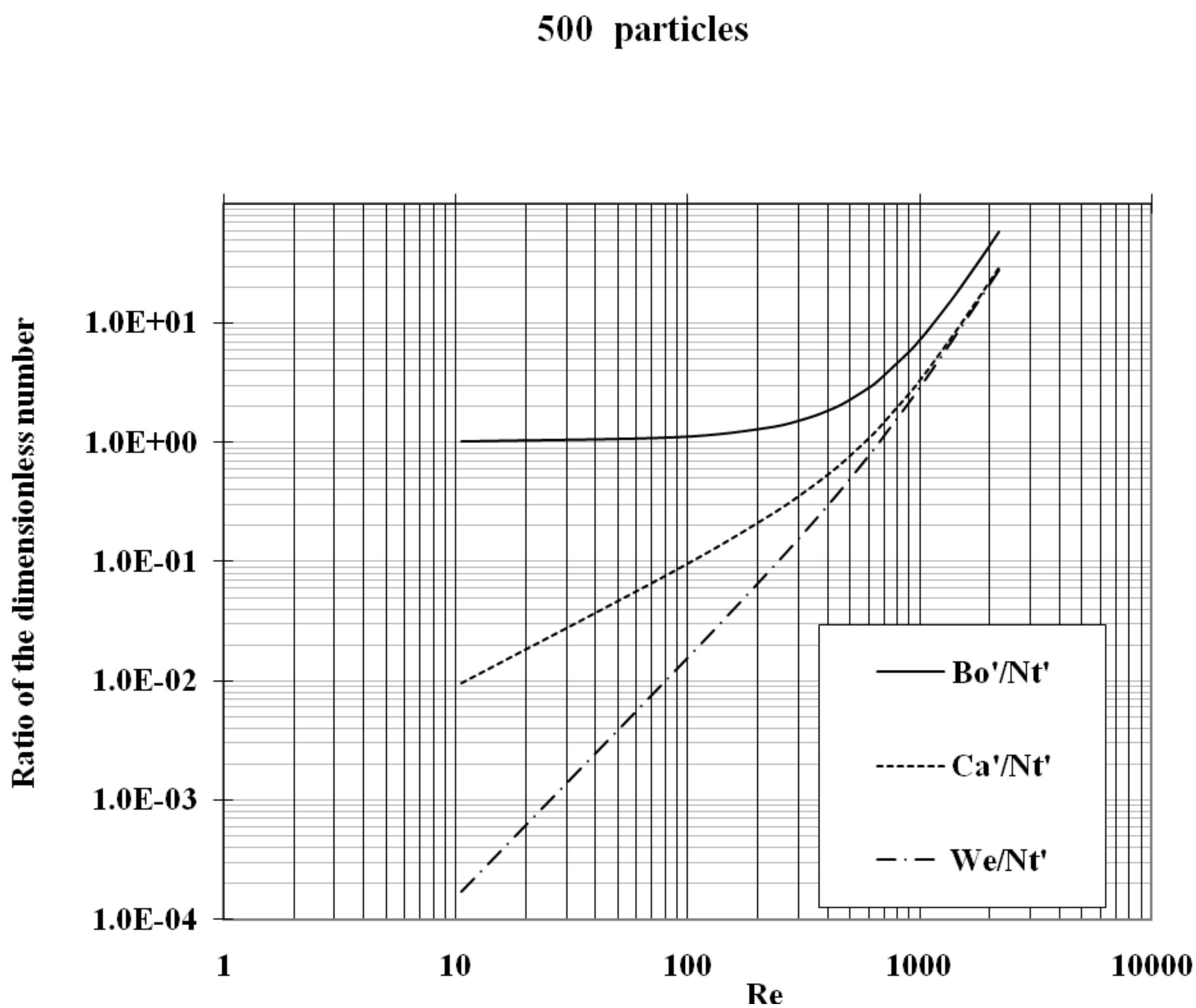


Figure 5.19 The ratio of modified dimensionless numbers (Bo′, Ca′, We) to Trapping number (Nt′) with Reynolds number (Re) when 500 particles are attached on a bubble

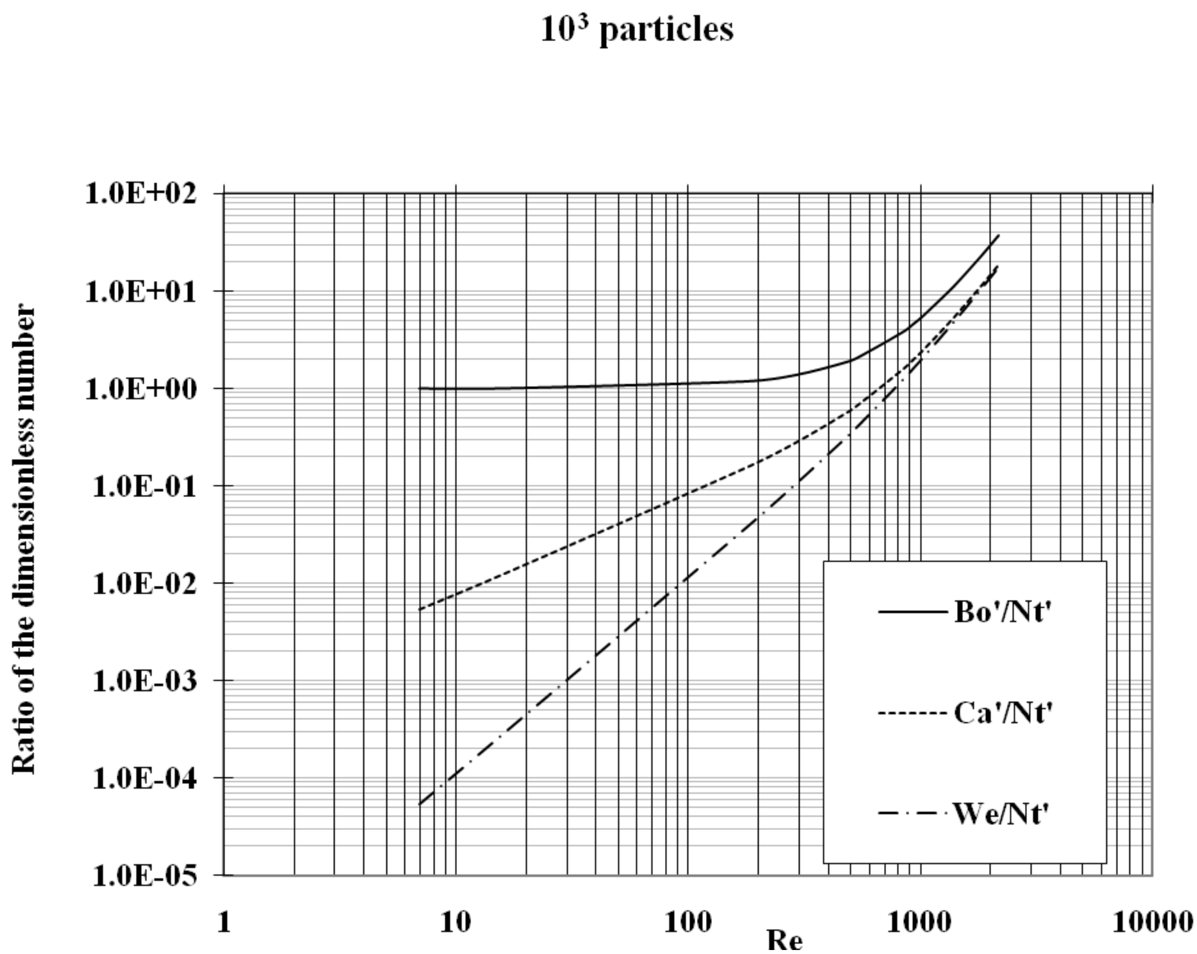


Figure 5.20 The ratio of modified dimensionless numbers (Bo′, Ca′, We) to Trapping number (Nt′) with Reynolds number (Re) when $10^3$ particles are attached on a bubble

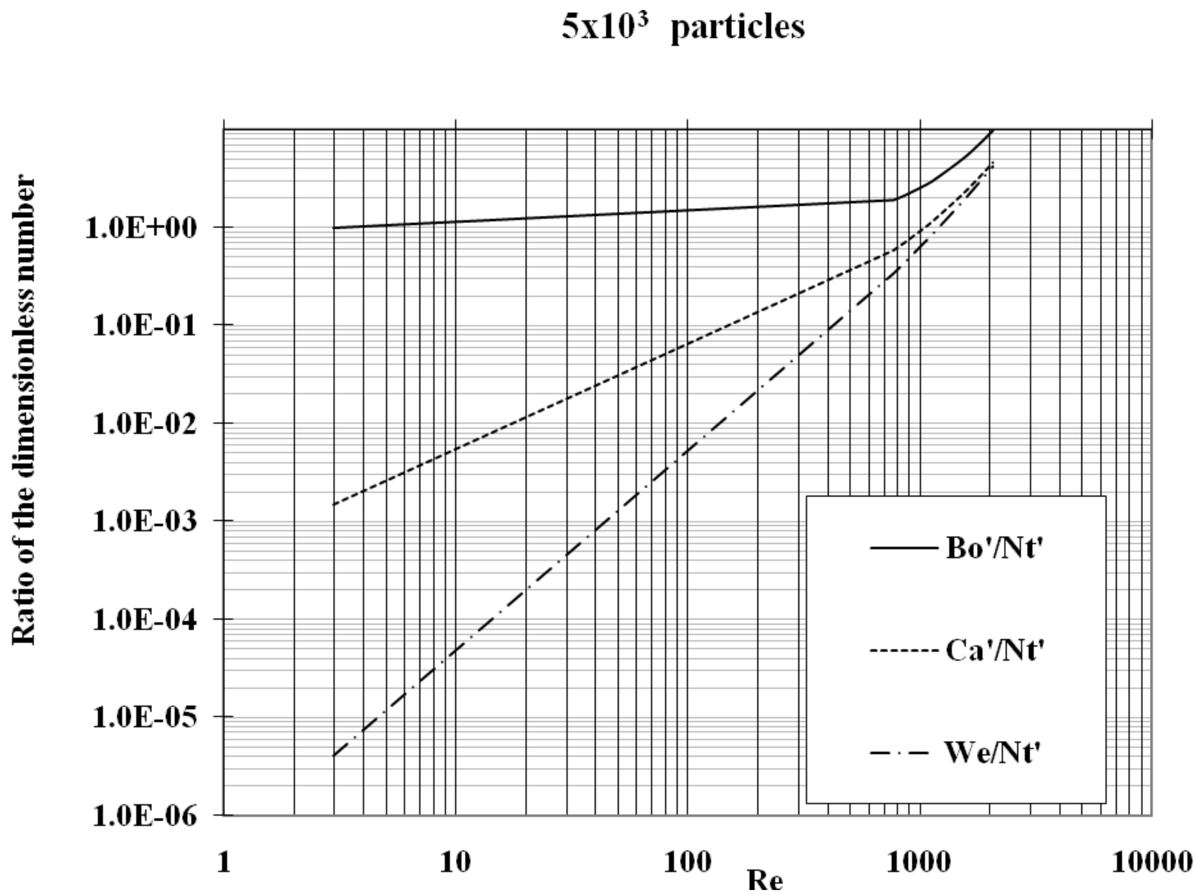


Figure 5.21 The ratio of modified dimensionless numbers (Bo′, Ca′, We) to Trapping number (Nt′) with Reynolds number (Re) when $5x10^3$ particles are attached on a bubble

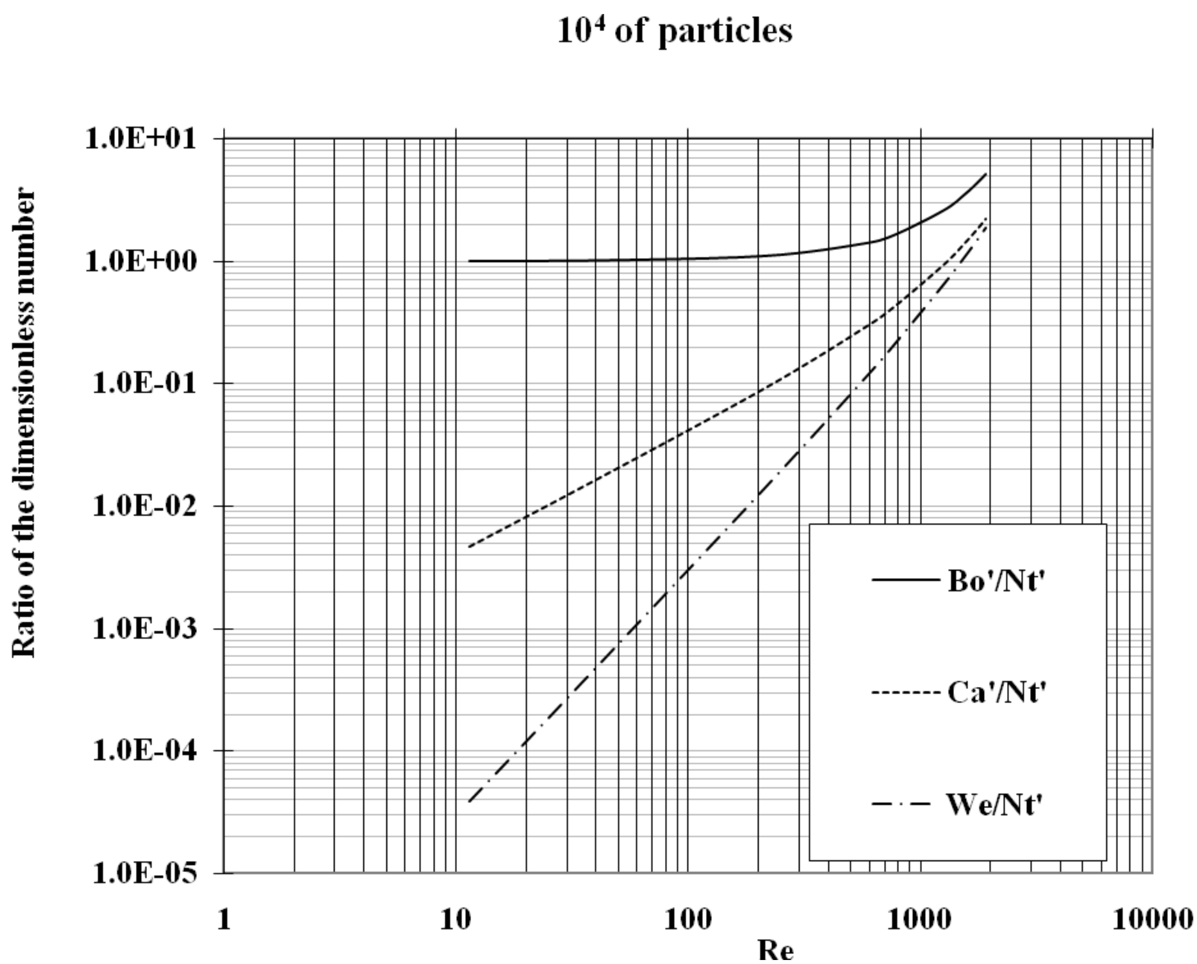


Figure 5.22 The ratio of modified dimensionless numbers (Bo′, Ca′, We) to Trapping number (Nt′) with Reynolds number (Re) when $10^4$ particles are attached on a bubble

point is 0.22 cm. When $R_b \leq 0.22$ cm, $Re \leq 601$, $Bo'/Nt'$ is almost constant and a slope of $We/Nt'$ to Re is 2.2 and a slope of $Ca'/Nt'$ to Re is 1.3. Reversely, When $R_b \geq 0.22$ cm, $Re \geq 601$, a slope of $Bo'/Nt'$ to Re is 2, a slope of $We/Nt'$ to Re is 2.6 and a slope of $Ca'/Nt'$ to Re is 1.8. In case of the particle-bubble unit with 1000 particles, the critical Re at the turning point is 670 and the particle-bubble unit's radius at this point is 0.25 cm. When $R_b \leq 0.25$ cm, $Re \leq 670$, $Bo'/Nt'$ is almost constant and a slope of $We/Nt'$ to Re is 2.1 and a slope of $Ca'/Nt'$ to Re is 1.3. Reversely, When $R_b \geq 0.25$ cm, $Re \geq 670$, a slope of $Bo'/Nt'$ to Re is 2, a slope of $We/Nt'$ to Re is 3.1 and a slope of $Ca'/Nt'$ to Re is 2.4.

In case of the particle-bubble unit with 5000 particles, the critical Re at the turning point is 1000 and the particle-bubble unit's radius at this point is 0.38 cm. When $R_b \leq 0.38$ cm, $Re \leq 1000$, $Bo'/Nt'$ is almost constant and a slope of $We/Nt'$ to Re is 2.1 and a slope of $Ca'/Nt'$ to Re is 1.1. Reversely, When $R_b \geq 0.38$ cm, $Re \geq 1000$, a slope of $Bo'/Nt'$ to Re is 5, a slope of $We/Nt'$ to Re is 8 and a slope of $Ca'/Nt'$ to Re is 3. In case of the particle-bubble unit with 10000 particles, the critical Re at the turning point is 1440 and the particle-bubble unit's radius at this point is 0.51 cm. When $R_b \leq 0.51$ cm, $Re \leq 1440$, $Bo'/Nt'$ is almost constant and a slope of $We/Nt'$ to Re is 1.9 and a slope of $Ca'/Nt'$ to Re is 1.2. Reversely, When $R_b \geq 0.51$ cm, $Re \geq 1440$, a slope of $Bo'/Nt'$ to Re is 4, a slope of $We/Nt'$ to Re is 6 and a slope of $Ca'/Nt'$ to Re is 2. Table 5.3 indicates summary of a slope of the ratio of the modified dimensionless number to Reynolds number with various numbers of attached particle. According to table 5.3, before the turning point, the ratio of the modified Bond number to the modified Trapping number is almost constant and the range of a slope of $Ca'/Nt'$ to Reynolds number is 1~1.3 and the range of a slop of $We/Nt'$ to Reynolds number is 1.9~2.2. That means small bubble is more affected by attachment of particles on a bubble than large bubble.

Table 5. 3 Summary of a slope of the ratio of the modified dimensionless number to Reynolds number for a bubble without or with a particle

| | *Before the turning point* | | | *After the turning point* | | |
|---|---|---|---|---|---|---|
| *Number of particle* | $\frac{Bo'/Nt'}{\mathrm{Re}}$ | $\frac{Ca'/Nt'}{\mathrm{Re}}$ | $\frac{We/Nt'}{\mathrm{Re}}$ | $\frac{Bo'/Nt'}{\mathrm{Re}}$ | $\frac{Ca'/Nt'}{\mathrm{Re}}$ | $\frac{We/Nt'}{\mathrm{Re}}$ |
| 0 | Constant | 1 | 2 | 2.5 | 2.5 | 2.5 |
| 100 | Constant | 1 | 2 | 2.6 | 2 | 2 |
| 500 | Constant | 1.3 | 2.2 | 2 | 1.8 | 2.6 |
| 1000 | Constant | 1.3 | 2.1 | 2 | 2.4 | 3.1 |
| 5000 | Constant | 1.1 | 2.1 | 5 | 3 | 8 |
| 10000 | Constant | 1.2 | 1.9 | 4 | 2 | 8 |

# 6 APPLICATION OF TERMINAL VELOCITY OF A SINGLE BUBBLE WITH OR WITHOUT THE PARTICLES IN POROUS MEDIA

## 6-1 EFFECT OF THE PROPERTY OF THE PARTICLE DURING THE MOVEMENT OF THE PARTICLE-BUBBLE UNIT IN POROUS MEDIA

In previous Sections 3, 4 and 5, the used parameters of the particle's properties are based on the hydrophobic particle for a rising the particle-bubble unit in porous media. Many researchers have classified two different types of particles which are hydrophilic and hydrophobic. [*Wan et. al*., 1994, *Wan and Wilson*, 1994, *Corapcioglu and Choi*, 1996] They have performed the colloid transport and developed a mathematical model in unsaturated porous media. They have different results of hydrophobic and hydrophilic colloid. Thus, in our study, we compared the effects of the hydrophilic particle with that of hydrophobic particle.

### 6-1-1 Definition of hydrophilic and hydrophobic particle

When a particle is attached on bubble, there are two types of particle attachment mechanism. One is the hydrophilic particle's attachment and the other is the hydrophobic particle's attachment. Definition of the hydrophilic particle is that a particle has an affinity for water and that of the hydrophobic particle is that a particle repels water. Figure 6.1 shows a diagram of hydrophilic and hydrophobic particle attachment on the bubble. As seen in figure 6.1, the hydrophilic particle is placed to inside of bubble and the hydrophobic particle is placed to outside of bubble. According to *Wan et al*. [1994], particle surface hydrophobicity is one of the most important factors to classify the hydrophilic and hydrophobic particle.

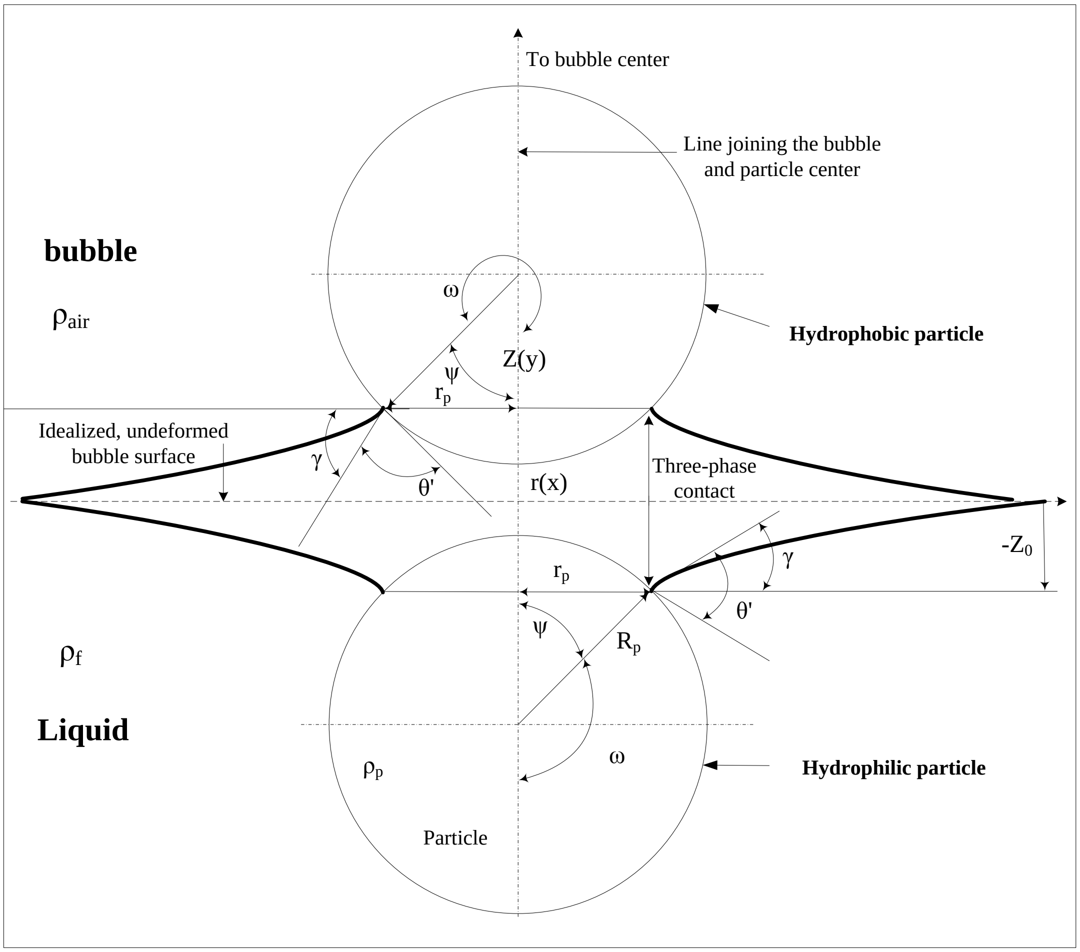


Figure 6.1 A schematic diagram of hydrophilic and hydrophobic particle attachment on the bubble

Thus, they have used "water-air contact angles of particle surfaces to characterize the relative hydrophobicity". In our study, this contact angle is used a main classification factor for the hydrophilic and the hydrophobic particle's attachment on bubble. In figure 6.1, contact angle between a particle and bubble is $\Theta'$ . If contact angle is changed, $\omega$ being the angle indicated in figure 6.1 is changed. When $\omega$ is $\pi$, a particle is completely immersed into a bubble. From the data of Wan and Wilson [1994], the contact angle ($\Theta'$) of hydrophilic particle is applied by $24.7^{o}$ and that of hydrophobic particle is applied by $77^{o}$ in our study. In geometry, an angle $\omega$ is defined by $\pi - (\Theta'-\gamma)$. Definition of an angle $\gamma$ is angular inclination of the gas-liquid meniscus at three phase contact. An angle $\gamma$ is indicated in figure 6.1 and is assumed by $30^{o}$. Therefore, an angle $\omega$ of hydrophilic particle is $185.3^{o}$ and that of hydrophobic particle is $133^{o}$. Table 6.1 indicates the summary of contact angle between a particle and bubble, an angle $\gamma$, and an angle $\omega$. This variable is applied to equation 4.24, and then the terminal velocity of the particle-bubble in porous media is calculated and simulated.

Table 6. 1 Summary of $\Theta'$ between a particle and bubble, an angle $\gamma$, and an angle $\omega$

| *Particle type* | *Contact angle ($\Theta'$)* | *Angle $\gamma$* | *Angle $\omega$* |
|---|---|---|---|
| Hydrophilic particle | $24.7^{o}$ | $30^{o}$ | $185.3^{o}$ |
| Hydrophobic particle | $77^{o}$ | $30^{o}$ | $133^{o}$ |

*Wan and Wilson* [1994]

**6-1-2 Effect of hydrophilic and hydrophobic particle for the movement of the particle-bubble unit in porous media**

Figure 6.2 shows the terminal velocity of the particle-bubble unit in porous media for the hydrophilic particle with various particle attachment and figure 6.3 illustrate the terminal velocity of the particle-bubble unit in porous media for the hydrophobic particle with various particle attachments. As seen in figure 6.2 and figure 6.3, there are big different velocity profiles with various particles attachment and starting point of the particle-bubble unit in porous media. In hydrophilic particle attachment, the terminal velocity profile of the particle-bubble unit with less than 1000 particles is similar to that of bubble without particle. The terminal velocity of the particle-bubble unit in porous media with 5000 and 10000 particles is slower than that of bubble without particle. As mentioned before, starting point of bubble radius without particle is 0.119 cm. In attachment of particles on bubble in porous media, that of bubble radius with 100 particles is 0.119 cm, that of bubble radius with 500 particles is 0.122 cm, that of bubble radius with 1000 particles is 0.125 cm, that of bubble radius with 5000 particles is 0.142 cm, and that of bubble radius with 10,000 particles is 0.16 cm.

Otherwise, in hydrophobic particle attachment, the terminal velocity profile of the particle-bubble unit with 100 particles in porous media is almost same as that of bubble without particle in porous media. That of the particle-bubble unit in porous media with over 500 particle moves to right hand side of graph that means this bubble is much slower than that of bubble without particle in porous media. Starting point of bubble radius with 100 particles is 0.128 cm, that of bubble radius with 500 particles is 0.152 cm, that of bubble radius with 1000 particles is 0.179 cm, that of bubble radius with 5000 particles is 0.279 cm, and that of

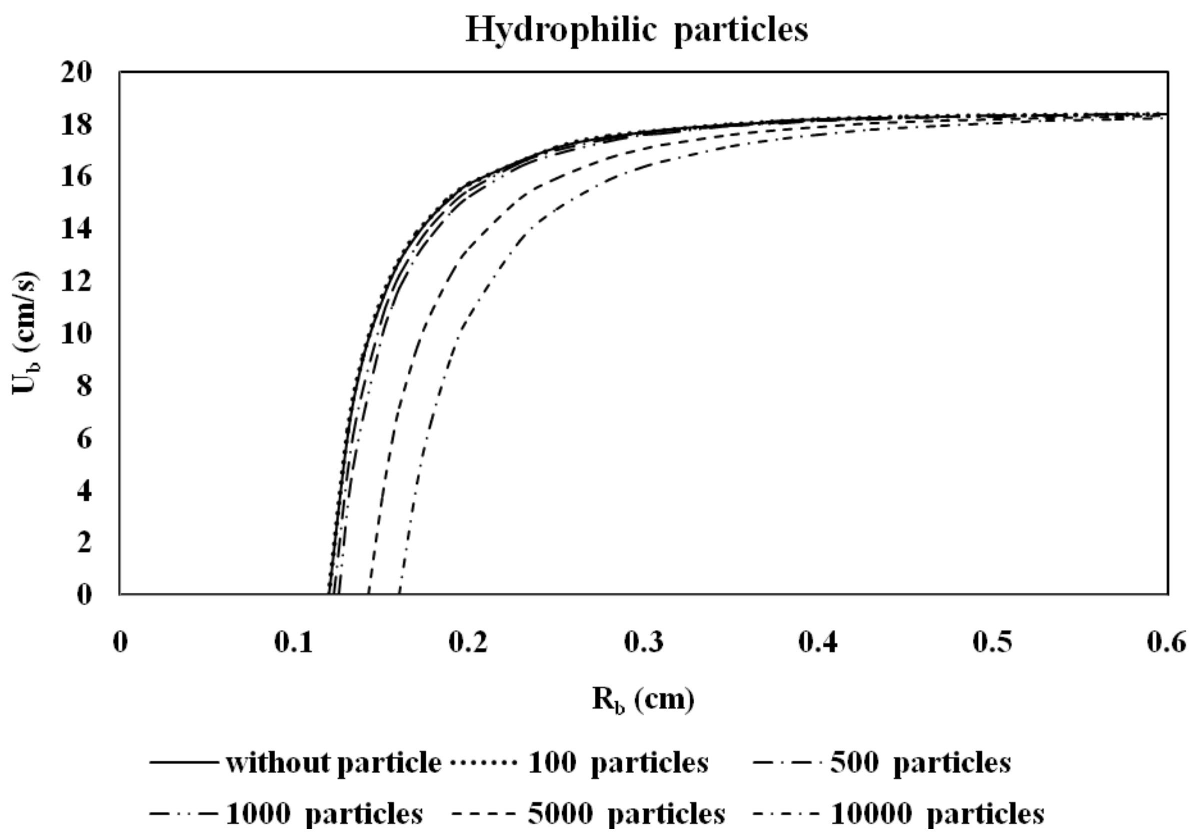


Figure 6.2 The terminal velocity of the particle-bubble unit in porous media for the hydrophilic particle with various particles attachment

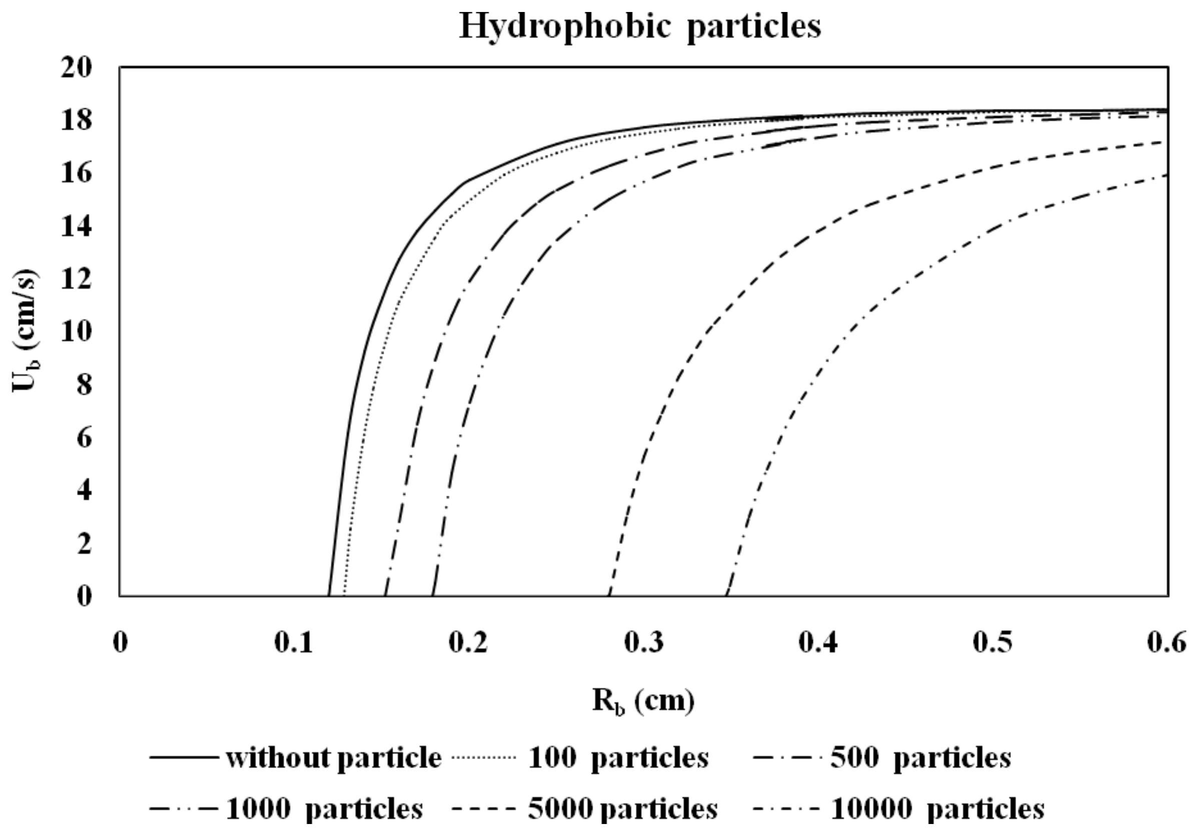


Figure 6.3 The terminal velocity of the particle-bubble unit in porous media for the hydrophobic particle with various particles attachment

bubble radius with 10,000 particles is 0.347 cm. As these results, the terminal velocity of bubble with hydrophobic particle is much slower than that of bubble with hydrophilic particle. In other words, effect of hydrophobic particle is much higher than that of hydrophilic particle. The force acting on rising bubble with particle consists of buoyant force, drag force, and surface tension force. Contact angle between the particle and bubble is related to surface tension force. According to *Corapcioglu and Choi* [1996], the hydrophobic particle has more affinity to the air-water interface than to the solid grain and the hydrophilic particle has less affinity for both solid grain and the air-water interface. When a bubble with particle goes upward in porous media, the sum of surface tension of the hydrophilic particle-bubble unit is less affected than that of the hydrophobic particle-bubble unit. As described in Section 3, surface tension is key factor of decreasing the terminal rising velocity of a bubble with or without particle. Thus, the terminal velocity of a bubble with hydrophilic particle is much faster than that of a bubble with hydrophobic particle in porous media and the trapping possibility of a bubble with hydrophobic particle is much higher than that of a bubble with hydrophilic particle. Figure 6.4 - 6.8 illustrate the comparison between the terminal velocity with hydrophilic particle and with hydrophobic particle as increasing the number of particles (100, 500, 1000, 5000, 10000). The terminal velocity of a bubble with less than 1000 of hydrophilic particles is almost same as that of a bubble without particle. Otherwise, the terminal velocity of a bubble with less than 100 of hydrophobic particles is similar to that of a bubble without particle. Thus, effect of a bubble with hydrophobic particle is 10 times more than that of a bubble with hydrophilic particle.

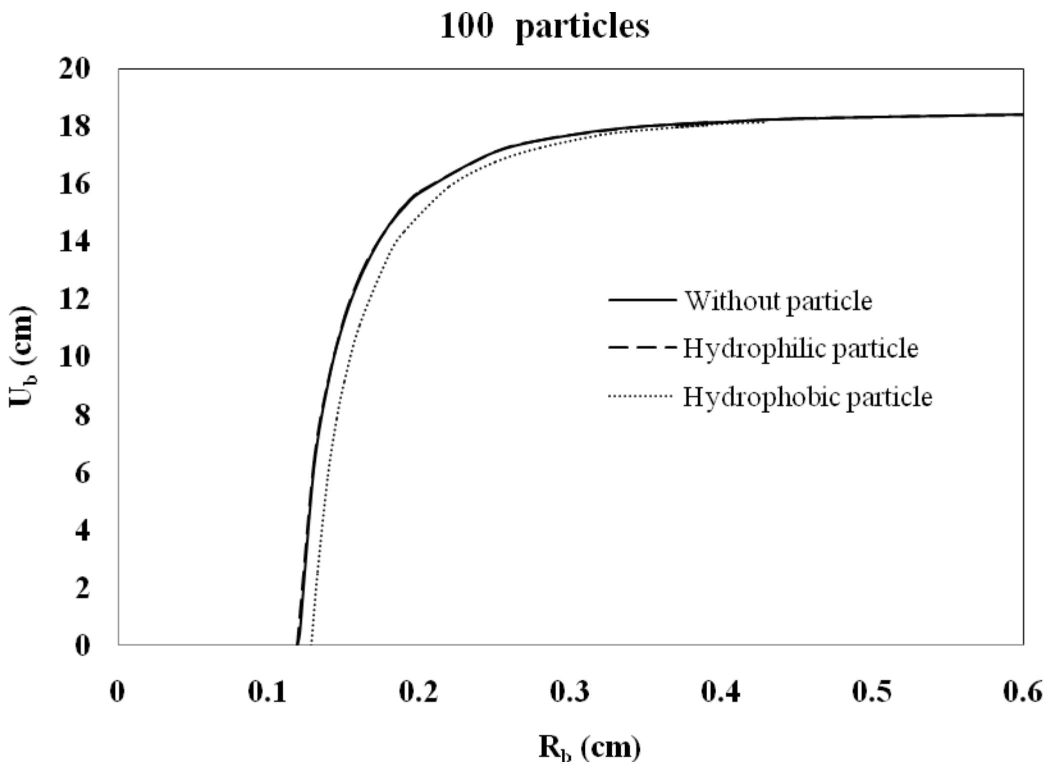


Figure 6.4 Comparison between the terminal velocity with hydrophilic particles and with hydrophobic particles when 100 particles are attached on a bubble in porous media

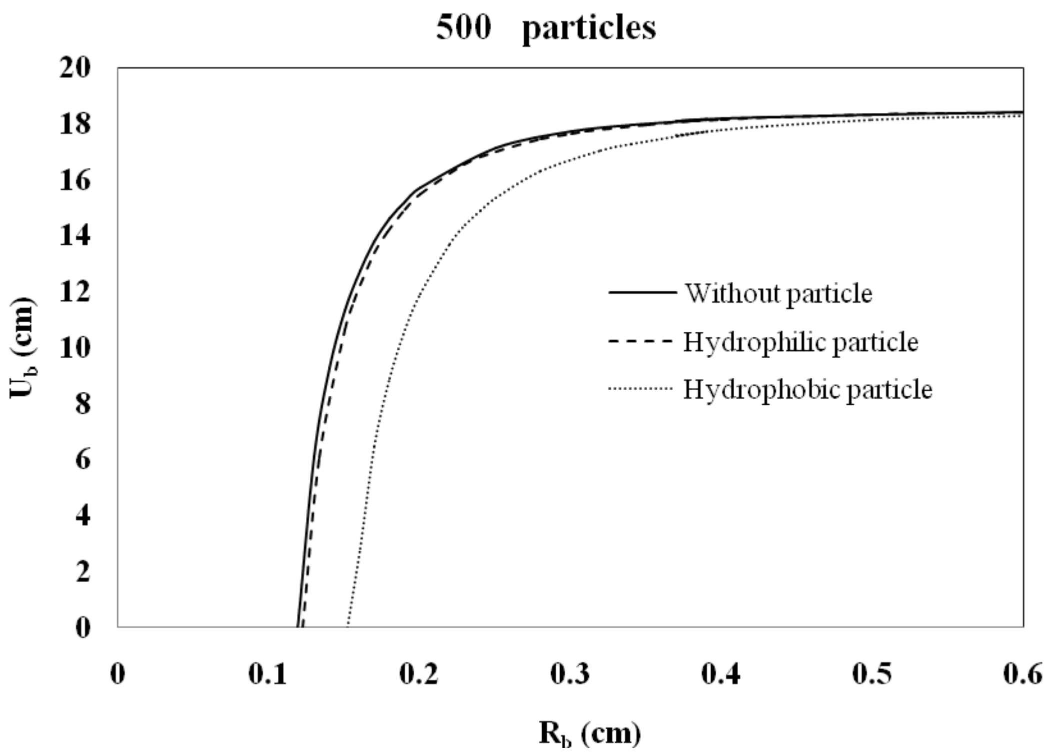


Figure 6.5 Comparison between the terminal velocity with hydrophilic particles and with hydrophobic particles when 500 particles are attached on a bubble in porous media

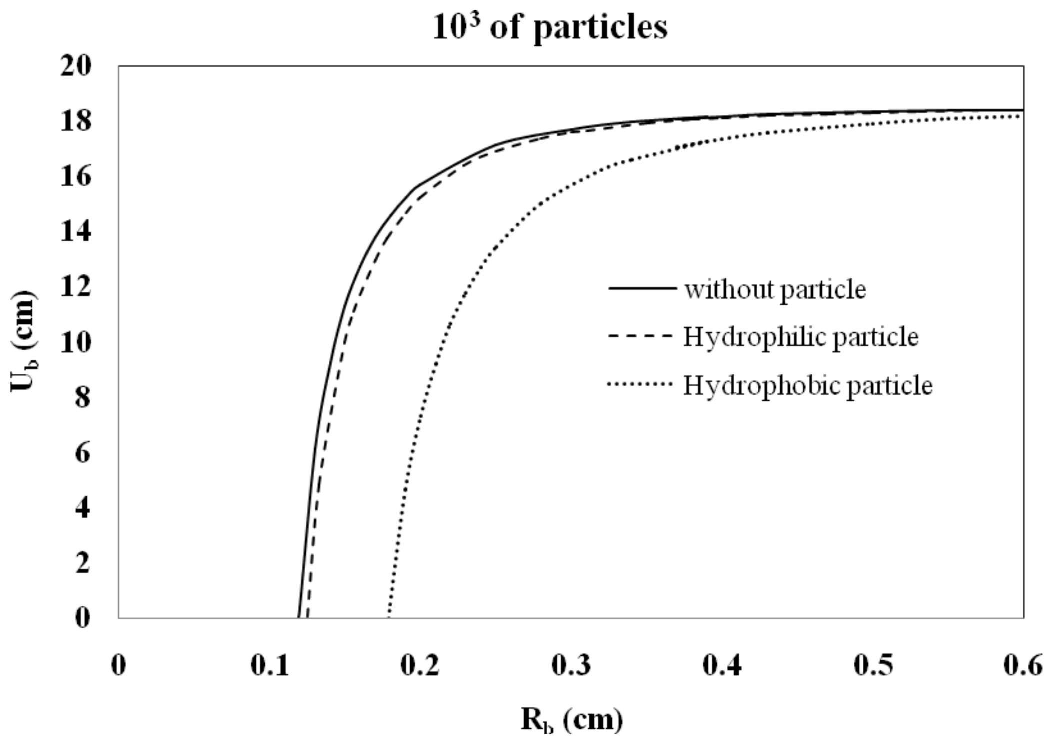


Figure 6.6 Comparison between the terminal velocity with hydrophilic particles and with hydrophobic particles when $10^3$ particles are attached on a bubble in porous media

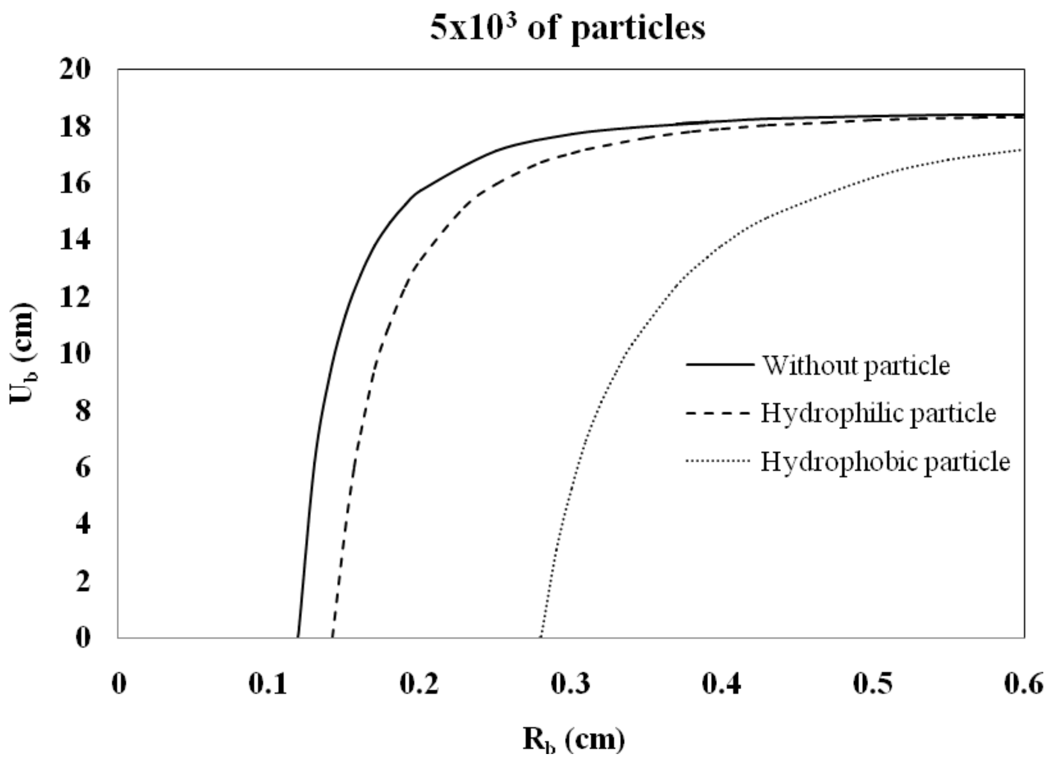


Figure 6.7 Comparison between the terminal velocity with hydrophilic particles and with hydrophobic particles when $5x10^3$ particles are attached on a bubble in porous media

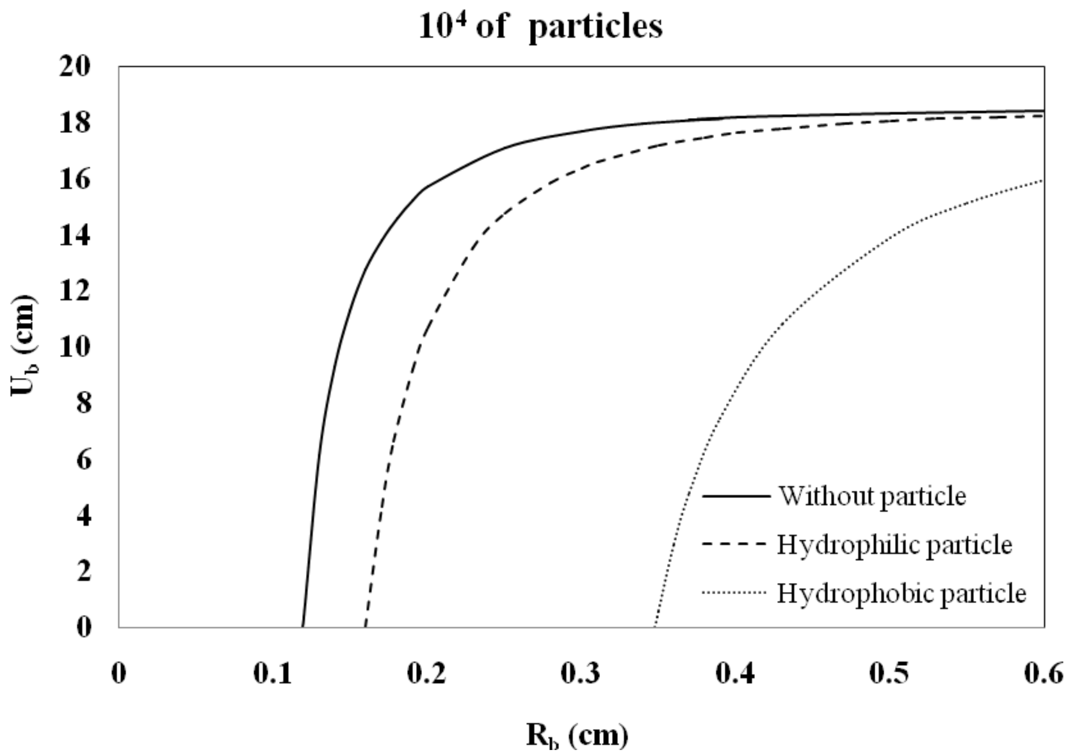


Figure 6.8 Comparison between the terminal velocity with hydrophilic particles and with hydrophobic particles when $10^4$ particles are attached on a bubble in porous media

## 6-2 APPLICATION OF THE TERMINAL VELOCITY OF THE PARTICLE-BUBBLE UNIT IN POROUS MEDIA

### 6-2-1 Overview

The principle of contaminant removal in air sparging technique is based on the mass transfer process between air and water phase in a saturated porous media. An air-water mass transfer mechanism occurs when an air bubble is injected to the groundwater and gets in touch with water. In simple model, it can be assumed that the contaminant is present only as dissolved Volatile Organic Compound (VOC) which dose not react with water or with solid grains and sorption effects of contaminant with solid grains may be neglected. Therefore, molecular diffusion and advection are only processes which are included in this simple model occurring in a single bubble movement. When a bubble rise through a porous medium, dissolved VOC in groundwater can be moved to a single bubble from the groundwater. This contaminated bubble need to be removed or treated by a soil vapor extraction (SVE). This Section consists of two parts. The first part of this Section presents a derivation of the governing equation of VOC removal concentration in a single bubble. The equation indicates the rising of a single bubble containing the VOC in a porous media. This equation is derived using mass transfer between immobile water and mobile gas phase in a steady state. Secondly, based on the governing equation of VOC removal, effect of various radii of a bubble and numbers of particle is performed.

### 6-2-2 Governing equation of VOC removal concentration in a single bubble

For this simple model, the first step in the derivation of the governing equation of the VOC removal rate in the bubble movement needs a review of the physical laws used to build the model. The mass transfer model between the bubble and groundwater is derived from the mass transfer flux and the rate of mass transfer based on film theory and Henry's law.

From fluid mechanics, the mass flux is expressed by

$$J = \frac{1}{A_b}\frac{dm_g}{dt} \tag{6.1}$$

Where $A_b$ is the surface area of a bubble and $m_g$ is the mass of VOC in a bubble.

The mass of VOC in a bubble is the gas concentration of VOC in a bubble multiply by the volume of a bubble. Its expression is given by

$$m_g = C_g \forall_b \tag{6.2}$$

Where $C_g$ is the gas concentration of VOC in a bubble and $V_b$ is the volume of bubble.

According to the equation 6.1~2, the mass flux of a gas is expressed by

$$J = \frac{1}{A_b}\frac{dC_g \forall_b}{dt} \tag{6.3}$$

In this equation, the volume of bubble is constant since a bubble is assumed by incompressible fluid, thus equation 6.3 can be expressed by

$$\frac{dC_g}{dt} = J\,\frac{A_b}{\forall_b} \tag{6.3}$$

The rate of mass transfer is expressed by film theory in the form

$$J = k\Delta C \tag{6.4}$$

Where k is a mass transfer coefficient and ΔC is the concentration gradient between a bubble and water phase.

The equilibrium between a bubble and water phase at the interface is expressed by Henry's law in dimensionless form

$$C_g = HC_e \tag{6.5}$$

Where H is the dimensionless Henry's constant and $C_e$ is the equilibrium concentration related to solubility of a gas.

The concentration gradient is expressed by

$$\Delta C = C_0 - \frac{C_g}{H} \tag{6.6}$$

Where $C_0$ is initial concentration in water.

From equation 6.4~6, the rate of mass transfer is given by

$$J = k\left(C_0 - \frac{C_g}{H}\right) \tag{6.7}$$

Substituting equation 6.7 into equation 6.3, its expression is given by

$$\frac{dC_g}{dt} = k\frac{A_b}{\forall_b}\left(C_0 - \frac{C_g}{H}\right) \tag{6.8}$$

Inserting $A_b=4\pi R_b^2$, $V_b=4/3\pi R_b^3$ to equation 6.3 is given by

$$\frac{dC_g}{dt} = k\frac{4\pi R_b^2}{4/3\pi R_b^3}\left(C_0 - \frac{C_g}{H}\right) = \frac{3k}{HR_b}\left(HC_0 - C_g\right) \tag{6.9}$$

The solution of the equation 6.9 will be obtained by the solution of ordinary differential equation. Rearranging of the equation 6.9 is given by

$$dt = \frac{dx}{u_b} = \frac{HR_b dC_g}{3k\left(HC_0 - C_g\right)} \tag{6.10}$$

Based on this equation, the following three ordinary differential equations are obtained from the equation 6.10:

$$dt = \frac{dx}{u_b} \rightarrow t = \frac{x}{u_b} \tag{6.11}$$

$$dt = \frac{HR_b dC_g}{3k\left(HC_0 - C_g\right)} \tag{6.12}$$

$$\frac{dx}{u_b} = \frac{HR_b dC_g}{3k\left(HC_0 - C_g\right)} \tag{6.13}$$

Integrating the equation 6.12 for the initial condition $C_g = 0$ at t=0 is given by

$$C_g(t) = HC_0\left(1 - e^{-\frac{3k}{HR_b}t}\right) \tag{6.14}$$

Integrating the equation 6.13 for the initial condition $C_g = 0$ at x=0 is given by

$$C_g(x) = HC_0\left(1 - e^{-\frac{3k}{HR_b}\frac{x}{u_b}}\right) \tag{6.15}$$

Equation 6.14 indicates that the gas mass concentration of VOC accumulated inside the bubble exponentially increases with time. From this equation, we can predict VOC removal amounts with time as increasing a radius of a bubble in porous media. And the change of gas mass concentration of VOC accumulated inside the bubble with the different injected depths can be obtained by equation 6.15.

**6-2-3 Effect of a bubble's radius and particle's numbers for VOC removal by using the equation of the terminal rise velocity of a bubble in porous media**

From equation 6.14, Henry's dimensionless constant (H) and the mass transfer coefficient (k) plays an important role in a volatile organic contaminants (VOC) removal in porous media. Two factors , H and k, are related to the solubility of VOC, and more gas mass concentration of contaminant in a bubble is removed from the groundwater for high Henry's dimensionless constants. The contaminants with higher Henry's dimensionless constants are more soluble than that with lower ones. The equilibrium concentration of VOC is fastest achieved for the highest k. Many researchers have studied about the mass transfer coefficient (k) in rise phenomena for a single bubble [*Leonard and Houghton*, 1963, *Calderbank and Lochiel*, 1964]. In our study, Henry's dimensionless constant (H) and the mass transfer coefficient (k) is not considerable factor for VOC removal in porous media.

In order to predict the effect of a radius of a single bubble in porous media for VOC removal, equation 6.14 is used. And it is assumed that Henry's dimensionless constant (H) is 0.195 for benzene, the mass transfer coefficient (k) is $3 \times 10^{-5}$ cm/s for benzene and the initial concentration of contaminant is 10 mg/l. These data are represented by *Braida and Ong* [1998]. Figure 6.9 shows VOC removal concentrations with various radii (0.2, 0.3, 0.4, 0.5 and 0.6 cm) of a single bubble without particle. As seen in figure 6.9, VOC removal concentration (mg/l) inside a single bubble is increased with increasing time.

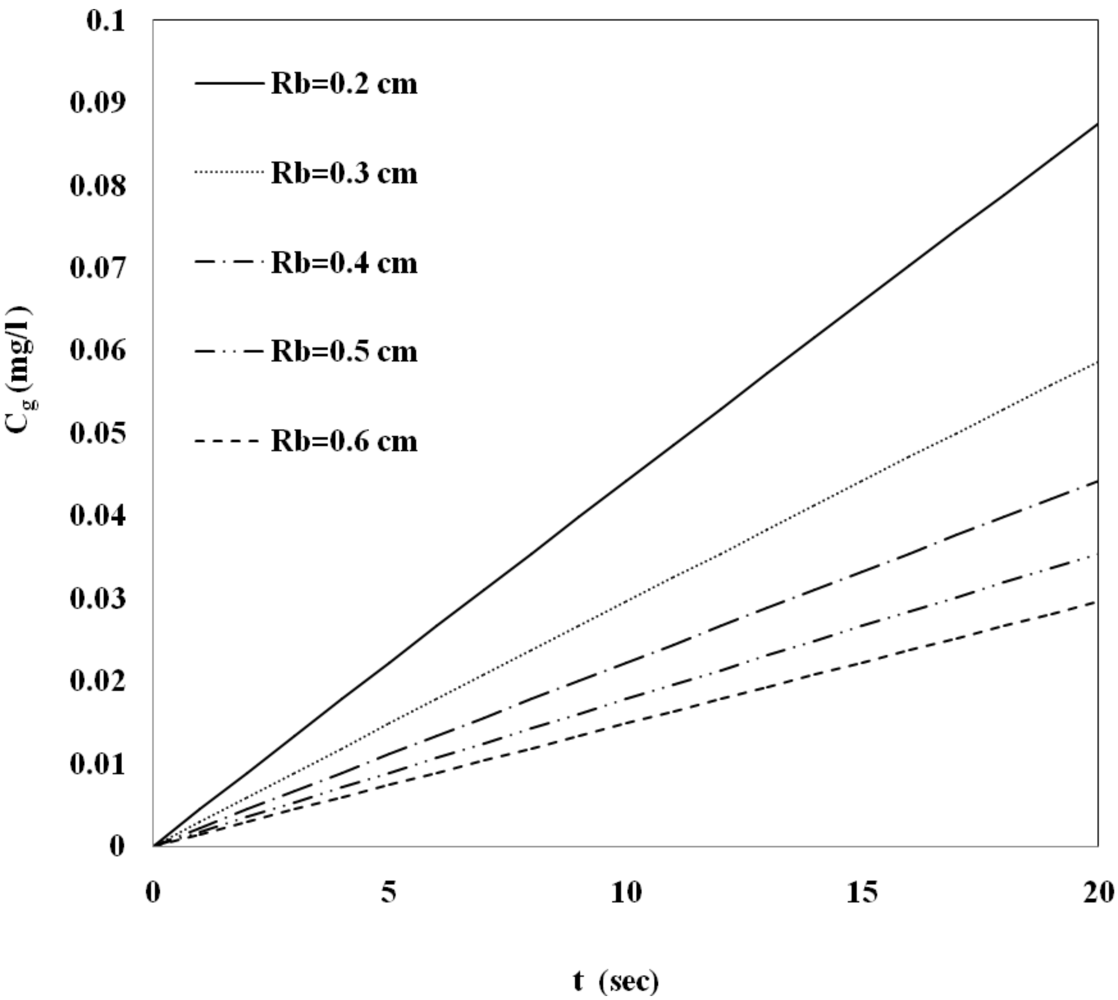


Figure 6.9 VOC removal concentrations with various radii of a single bubble without particle

The gas mass concentration of contaminant accumulated inside a bubble is increased with decreasing the radius of a bubble which means that small bubble is more effective than large bubble for VOC removal in porous media. The reason is that the terminal velocity of small bubble is slower than that of large bubble. When the terminal velocity of a bubble in porous media is slow, the contact time between a bubble and the contaminated water is long. Thus, the contact time between a bubble and the contaminated water in small bubble is much longer than that in large bubble in porous media. When the contact time is long, the mass transfer rate between a bubble and water is high. As a result, small size of a bubble is more effective and useful than large size of a bubble in VOC removal mechanism.

In order to investigate the effect of numbers of attached particles on the particle-bubble unit in porous media, equation 6.15 is applied and it is assumed that Henry's dimensionless constant, the mass transfer coefficient and the initial concentration of contaminant is same as above and the depth of column is 2m. Figure 6.10 shows VOC removal concentration with various numbers of attached particle on the particle-bubble unit with $R_b$=0.4 cm in porous media as increasing the depth. As seen in figure 6.10, VOC removal concentration is increased with increasing the numbers of attached particle on a bubble in porous media. There is no big difference at less than 1000 of particles on a bubble at 200 cm of depth. However, the effect of 5000 and 10000 of particles is noticeable. When a bubble is rising up at 200 cm of depth, the VOC removal concentration of the bubble-particle unit with less than 1000 of attached particles is about 0.024~5 mg/l. That of a bubble with 5000 attached particles is 0.032 mg/l. This value is increased by about 25 % of the VOC removal concentration of a bubble with less than 1000 of particles. In 10000 of particles attached bubble, the VOC removal concentration is 0.052 mg/l and this value is increased by over 2 times of ones of a bubble with less than 1000 of particles. As a result, the VOC removal concentration of a single bubble with higher numbers of particles is larger than that of ones with lower numbers of particles, since the terminal velocity of a bubble with higher numbers of attached particles is slower than that of ones with lower numbers of attached particles in porous media. This effect of attached particle is similar to that of size of a bubble. The terminal velocity of a bubble with lower numbers of attached particles is faster than that of ones with higher numbers of attached particles. When the terminal velocity of a bubble is fast, the contact time between gas and water phase is little. Thus, the contact time between a bubble with lower numbers of attached particles and water phase is much shorter than ones between a bubble with higher numbers of attached particles and water phase. When this time is short, the mass transfer rate between bubbles with lower numbers of attached particles is lower than ones between bubbles with higher numbers of attached particles.

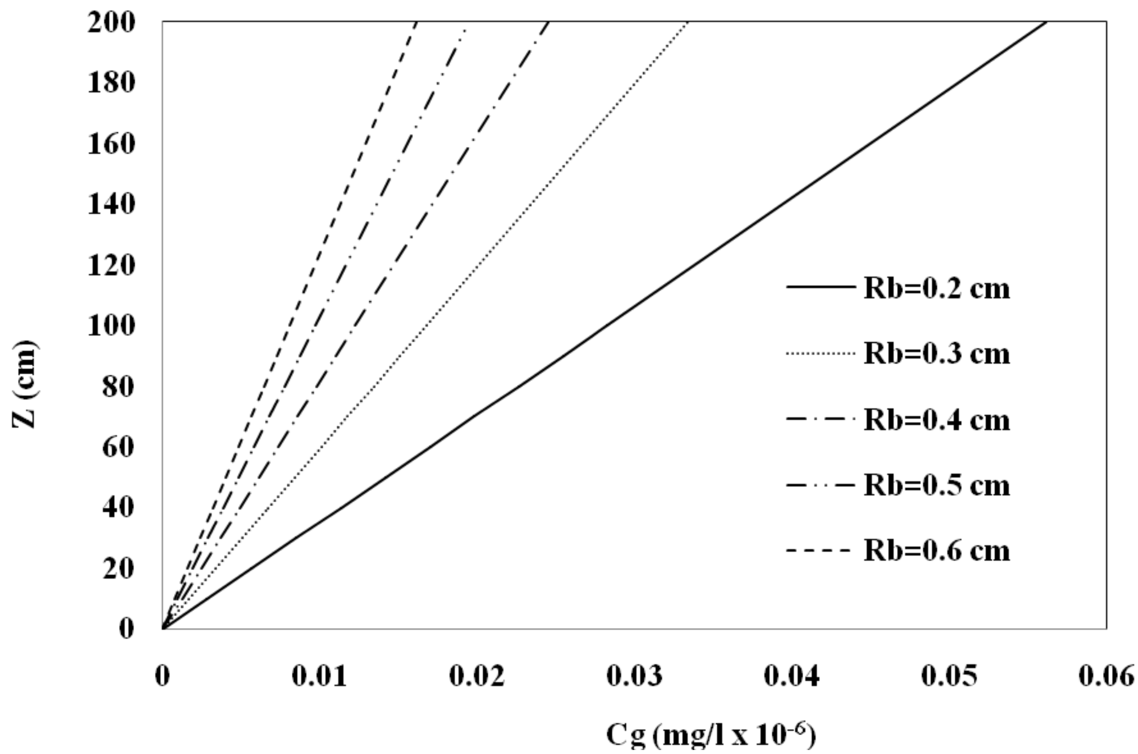


Figure 6.10 VOC removal concentration with various numbers of attached particle on a single bubble with $R_b$=0.4 cm as increasing the depth Z (cm)

# 7 SUMMARY AND CONCLUSION

When a bubble moves upward in porous media, the terminal velocity of an air bubble might be changed because of the momentum exchange between air and solid phase and between air and water phase. This change of momentum is equal to the sum of external forces acting on a bubble in porous media. These external forces are balanced by the buoyant force, surface tension, and drag force. After established external forces balance of a bubble in porous media, we can obtain the terminal rising velocity of a bubble.

When a colloidal particle is attached on a bubble in porous media, the sum of external forces could be changed by adding external forces acting on the particle-bubble unit. The additional forces for the movement of the particle-bubble unit are gravitational force, buoyant force, hydrostatic pressure force, capillary force, capillary pressure force, and drag force. However, these additional forces are presented by interaction between a bubble and an attached particle in porous media. Two of them which are hydrostatic pressure force and capillary pressure force are generated by the difference between the excess pressure in the bubble and the hydrostatic force. We can neglect these two forces because of our assumption which is that sorption process between a bubble and a particle is irreversible and there is no detachment on a particle-bubble unit. In the particle-bubble unit's movement, the buoyant force acting on the particle-bubble unit is balanced by gravitational force, surface tension, and drag force acting on the particle-bubble unit. Thus, the equation of the particle-bubble unit acting on external forces is modified and changed and then we can find the terminal rising velocity of the particle-bubble unit in porous media.

After set up the force balance equation, the terminal rising velocity of a bubble without and with a particle can be obtained. The equation of the terminal velocity has two unknown variables which are the velocity and the radius of a bubble in porous media. The other variables (such as liquid properties which are density, viscosity, and surface tension of water, gas properties which are density, viscosity of gas in a bubble, porous medium properties which are porosity and radius of pore throat and the properties of a particle which are density and size of a particle) are known parameters. Thus, the solution of the terminal velocity of a bubble without and with a particle can be obtained. The conclusions of the terminal velocity profile of a bubble without a particle are that:

- The radius of a bubble determine the bubble rise velocity
- The terminal velocity of bubble in liquid is faster than that of bubble in porous medium because of surface tension.
- The conclusions of the terminal velocity profile of a bubble with the particles are that:
- As increased the numbers of attached particle, the terminal velocity profile of the particle-bubble unit in porous media is decreased.
- Attached particle on the bubble in porous media might prevent the movement of a bubble in porous media due to surface tension of the particles.
- Surface tension of the particles is more affected than buoyant force of the particles for the particle-bubble's movement in porous media.

As the number of attached particle on the particle-bubble unit in porous media is increased, the starting point of the radius of the particle-bubble unit in porous media is increased. That means a bubble with higher numbers of the particles can be easily trapped than ones with lower numbers of the particles. As these results, the presence of the particles in porous media might enhance and improve the efficiency of an air sparging system. The effect of solid grain size ($d_p$) is another important factor for a rising bubble in porous media. The terminal velocity of a bubble without or with the particles is decreased with decreasing the size of solid grain size ($d_p$). The reason is that a bubble is hard to pass through the small size of pore throat and needs more driving force such as a buoyant force in porous media.

In the dimensionless analysis of a bubble without or with the particles, the Bond number is constant with increasing the radius of a bubble because the increase in the density of a bubble without or with the particles with decreasing the volume of bubble is not significant enough compared to the density of the water. The reason is that the movement of a bubble without or with the particles is not affected by the bubble's density with this range of the volume of bubble. In the other side, the Capillary number and Weber number is increased with increasing the radius of a bubble. This can be concluded that the viscous and the inertial force dominate the surface tension force heavily. Compared the Capillary number with Weber number, the viscous force is more affected than the inertial force for the movement of a bubble without or with the particles in porous media. Trapping number is decreased with increasing the radius of a bubble without or with the particles. This may be explained that a small size of a bubble can be more easily trapped that a large size of ones without or with the particles in porous media.

In relationship between various dimensionless numbers and the Reynolds number, the Bond number does not change with the Reynolds number because of a big difference of the density of gas and water phase. However, Capillary number, Weber number and Trapping number with increasing the Reynolds number indicates different lines with sharp changes at the almost same range of Re value. This sharp change in behavior indicates that different types of bubble movement are predicted before and after turning point. At this turning point, the magnitude of inertial force and viscous force of a bubble without or with the particles is much smaller than that of surface tension force of a bubble without a particle with less than the radius of a bubble at this turning point. Thus, the small size of a bubble without or with the particles is dominated by surface tension. In before the turning point, Trapping number is initially almost constant with increasing Reynolds number. Thus, bubble size is insignificant for the Trapping number. Capillary number initially is increased with increasing Reynolds number until the effect of viscous forces against the drag forces becomes insignificant at the turning point. Weber number (We) is increased with increasing Reynolds number until the effect of inertial forces against the drag forces becomes negligible at this turning point.

After turning point, Trapping number is gradually decreased with increasing Reynolds number (Re) since bubble size is important for the Trapping number. Capillary number is almost constant as increasing Reynolds number after turning point, thus the effect of viscous forces against the drag forces become a significant factor for rising bubble movement in porous media. The value of Capillary number is equal to that of Weber number which means that effect of viscous force is same as that of inertial force after the turning point.

In the effect of particle for the particle-bubble unit in porous media, the numbers of particles are increased with decreasing the modified Bond number. And the modified Capillary number and Weber number is decreased with increasing attached particles on a bubble. The modified Trapping number is increased with increasing attached particles on a bubble. As a result, the particle-bubble unit in porous media can be stuck or trapped among pore body or pore throat by attachment of particles on a bubble.

In the effect of the property of the particle, the terminal rise velocity of a bubble with hydrophobic attached particles is much slower than that of ones with hydrophilic attached particles. Based on our simulation, the effect of a bubble with hydrophobic particles is 10 times more than that of ones with hydrophilic particles.

The gas mass concentration of contaminant accumulated inside a bubble is increased with decreasing the radius of a bubble which means that small bubble is more effective than large bubble for VOC removal in porous media. The reason is that the terminal velocity of small bubble is slower than that of large bubble. When the terminal velocity of a bubble in porous media is slow, the contact time between a bubble and the contaminated water is long. Thus, the contact time between a bubble and the contaminated water in small bubble is much longer than that in large bubble in porous media. When the contact time is long, the mass transfer rate between a bubble and water is high. As a result, small size of a bubble is more effective and useful than large size of a bubble in VOC removal mechanism.

As a result, the VOC removal concentration of a single bubble with higher numbers of particles is larger than that of ones with lower numbers of particles, since the terminal velocity of a bubble with higher numbers of attached particles is slower than that of ones with lower numbers of attached particles in porous media. This effect of attached particle is similar to that of size of a bubble. The terminal velocity of a bubble with lower numbers of attached particles is faster than that of ones with higher numbers of attached particles. When the terminal velocity of a bubble is fast, the contact time between gas and water phase is little. Thus, the contact time between a bubble with lower numbers of attached particles and water phase is much shorter than ones between a bubble with higher numbers of attached particles and water phase. When this time is short, the mass transfer rate between bubbles with lower numbers of attached particles is lower than ones between bubbles with higher numbers of attached particles.

The results of our modeling works indicate that the effect of the colloidal particles presented in subsurface is very important for the migration of a discrete bubble in porous media. As increased the particles, the terminal velocity of a single bubble in porous media is decreased. As decreased the velocity of a bubble, the mass transfer rate of VOC is increased. Thus, the efficiency of air sparging may be increased. However, if the colloidal particles are one of target contaminant, we need more careful design criteria for air sparging. As increased the particles on a bubble, the radius of a bubble should be bigger than the possible trapped radius of a bubble.

**REFERENCES**

Adams, J.A., and K.R. Reddy (1997), The effect of grain size distribution on air sparging efficiency, in *In situ and on-site Bioremediation*, edited by B.C. Alleman, and A. Lesson, pp. 165-172, Battelle Press, Columbus, Ohio.

Bloom, F., and T. J. Heindel (1997), A theoretical model of flotation deinking efficiency, *J. Colloid Interface Sci*., *190*,182-197.

Braida, W. J., and S. K. Ong (1998), Air sparging: Air-water mass transfer coefficients, *Water Resour. Res*., *34*, 3245-3253.

Brooks, M. C., W. R. Wise, and M. D. Annable (1999). Fundamental changes in in-situ air sparging flow patterns, *Ground Water Monit. Rem.*, *19*, 105-113.

Calderbank, P. H., and A. C. Lochiel (1964), Mass transfer coefficients, velocities and shapes of carbon dioxide bubbles in free rise through distilled water, *Chem. Eng. Sci*., *19*, 485-503.

Chu, Y., Y. Jin, M. Flury, and M. V. Yates (2001), Mechanisms of virus removal during transport in unsaturated porous media, *Water Resour. Res.*, *37*, 253-263.

Corapcioglu, M. Y., and H. C. Choi (1996), Modeling colloid transport in unsaturated porous media and validation with laboratory column data, *Water Resour. Res.*, *32*, 3437-3449.

Corapcioglu, M. Y., A. Cihan, and M. Drazenovic (2004), Rise velocity of an air bubble in porous media, *Water Resour. Res*., *40*:doi:10.1029/2003WR002618.

Dai, Z., D. Fornasiero, and J. Ralston (2000), Particle-bubble collision models-a review, *Adv. Colloid and Interface Sci.*, *85*, 231-256.

DeNovio, N. M., J. E. Saiers, and J. N. Ryan (2004), Colloid movement in unsaturated porous media: Recent advances and future directions, *Vadose Zone J.*, *3*, 338-351.

Elder C.R, and C.H. Benson (1999), Air channel formation, size, spacing, and tortuosity during air sparging, *Ground Water Monit. Rem.*, *19*,171-181.

Ergun, S. (1953), Fluid flow through packed columns, *Chem.Eng.Prog*., *48*, 89-94.

Goldenberg, L. C., I. Hutcheon, and N. Wardlaw (1989), Experiments on transport of hydrophobic particles and gas bubbles in porous media, *Transp. Porous Media*, *4*, 129-145

Graton, L. C., and H. J Fraser (1935), Systematic packing of spheres with particular relation to porosity and permeability, *J.Geol*., *43*,786-909

Haberman, W. L. and R. K. Morton (1953), An experimental investigation of the drag and shape of air bubbles rising in various liquid, *Rep. 802*, David Taylor Model Basin, U.S. Dept. of the Navy, Washington, DC.

Ji, W., M. A. Dahmani, D. P. Ahlfeld, J.D. Lin, and E. Hill (1993), Laboratory study of air sparging: air flow visualization, *Ground Water Monit. Rem.*, *13*, 115-126.

Keller, A., and S. Sirivithayapakorn (2004), Transport of colloids in unsaturated porous media: Explaining large-scale behavior based on pore-scale mechanisms, *Water Resour. Res.*, *40*: doi: 10.1029/2004WR003315.

Kovscek, A. R., and C. J. Radke (1994), Fundamentals of foam transport in porous media, in *Foams*, edited by L. L. Schramm, pp. 115-163, American Chemical Society., Washington, D. C.

Langmuir, I., and K. Blodgett (1945), A mathematical investigation of water droplet trajectories, *Coll. Works of I. Langmuir*, *10*, 348-393.

Leonard, J. H., and G. Houghton (1963), Mass transfer and velocity of rise phenomena for single bubbles, *Chem. Eng. Sci*., *18*, 133-142.

Levich, V.G. (1962), *Physicochemical Hydrodynamics*, Prentice-Hall, Englewood Cliffs, N.J.

Mendelson, H. D. (1967), The prediction of bubble terminal velocities form wave theory, *AICHE J*., *13*, 250-253

Nguyen, A. (1994), The collision between fine particles and single air bubbles in flotation, *J. Colloid Interface Sci.*, *162*,123-128.

Nguyen, A., and G. M. Evans (2003), Stream function, flow separation and force equation for stagnation flow passing a small solid sphere touching a rising gas bubble, *J. of Physics A.*, *36*,9105-9117.

Ortiz-Arroyo, A., F. Larachi, and I. Iliuta (2003), Method for inferring contact angle and for correlating static liquid hold-up in packed beds, *Chem. Eng. Sci*., *58*, 2835-2855.

Peebles, F.N., and H. J. Garber (1953), Studies on the motion of gas bubbles in liquids, *Chem. Eng. Prog*., *49*, 88-97

Peterson, J. W., K. S. Murray., Y. I. Tulu., B. D. Peuler., and D. A. Wilkens (2001), Air-flow geometry in air sparging of fine-grained sands, *Hydrogeology J.*, *9*, 168-176.

Ralston, J., and S. S. Dukhin (1999), The interaction between particles and bubbles, *Colloid. Surfaces A.*, *151*, 3-14.

Ryan, J. N., and M. Elimelech (1996), Colloid mobilization and transport in groundwater, *Colloid. Surfaces A.*, *107*,1-56.

Schäfer, A., H. Harms, and A. J. B. Zehnder (1998), Bacterial accumulation at the air-water interface, *Environ. Sci. Technol.*, *32*, 3704-3712.

Schulze, H. J. (1977), New theoretical and experimental investigations on stability of bubble/particle aggregates in flotation: A theory on the upper particle size of floatability, *Int. J. Miner. Process*, *4*, 241-259.

Schulze, H. J., B. Radoev, T. Geidel, H. Stechemesser, and E. Topfer (1989), Investigations of the colloision process between particles and gas bubbles in flotation - A theoretical analysis, *Inter. J. of Min. Processing*, *27*, 263-278.

Sutherland, K. (1948), Physical chemistry of flotation XI. Kinetics of the flotation process, *J. Phys. Chem.*, *52*,394–425

Tung, V.X., and V.K. Dhir (1988), A hydrodynamic model for two-phase flow through porous media, *Inter. J.of MultiphaseFlow*, *14*,47-65

Wan, J., and T. K. Tokunaga (1997), Film straining of colloids in unsaturated porous media: Conceptual model and experimental testing, *Environ. Sci. Technol.*, *31*, 2413-2420.

Wan, J., J. L. Wilson, and T. L. Kieft (1994), Influence of the gas-water interface on transport of microorganisms through unsaturated porous media, *App. Env. Microbio.*, *60*, 509-516.

Wan, J., and J. L. Wilson (1994), Visualization of the role of the gas-water interface on the fate and transport of colloids in porous media, *Water Resour. Res.*, *30*, 11-23.

Weber, M. E., D. C. Blanchard, and L. D. Syzdek (1983), The mechanism of scavenging of waterborne bacteria by a rising bubble, *Limnol. Oceanogr.*, *28*, 101-105.

Wilson, D. J., R. D. Norris, and A. N. Clarke (1998), Groundwater cleanup by in-situ sparging. XIV. An air channeling model for biosparging with a horizontal pipe, *Sep. Sci. and Technol.*, *33*, 97-118.

# APPENDIX A

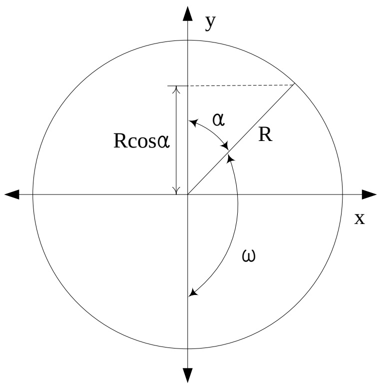


$$R^2 = X^2 + Y^2$$

$$V_{part} = \int_0^{R\cos\alpha} \pi Y^2 dx + \frac{2}{3}\pi R^3$$

$$= \int_0^{R\cos\alpha} \pi\left(R^2 - X^2\right)dx + \frac{2}{3}\pi R^3$$

$$= \left[\pi\left(R^2 X - \frac{X^3}{3}\right)\right]_0^{R\cos\alpha} + \frac{2}{3}\pi R^3$$

$$= \pi R^3 \cos\alpha - \frac{\cos^3\alpha}{3} R + \frac{2}{3}\pi R^3$$

$$= \frac{\pi}{3}\left[2 + 3\cos\alpha - \cos^3\alpha\right]R^3$$

*where* $\cos\alpha = -\cos\omega$

$$V_{part} = \frac{\pi}{3}R^3\left[2 - 3\cos\omega + \cos^3\omega\right]$$

$$= \frac{\pi}{3}R^3\left[\left(1 - \cos\omega\right)^2\left(2 + \cos\omega\right)\right]$$

# APPENDIX B

| Symbol | Meaning |
|---|---|
| $\Sigma F$ | Sum of the external forces acting on a bubble |
| $t$ | Time |
| $m$ | Mass of a bubble |
| $u_b$ | Rise velocity of bubble |
| $u_{bp}$ | Velocity of the particle-bubble unit |
| $u_{bw}$ | Velocity of bubble in liquid |
| $\rho_g$ | Density of a gas bubble |
| $\rho_f$ | Density of water |
| $\rho_p$ | Density of particle |
| $n$ | Porosity |
| $C_D$ | Drag coefficient in liquid |
| $D_b$ | Bubble diameter |
| $d_p$ | Diameter of solid grain |
| $\alpha_0$ | Void fraction |
| $\forall_b$ | Volume of the bubble |
| $R_b$ | Bubble radius |
| $R_p$ | Particle radius |
| $R_{b\_T}$ | Trapped bubble radius in porous media |
| $R'$ | Equivalent radius of a pore throat |
| $F_b$ | Buoyant force for bubble |
| $F_{st}$ | Surface tension force for bubble |
| $F_d$ | Drag force for bubble |
| $F_b^{B+P}$ | Buoyant force for particle-bubble unit |
| $F_g^{B+P}$ | Gravitational force for particle-bubble unit |
| $F_{st}^{B+P}$ | Surface tension force for particle-bubble unit |
| $F_d^{B+P}$ | Drag force for particle-bubble unit |
| $\sigma$ | Surface tension |

| | |
|---|---|
| $\Theta$ | Contact angle |
| $R'$ | Equivalent radius of a pore throat |
| $d_p$ | Diameter of the solid grains |
| $\mu_b$ | Effective dynamic viscosity of the bubble |
| $\mu_w$ | Dynamic viscosity of water |
| A | Correction factor |
| $\Theta$’ | Contact angle of particle |
| $\gamma$ | Angular inclination of the gas-liquid meniscus |
| $\omega$ | $\pi – (\Theta’-\gamma)$ |
| $A_b$ | Surface area of a bubble and |
| $m_g$ | Mass of VOC in a bubble. |
| $C_g$ | Gas concentration of VOC in a bubble |
| k | Mass transfer coefficient |
| $\Delta C$ | Concentration gradient between a bubble and water phase |
| H | Dimensionless Henry’s constant |
| $C_e$ | Equilibrium concentration related to solubility of a gas |
| $C_0$ | Initial concentration in water |

# VITA

Ji-Seok Han was born in Seoul, Korea. Upon graduation from Seoul High School in 1989, he attended Korea University. Majoring in environmental engineering, he earned his Bachelor of Science degree from the university in 1995. He worked for three years as a maintenance officer in the Korea Air Force and enrolled in the graduate program in Civil Engineering at Texas A&M University in 1999. His research for his M.S. thesis was the feasibility of electrophoretic repair of impoundment leaks. He completed his Master of Science in civil engineering at Texas A&M University in May 2002. His research and coursework have focused on understanding the transport and fate of organic contaminants in the subsurface and the development of mathematical models and remediation techniques. His research interests are environment friendly remediation technology and model development with a multiphase and multimedia approach, and risk assessment.

His permanent address is as follows:

Jukong APT. 506-605, Byul-yang Dong

Kwachun City, Kyungki-Do, Korea

Tel. 011-82-2-502-2398